ADVANCED TOPICS IN ASTRODYNAMICS

SUMMER COURSE

BARCELONA, JULY–2004

NOTES FOR THE

GRAVITATIONAL ASSISTED TRAJECTORIES

LECTURES

E. Barrabés, G. Gómez and J. Rodríguez-Canabal

Contents

1 Introduction

Interplanetary gravitational assisted trajectories appear when a spacecraft, on its way from one celestial body to another, approaches a third attracting body which produces a significant change in the trajectory of the spacecraft.

Due to the large distances between the attracting masses in the solar system, as well as the values of the ratios between the masses of the planets and the sun, in a first approximation the gravity field in the solar system can be decoupled. When the motion takes place far from a planet (heliospheric region) the dominant effect is due to the Sun, while the dominant term of the equations of motion corresponds to the planet when the spacecraft moves in the so called planetary gravispheres. The boundaries of the gravispheres can be defined in a number of different ways, such as: spheres of gravitation, Laplace's spheres of influence, Hill's regions, Belbruno's weak stability boundaries, etc.

According to this, the motion of the spacecraft can be expressed as a sequence of perturbed keplerian arcs. In the first order approximation, the trajectory is represented by a series of segments of undisturbed keplerian motion. In a further step, asymptotic expansions can be obtained for the so called "inner" and "outer" solutions, corresponding to the motion inside or outside a gravisphere. Of course, matching conditions on both kinds of solutions must be added at the boundaries.

The analytical solutions obtained with the above approximations are used as initial guesses in the determination of the trajectory, or the domain of admissible trajectories, to be used by a spacecraft in order to accomplish a certain interplanetary mission. For this purpose, the use of numerical nonlinear programming procedures are required, in order to take into account the restrictions required for the mission.

Within this frame of reference, the objectives of the course will be:

- To explain and analyse the concepts and techniques, both analytical and numerical, related to gravity assist,
- To illustrate the gravitational assist procedures with some spacecraft missions developed by ESA.

1.1 Transfers within the Solar System

Assume that we want to reach, from one circular orbit around the Sun, another circular orbit of different radius but in the same plane. Let the radii of the two circular orbits be r_1 and r_2 as shown in Fig. 1.

From the energy integral

$$\frac{v^2}{2} - \frac{\mu_S}{r} = -\frac{\mu_S}{2a},$$

where $\mu_S = Gm_S$ (m_S is the mass of the Sun and G the gravitation constant) and $a = (r_1 + r_2)/2$ (the semi-major axis of the transfer orbit), one easily gets

$$r_1 \frac{v_1^2}{\mu_S} = \frac{2\sigma}{1+\sigma},$$

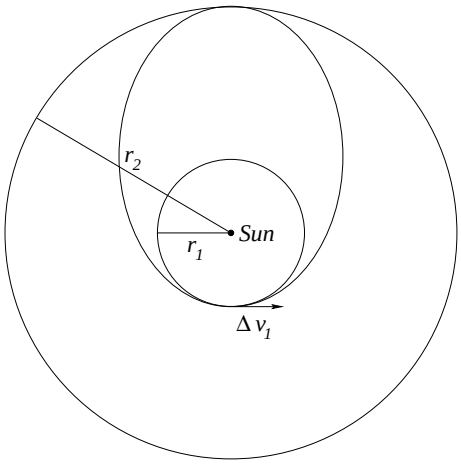

Figure 1: Transfer between circular coplanar orbits.

with $\sigma = r_2/r_1$. Since the velocity in the inner circular orbit is $\sqrt{\mu_S/r_1}$, the required change of velocity at the periapsis of the transfer ellipse is

$$\Delta v_1 = v_1 - \sqrt{\mu_S/r_1} = \sqrt{\mu_S/r_1}\left(\sqrt{\frac{2\sigma}{1+\sigma}} - 1\right).$$

As we are only interested in an encounter with the outer planet (or inner if $r_2 < r_1$), we are not going to compute the second Δv completing the Hohmann transfer.

Consider now how injection into the interplanetary orbit is achieved from a circular parking orbit around the Earth. Relative to the Earth, the interplanetary orbit is initially a hyperbola and becomes subsequently an elliptic orbit relative to the Sun. Again, from the energy first integral

$$v_0 = \sqrt{v_\infty^2 + 2\mu_E/r_0}, \qquad \text{with} \qquad v_\infty^2 = -\mu/a_h,$$

where now $\mu_E = Gm_E$ (see Fig. 2).

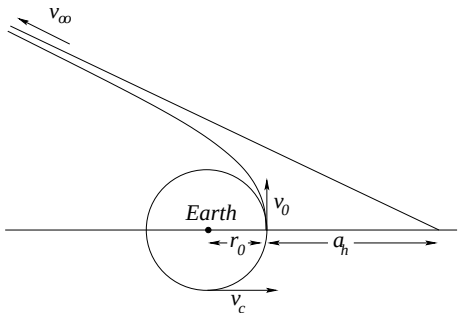

Figure 2: Hyperbolic escape.

Since the velocity in circular orbit is $v_c = \sqrt{\mu_E/r_0}$, the required increment of velocity to escape is

$$\Delta v_0 = \sqrt{v_\infty^2 + 2\mu_E/r_0} - \sqrt{\mu_E/r_0}. \tag{1}$$

In this way, we can compute the Δv required to inject a spacecraft (initially in a circular orbit about the Earth) into a heliocentric orbit with an aphelion equal to that of a planet, i.e. the minimum energy to encounter that planet.

The required hyperbolic escape velocity v_∞ is equivalent to the Δv_1 and the velocity increment Δv_0 to be applied from the circular Earth orbit to achieve a given v_∞ is given by (1). Departing from circular orbit around the Earth, at an altitude of 185 km, The velocity increments are

Planet	v_∞	Δv_0
Mercury	–7.533	5.556
Venus	–2.495	3.507
Mars	2.945	3.615
Jupiter	8.793	6.306
Saturn	10.289	7.284
Uranus	11.280	7.978
Neptune	11.654	8.247
Pluto	11.813	8.363

Table 1: Minimum Δv requirements (in km/s) to encounter the planets.

From the above Table it is seen that only Venus and Mars have low requirements and that the exploration of the outer planets is difficult in terms of conventional chemical propulsion.

2 Equations of motion

2.1 The n-body problem as a perturbation of the Kepler problem

In an inertial reference frame, and according to Newton's laws, the equations of motion of n punctual masses m_1,m_2,...,m_n are

$$m_k \ddot{\mathbf{r}}_k = G \sum_{j=1,\, j\neq k}^{n} \frac{m_j m_k}{r_{jk}^3}(\mathbf{r}_j - \mathbf{r}_k), \quad k = 1, 2, ..., n, \tag{2}$$

where $r_{jk} = |\mathbf{r}_j - \mathbf{r}_k|$. For $k = 1, 2$ we have

$$\begin{aligned} \frac{d^2\mathbf{r}_1}{dt^2} &= G\frac{m_2}{r_{21}^3}(\mathbf{r}_2 - \mathbf{r}_1) + G\sum_{j=3}^{n} \frac{m_j}{r_{j1}^3}(\mathbf{r}_j - \mathbf{r}_1), \\ \frac{d^2\mathbf{r}_2}{dt^2} &= G\frac{m_1}{r_{12}^3}(\mathbf{r}_1 - \mathbf{r}_2) + G\sum_{j=3}^{n} \frac{m_j}{r_{j2}^3}(\mathbf{r}_j - \mathbf{r}_2). \end{aligned} \tag{3}$$

Subtracting these two equations we get the one corresponding to the relative

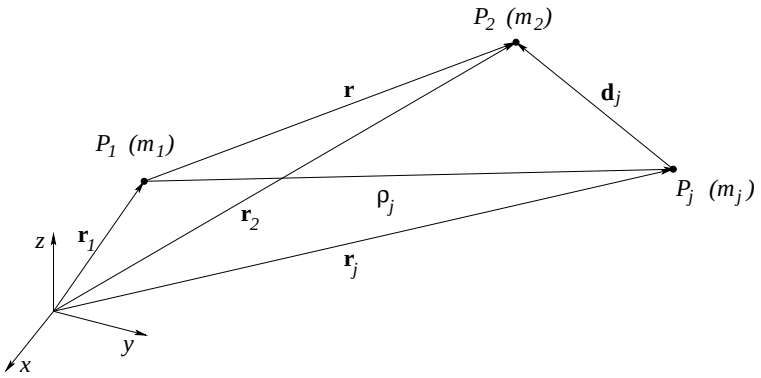

Figure 3: Inertial and relative coordinates.

motion of m_2 with respect to m_1

$$\frac{d^2\mathbf{r}}{dt^2} + \mu\,\frac{\mathbf{r}}{r^3} \;=\; -G\sum_{j=3}^{n} m_j \left(\frac{\mathbf{d}_j}{d_j^3} + \frac{\boldsymbol{\rho}_j}{\rho_j^3}\right), \tag{4}$$

where we have defined, as is shown in Figure 3, $\mathbf{r} = \mathbf{r}_2 - \mathbf{r}_1$, $\boldsymbol{\rho}_j = \mathbf{r}_j - \mathbf{r}_1$, $\mathbf{d}_j = \mathbf{r} - \boldsymbol{\rho}_j$ and $\mu = G(m_1 + m_2)$. If $m_3 = ... = m_n = 0$, then either (3) as (4) are the equations of the two body problem.
Is easy to verify that

$$\frac{\mathbf{d}_j}{d_j^3} + \frac{\boldsymbol{\rho}_j}{\rho_j^3} = -\frac{\partial}{\partial \mathbf{r}}\left(\frac{1}{d_j} - \frac{\mathbf{r}\cdot\boldsymbol{\rho}_j}{\rho_j^3}\right).$$

So, defining

$$V_j = Gm_j\left(\frac{1}{d_j} - \frac{\mathbf{r}\cdot\boldsymbol{\rho}_j}{\rho_j^3}\right), \tag{5}$$

as the disturbing potential associated to m_j, the equation of relative motion (4) becomes

$$\frac{d^2\mathbf{r}}{dt^2} + \mu\,\frac{\mathbf{r}}{r^3} \;=\; \sum_{j=3}^{n} \frac{\partial V_j}{\partial \mathbf{r}}. \tag{6}$$

2.1.1 Developments of the disturbing function

Next we are going to develop V_j as a power series in r/ρ_j. To simplify the notation we will remove the subindex j in V_j, so

$$V = Gm\left(\frac{1}{d} - \frac{\mathbf{r}\cdot\boldsymbol{\rho}}{\rho^3}\right) = Gm\left(\frac{1}{d} - \frac{r\,\cos\alpha}{\rho^2}\right) = \frac{Gm}{\rho}\left(\frac{\rho}{d} - \frac{r}{\rho}\cos\alpha\right), \tag{7}$$

where α is the angle between $\mathbf{r}$ and $\boldsymbol{\rho}$, as is shown in Figure 4.

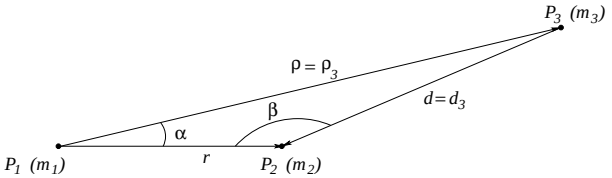

Figure 4: Relative coordinates.

If $\mathbf{r} = (x, y, z)$ and $\boldsymbol{\rho} = (\xi, \eta, \zeta)$, then

$$d^2 = (x-\xi)^2 + (y-\eta)^2 + (z-\zeta)^2 = \rho^2 - 2\rho\, r\,\cos\alpha + r^2,$$

and so

$$\frac{\rho}{d} = \left[1 - 2\,\frac{r}{\rho}\cos\alpha + \frac{r^2}{\rho^2}\right]^{-1/2} = (1+q)^{-1/2}, \tag{8}$$

with $q = r^2/\rho^2 - 2\,(r/\rho)\,\cos\alpha$. Using Taylor's formula

$$\begin{array}{rcl} (1+q)^{-1/2} & = & \sum_{k\geq 0} \dfrac{-1/2(-3/2)(-5/2)...((1-2k)/2)}{k!} q^k \\ & = & \sum_{k\geq 0} (-1)^k \dfrac{(2k-1)!!}{2^k k!} q^k \;=\; \sum_{k\geq 0} (-1)^k \dfrac{(2k)!}{(2^k\ k!)^2} q^k, \end{array} \tag{9}$$

where the equality between the coefficients in the last two summations is easily proved by induction. On the other hand, defining $t = r/\rho$, $q^k = (t^2 - 2t\cos\alpha)^k$ and using the binomial formula, we get

$$q^k = \sum_{l=0}^{k} \frac{k!}{l!\,(k-l)!} t^{k+l} (-2)^{k-l} \cos^{k-l}\alpha. \tag{10}$$

Substituting (10) in (9) we get

$$(1+q)^{-1/2} = \sum_{k\geq 0} \sum_{l=0}^{k} (-1)^l \frac{(2k)!}{2^{k+l}\ k!\,(k-l)!\,l!}\ \cos^{k-l}\alpha\ t^{k+l}.$$

In order to write this development as a power series in t, we change the summation index by defining $n = k + l$ and replacing k by $n - l$. In this way we get

$$(1+q)^{-1/2} = \sum_{n\geq 0} \sum_{l=0}^{[n/2]} (-1)^l \frac{(2n-2l)!}{2^n\ (n-l)!\ (n-2l)!\ l!} \cos^{n-2l}\alpha\, t^n.$$

where $[\ ]$ denotes the integer part. The coefficients of t^n are polynomials in $\cos\alpha$, which are denoted by $P_n(\cos\alpha)$. Summarising, we have seen that

$$\frac{\rho}{d} = (1+q)^{-1/2} = 1 + \sum_{n\geq 1} \left(\frac{r}{\rho}\right)^n P_n(\cos\alpha), \tag{11}$$

where

$$P_n(z) = \frac{1}{2^n} \sum_{l=0}^{[n/2]} (-1)^l \frac{(2n-2l)!}{l!\ (n-l)!\ (n-2l)!} z^{n-2l},$$

are the Legendre polynomials, which are usually defined as

$$P_n(z) = \frac{1}{2^n\, n!} \frac{d^n}{dz^n}(z^2-1)^n.$$

The equivalence between the two definitions follows from

$$\begin{aligned} \frac{d^n}{dz^n}(z^2-1)^n &= \frac{d^n}{dz^n}\left[\sum_{l=0}^{n} (-1)^l \frac{n!}{l!\ (n-l)!} z^{2n-2l}\right] \\ &= \sum_{l=0}^{[n/2]} (-1)^l \frac{n!}{l!\ (n-l)!} \frac{(2n-2l)!}{(n-2l)!} z^{n-2l}. \end{aligned} \tag{12}$$

The first Legendre polynomials are $P_0(z) = 1$, $P_1(z) = z$, $P_2(z) = \frac{1}{2}(3z^2-1)$, $P_3(z) = \frac{1}{2}(5z^3 - 3z)$.

Using (11), we can write the disturbing function as

$$V = \frac{Gm}{\rho}\left(\frac{\rho}{d} - \frac{r}{\rho}\cos\alpha\right) = \frac{Gm}{\rho}\left(1 + \sum_{n\geq 2}\left(\frac{r}{\rho}\right)^n P_n(\cos\alpha)\right).$$

If r/ρ is small, this series converges quite rapidly and only a few terms are required for satisfactory accuracy in many applications. In order to use these developments in the equations of motion (6) we need to compute $\partial V/\partial \mathbf{r}$. We have that

$$\frac{\partial P_n(\cos\alpha)}{\partial \mathbf{r}} = {P_n}'(\cos\alpha)\, \frac{\partial \cos\alpha}{\partial \mathbf{r}}.$$

If $\mathbf{r} = (x,y,z)^T$, $\boldsymbol{\rho} = (\xi,\eta,\zeta)^T$, one can easily compute

$$\frac{\partial \cos\alpha}{\partial x} = \frac{\partial}{\partial x}\left(\frac{\mathbf{r}\,\boldsymbol{\rho}}{r\rho}\right) = \frac{\xi r\rho - \mathbf{r}\,\boldsymbol{\rho}\,\rho\,(x/r)}{r^2\rho^2} = \frac{\xi}{r\rho} - \frac{x\cos\alpha}{r^2}.$$

The derivatives with respect to y and z can be computed in a similar way. Using the equality $\cos\alpha {P'}_n(\cos\alpha) = nP_n(\cos\alpha) + {P'}_{n-1}(\cos\alpha)$, we get

$$\begin{aligned} \frac{\partial P_n(\cos\alpha)}{\partial \mathbf{r}} &= \frac{1}{r}{P'}_n(\cos\alpha)\left(\frac{\boldsymbol{\rho}}{\rho} - \cos\alpha\,\frac{\mathbf{r}}{r}\right) \\ &= \frac{1}{r}\left({P'}_n(\cos\alpha)\frac{\boldsymbol{\rho}}{\rho} - nP_n(\cos\alpha)\frac{\mathbf{r}}{r} - {P'}_{n-1}(\cos\alpha)\frac{\mathbf{r}}{r}\right). \end{aligned}$$

Using this last formula and introducing the unit vectors $\mathbf{i_r} = \mathbf{r}/r$, $\mathbf{i}_\rho = \boldsymbol{\rho}/\rho$ we finally obtain

$$\begin{aligned}
\frac{\partial V}{\partial \mathbf{r}} &= \frac{Gm}{\rho}\sum_{n\geq 2}\frac{\partial}{\partial \mathbf{r}}\left[\left(\frac{r}{\rho}\right)^n P_n(\cos\alpha)\right] \\
&= \frac{Gm}{\rho}\sum_{n\geq 2}\left[\frac{n}{\rho}\left(\frac{r}{\rho}\right)^{n-1} P_n(\cos\alpha)\,\mathbf{i_r} + \left(\frac{r}{\rho}\right)^n \frac{\partial P_n(\cos\alpha)}{\partial \mathbf{r}}\right] \\
&= \frac{Gm}{\rho}\sum_{n\geq 2}\left[\frac{n}{\rho}\left(\frac{r}{\rho}\right)^{n-1} P_n(\cos\alpha)\,\mathbf{i_r} + \frac{1}{r}\left(\frac{r}{\rho}\right)^n P'_n(\cos\alpha)\,\mathbf{i}_\rho \right. \\
&\qquad \left. -\frac{n}{r}\left(\frac{r}{\rho}\right)^n P_n(\cos\alpha)\,\mathbf{i_r} - \frac{1}{r}\left(\frac{r}{\rho}\right)^n P'_{n-1}(\cos\alpha)\,\mathbf{i_r}\right] \\
&= \frac{Gm}{\rho^2}\sum_{n\geq 1}\left(\frac{r}{\rho}\right)^n \left[P'_{n+1}(\cos\alpha)\,\mathbf{i}_\rho - P'_n(\cos\alpha)\,\mathbf{i_r}\right].
\end{aligned}$$

So, the equation of motion (6) can be written as

$$\frac{d^2\mathbf{r}}{dt^2} + \mu\frac{\mathbf{r}}{r^3} = G\sum_{j=3}^{n}\frac{m_j}{\rho_j^2}\sum_{k\geq 1}\left(\frac{r}{\rho_j}\right)^k \left[P'_{k+1}(\cos\alpha)\,\mathbf{i}_{\rho_j} - P'_k(\cos\alpha)\,\mathbf{i_r}\right]. \quad (13)$$

2.2 The restricted three body problem

According to (2), in an inertial reference frame, the equations of the three body problem are

$$\begin{aligned}
\ddot{\mathbf{r}}_1 &= -Gm_2\frac{\mathbf{r}_1-\mathbf{r}_2}{r_{21}^3} - Gm_3\frac{\mathbf{r}_1-\mathbf{r}_3}{r_{31}^3}, \\
\ddot{\mathbf{r}}_2 &= -Gm_1\frac{\mathbf{r}_2-\mathbf{r}_1}{r_{12}^3} - Gm_3\frac{\mathbf{r}_2-\mathbf{r}_3}{r_{32}^3}, \\
\ddot{\mathbf{r}}_3 &= -Gm_1\frac{\mathbf{r}_3-\mathbf{r}_1}{r_{13}^3} - Gm_2\frac{\mathbf{r}_3-\mathbf{r}_2}{r_{23}^3},
\end{aligned} \quad (14)$$

where $r_{jk} = |\mathbf{r}_j - \mathbf{r}_k|$. If one of the masses can be neglected, in front of the other two, the above equations can be simplified. Taking, for instance, $m_3 = 0$ we get

$$\begin{aligned}
\ddot{\mathbf{r}}_1 &= -Gm_2\frac{\mathbf{r}_1-\mathbf{r}_2}{r_{21}^3}, \\
\ddot{\mathbf{r}}_2 &= -Gm_1\frac{\mathbf{r}_2-\mathbf{r}_1}{r_{12}^3}, \\
\ddot{\mathbf{r}}_3 &= -Gm_1\frac{\mathbf{r}_3-\mathbf{r}_1}{r_{13}^3} - Gm_2\frac{\mathbf{r}_3-\mathbf{r}_2}{r_{23}^3}.
\end{aligned} \quad (15)$$

The first two equations of this system describe the Keplerian motion of m_1 and m_2, which are usually known as *primaries*. Assuming some fixed motion for the primaries (circular, elliptic,..) the third equation defines the *restricted three body problem* (RTBP).

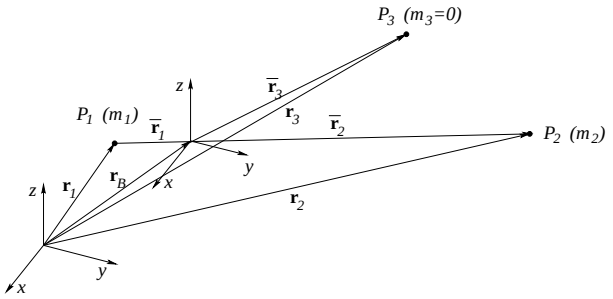

Figure 5: Barycentric coordinates.

To study the RTBP, is useful to write the equations in a *synodic* reference system which rotates about the barycenter. Let's first consider the third body acceleration as seen from the barycenter. Denoting by $\overline{\mathbf{r}}_i = \mathbf{r}_i - \mathbf{r}_B$, $i = 1, 2, 3$, the positions of the three bodies in this frame (where $\mathbf{r}_B$ is the position vector of the barycenter) and taking into account that

$$\overline{\mathbf{r}}_{jk} = \overline{\mathbf{r}}_j - \overline{\mathbf{r}}_k = \mathbf{r}_j - \mathbf{r}_k = \mathbf{r}_{jk}, \qquad \ddot{\overline{\mathbf{r}}}_k = \ddot{\mathbf{r}}_k - \ddot{\mathbf{r}}_B = \ddot{\mathbf{r}}_k,$$

due to conservation of linear momentum, we see that the equations of motion (14) and (15) are independent of any particular inertial frame. From now on, we will assume that (15) are the equations of the RTBP in an inertial barycentric reference frame.

One particular case of the RTBP is the *circular restricted three body problem*, in which m_1 and m_2 describe circular orbits around their barycenter. For this problem we will use a synodic reference system in which the two primaries remain at rest on the x–axis. If $R(t)$ is the transformation between both reference frames, defined by the constant angular velocity $\boldsymbol{\omega} = (0, 0, n)^T$ of the rotating frame with respect to the fixed one, we have

$$\boldsymbol{\rho} = R(t)\mathbf{r},$$

where $\boldsymbol{\rho}$ denotes the synodical position and $\mathbf{r}$ the corresponding barycentric one. Recall that

$$\frac{d^2\mathbf{r}}{dt^2} = \frac{d^2\boldsymbol{\rho}}{dt^2} + 2\boldsymbol{\omega} \wedge \frac{d\boldsymbol{\rho}}{dt} + \boldsymbol{\omega} \wedge (\boldsymbol{\omega} \wedge \boldsymbol{\rho}), \tag{16}$$

Denoting by $\boldsymbol{\rho} = (x, y, z)^T$ the synodic position of m_3, its Coriolis and centripetal accelerations are

$$\boldsymbol{\omega} \wedge \frac{d\boldsymbol{\rho}}{dt} = n \begin{pmatrix} \dot{y} \\ -\dot{x} \\ 0 \end{pmatrix}, \quad \boldsymbol{\omega} \wedge (\boldsymbol{\omega} \wedge \boldsymbol{\rho}) = n^2 \begin{pmatrix} x \\ y \\ 0 \end{pmatrix},$$

and the synodic equations of the RTBP become

$$\begin{aligned}
\ddot{x} - 2n\dot{y} - n^2 x &= -Gm_1 \frac{(x - x_1)}{r_{13}^3} - Gm_2 \frac{(x - x_2)}{r_{23}^3} = \frac{\partial}{\partial x}\left(\frac{Gm_1}{r_{13}} + \frac{Gm_2}{r_{23}}\right), \\
\ddot{y} + 2n\dot{x} - n^2 y &= -Gm_1 \frac{y}{r_{13}^3} - Gm_2 \frac{y}{r_{23}^3} = \frac{\partial}{\partial y}\left(\frac{Gm_1}{r_{13}} + \frac{Gm_2}{r_{23}}\right), \\
\ddot{z} &= -Gm_1 \frac{z}{r_{13}^3} - Gm_2 \frac{z}{r_{23}^3} = \frac{\partial}{\partial z}\left(\frac{Gm_1}{r_{13}} + \frac{Gm_2}{r_{23}}\right).
\end{aligned}$$

where $(x_1, 0, 0)$ and $(x_2, 0, 0)$ denote the two fixed synodic positions of m_1 and m_2, respectively.

It is useful to introduce a suitable set of units in such a way that the distance between the two primaries is equal to one, $n = 1$ and the unit of mass such that the sum of the masses of the primaries is also one, so

$$m_1 = 1 - \mu, \qquad m_2 = \mu,$$

with $\mu \in [0, 1]$. With this choice $G = 1$ and we can set $\boldsymbol{\rho}_1 = (\mu, 0, 0)^T$, $\boldsymbol{\rho}_2 = (\mu - 1, 0, 0)^T$ so

$$r_{13} = \sqrt{(x-\mu)^2 + y^2 + z^2}, \qquad r_{23} = \sqrt{(x-\mu+1)^2 + y^2 + z^2}.$$

Using the auxiliary function

$$\Omega = \frac{1}{2}(x^2 + y^2) + \frac{1-\mu}{r_1} + \frac{\mu}{r_2},$$

where $r_1 = r_{13}$ and $r_2 = r_{23}$, the RTBP equations become

$$\begin{aligned} \ddot{x} - 2\dot{y} &= \frac{\partial \Omega}{\partial x}, \\ \ddot{y} + 2\dot{x} &= \frac{\partial \Omega}{\partial y}, \\ \ddot{z} &= \frac{\partial \Omega}{\partial z}. \end{aligned} \tag{17}$$

System (17) has a first integral, the *Jacobian integral*, which can be obtained multiplying equations (17) by $\dot{x}$, $\dot{y}$ and $\dot{z}$, adding the results and integrating; in this way we get

$$\dot{x}^2 + \dot{y}^2 + \dot{z}^2 - 2\Omega(x, y, z) = C_J. \tag{18}$$

2.3 The n-body problem as a perturbation of the restricted three body problem

Consider Newton's equation for the motion of an infinitesimal body in the force field created by n punctual masses. These masses can be assumed to be the bodies of the Solar System, which will be denoted by $\mathcal{S}$. In an inertial reference frame, the equation of motion of the infinitesimal particle is

$$\mathbf{r}'' = G \sum_{i \in \mathcal{S}} m_i \frac{\mathbf{r}_i - \mathbf{r}}{\|\mathbf{r} - \mathbf{r}_i\|^3},$$

where $\mathbf{r}_i$ are the inertial coordinates of the bodies in $\mathcal{S}$ and $\mathbf{r}$ the ones of the infinitesimal body. The prime denotes derivative with respect to some dynamical time t^*.

The above system can be written in Lagrangian form with Lagrangian function

$$L(\mathbf{r}, \mathbf{r}', t^*) = \frac{1}{2}\mathbf{r}' \cdot \mathbf{r}' + \sum_{i \in \mathcal{S}} \frac{G m_i}{\|\mathbf{r} - \mathbf{r}_i\|},$$

where $\cdot$ stands for the Euclidean scalar product.

In order to write the previous system as a perturbed restricted three body problem, we first choose two bodies $I, J \in \mathcal{S}$, with $m_I > m_J$, which will play the role of primaries. In this way, the mass parameter, μ, is defined as $\mu = m_J/(m_I + m_J)$. Next, we must introduce the synodic reference frame. Recall that the origin of this system is set at the barycenter of I, J and that the positions of the primaries are fixed at $(\mu, 0, 0)$ and $(\mu - 1, 0, 0)$. The transformation from synodical coordinates $\boldsymbol{\rho} = (x, y, z)^T$ to inertial (sidereal) ones, $\mathbf{r}$, is defined by

$$\mathbf{r} = \mathbf{b} + kC\boldsymbol{\rho}, \tag{19}$$

where

- The translation $\mathbf{b}$, given by

$$\mathbf{b} = \frac{m_I \mathbf{r}_I + m_J \mathbf{r}_J}{m_I + m_J},$$

  puts the barycenter of the primaries at the origin.

- The orthogonal matrix $C = (\mathbf{e}_1, \mathbf{e}_2, \mathbf{e}_3)$, sets the primaries on the x-axis and turns the instantaneous plane of motion of the primaries into the xy plane (by requiring that the relative velocity of one primary with respect to the other has its third component equal to zero). The columns of C are

$$\mathbf{e}_1 = \frac{\mathbf{r}_{JI}}{\|\mathbf{r}_{JI}\|}, \quad \mathbf{e}_3 = \frac{\mathbf{r}_{JI} \times \mathbf{r}'_{JI}}{\|\mathbf{r}_{JI} \times \mathbf{r}'_{JI}\|}, \quad \mathbf{e}_2 = \mathbf{e}_3 \times \mathbf{e}_1,$$

  being $\mathbf{r}_{ij} = \mathbf{r}_j - \mathbf{r}_i$.

- $k = \|\mathbf{r}_{JI}\|$ is a scaling factor which makes the distance between the primaries to be constant and equal to 1.

Note that the previous change of coordinates is non-autonomous, because $\mathbf{b}$, k and C depend on time.

Additionally, we want to use the same time units as the one usual for the RTBP, where 2π time units correspond to one revolution of the primaries. If t^* is the dynamical time and n is the mean motion of J with respect to I, we introduce the *adimensional time* t by

$$t = n(t^* - t_0^*), \tag{20}$$

where t_0^* is a fixed epoch.

If we denote by a dot the derivative with respect to t, then the Lagrangian can be written as

$$\begin{aligned} L(\boldsymbol{\rho}, \dot{\boldsymbol{\rho}}, t) \;=\; & n^2\Big(\frac{1}{2}\dot{\mathbf{b}}\cdot\dot{\mathbf{b}} + \dot{k}\dot{\mathbf{b}}\cdot\mathbf{s} + k\dot{\mathbf{b}}\cdot\dot{\mathbf{s}} + \frac{1}{2}\dot{k}^2\boldsymbol{\rho}\cdot\boldsymbol{\rho} + k\dot{k}\mathbf{s}\cdot\dot{\mathbf{s}} + \frac{1}{2}k^2\dot{\mathbf{s}}\dot{\mathbf{s}}\Big) + \\ & + \frac{Gm_I}{k[(x-\mu)^2 + y^2 + z^2]^{1/2}} + \frac{Gm_J}{k[(x-\mu+1)^2 + y^2 + z^2]^{1/2}} + \\ & + \sum_{i \in \mathcal{S}^*} \frac{Gm_i}{k\|\boldsymbol{\rho} - \boldsymbol{\rho}_i\|}, \end{aligned}$$

where $\mathbf{s} = C\boldsymbol{\rho}$, $\boldsymbol{\rho}_i$ is the position of the body $i \in \mathcal{S}$ in dimensionless coordinates and $\mathcal{S}^*$ represents the Solar System bodies considered without the two primaries

I, J. To get the above expression we have used that C is an orthogonal matrix and, hence, it preserves the scalar product and the Euclidean norm.

Removing from the above function the term $\dot{\mathbf{b}}\cdot\dot{\mathbf{b}}$ (which does not affect the equations of motion), multiply by $a/(G(m_I+m_J)) = 1/(n^2a^2)$ (where a is the mean semi-major axis of the orbit of one primary around the other computed using Kepler's third law $G(m_I+m_J)=n^2a^3$) and using the properties of the orthogonal basis $\mathbf{e}_i$, we get

$$\begin{aligned} L(\boldsymbol{\rho},\dot{\boldsymbol{\rho}},t) &= a_1(\dot{x}^2+\dot{y}^2+\dot{z}^2)+a_2(x\dot{x}+y\dot{y}+z\dot{z})+a_3(x\dot{y}-\dot{x}y)+ \\ &\quad +a_4(y\dot{z}-\dot{y}z)+a_5x^2+a_6y^2+a_7z^2+a_8xz+ \\ &\quad +a_9\dot{x}+a_{10}\dot{y}+a_{11}\dot{z}+a_{12}x+a_{13}y+a_{14}z+ \\ &\quad +a_{15}\left(\frac{1-\mu}{[(x-\mu)^2+y^2+z^2]^{1/2}}+\frac{\mu}{[(x-\mu+1)^2+y^2+z^2]^{1/2}}+\right. \\ &\quad \left.+\sum_{i\in\mathcal{S}^*}\frac{\mu_i}{[(x-x_i)^2+(y-y_i)^2+(z-z_i)^2]^{1/2}}\right), \end{aligned}$$

where the a_i, $i=1,...,15$ are time dependent functions depending on k, C, $\mathbf{b}$ and a (see [7]).

¿From the above Lagrangian we can write the second-order differential equations of motion as

$$\begin{aligned} \ddot{x} &= b_1+b_4\dot{x}+b_5\dot{y}+b_7x+b_8y+b_9z+b_{13}\frac{\partial\Omega}{\partial x} \\ \ddot{y} &= b_2-b_5\dot{x}+b_4\dot{y}+b_6\dot{z}-b_8x+b_{10}y+b_{11}z+b_{13}\frac{\partial\Omega}{\partial y} \\ \ddot{z} &= b_3-b_6\dot{y}+b_4\dot{z}+b_9x-b_{11}y+b_{12}z+b_{13}\frac{\partial\Omega}{\partial z} \end{aligned} \tag{21}$$

being

$$\begin{aligned} \Omega &= \frac{1-\mu}{\sqrt{(x-\mu)^2+y^2+z^2}}+\frac{\mu}{\sqrt{(x-\mu+1)^2+y^2+z^2}} \\ &\quad +\sum_{i\in\mathcal{S}^*}\frac{\mu_i}{\sqrt{(x-x_i)^2+(y-y_i)^2+(z-z_i)^2}}. \end{aligned}$$

where

$$\begin{aligned} &b_1=-\frac{1}{k}\,\ddot{\mathbf{b}}\cdot\mathbf{e}_1, \quad b_2=-\frac{1}{k}\,\ddot{\mathbf{b}}\cdot\mathbf{e}_2, \quad b_3=-\frac{1}{k}\,\ddot{\mathbf{b}}\cdot\mathbf{e}_3, \\ &b_4=-\frac{2\dot{k}}{k}, \quad b_5=2\,\dot{\mathbf{e}}_1\cdot\mathbf{e}_2, \quad b_6=2\,\dot{\mathbf{e}}_2\cdot\mathbf{e}_3, \\ &b_7=\dot{\mathbf{e}}_1\cdot\dot{\mathbf{e}}_1-\frac{\ddot{k}}{k}, \quad b_8=\frac{2\dot{k}}{k}\dot{\mathbf{e}}_1\cdot\mathbf{e}_2+\ddot{\mathbf{e}}_1\cdot\mathbf{e}_2, \quad b_9=\dot{\mathbf{e}}_1\cdot\dot{\mathbf{e}}_3, \\ &b_{10}=\dot{\mathbf{e}}_2\cdot\dot{\mathbf{e}}_2-\frac{\ddot{k}}{k}, \quad b_{11}=\frac{2\dot{k}}{k}\dot{\mathbf{e}}_2\cdot\mathbf{e}_3+\ddot{\mathbf{e}}_2\cdot\mathbf{e}_3, \quad b_{12}=\dot{\mathbf{e}}_3\cdot\dot{\mathbf{e}}_3-\frac{\ddot{k}}{k}, \\ &b_{13}=\frac{a^3}{k^3}. \end{aligned}$$

We note that setting $b_i=0$ for $i\neq 5,7,10,13$, $b_5=2$, $b_7=b_{10}=b_{13}=1$ and skipping the sum over $\mathcal{S}^*$ in Ω, the equations of motion become the usual

RTBP equations with mass parameter μ. Therefore, we can see equations (21) as a perturbation of the RTBP equations. Once the primaries have been fixed, we will get an idea of the order of magnitude of he perturbation by looking at the first coefficient of the Fourier expansions of the b_i functions. The Fourier analysis of this functions is done in [7] for different systems.

3 Gravispheres

3.1 Spheres of gravitation

Consider three mass points m_1, m_2 and m_3. We will assume that $m_3 < m_2 < m_1$. The modulus of the gravitational forces acting on m_3 towards m_1 and m_2 are

$$F_{13} = G\frac{m_1 m_3}{r_{13}^2}, \quad F_{23} = G\frac{m_2 m_3}{r_{23}^2}.$$

The locus of points where $F_{13} < F_{23}$ defines the *sphere of gravitational attraction* of m_2 with respect to m_1. The location and radius of this sphere is determined by

$$F_{13} = G\frac{m_1 m_3}{r_{13}^2} = G\frac{m_2 m_3}{r_{23}^2} = F_{23},$$

this is

$$\frac{r_{23}}{r_{13}} = \sqrt{\frac{m_2}{m_1}} < 1. \tag{22}$$

The locus of points defined by this equation is a sphere, whose diameter is defined by points A and B, as shown in Figure 6. According to (22), when m_3

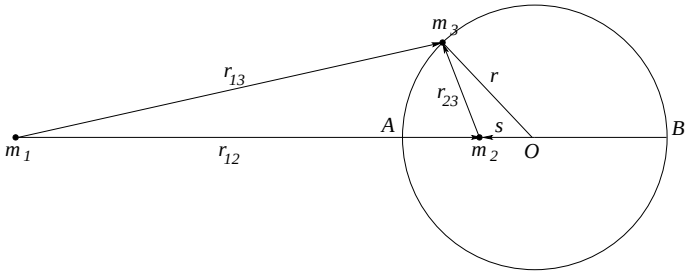

Figure 6: Sphere of gravitation.

is located at the collinear points A and B we have

$$\frac{r-s}{r_{12}-(r-s)} = \sqrt{\frac{m_2}{m_1}} = \frac{r+s}{r_{12}+r+s},$$

from which we get the radius r and the displacement s of the centre of the sphere of gravitation as a function of the distance r_{12}

$$r = \frac{\sqrt{m_2/m_1}}{1-m_2/m_1}\, r_{12}, \quad s = \frac{m_2/m_1}{1-m_2/m_1}\, r_{12}.$$

The spheres of gravitation are not of much interest since, for instance, the Moon is not inside the sphere of gravitation of the Earth. Denoting by S, E and M the Sun, the Earth and the Moon, respectively, the Moon should be inside the Earth's sphere of gravitation if

$$G\frac{m_S m_M}{r_{SM}^2} < G\frac{m_E m_M}{r_{EM}^2}, \quad \Leftrightarrow \quad r_{EM} < \sqrt{\frac{m_M}{m_S}} r_{SM},$$

When the Moon is between the Sun and the Earth (at point A of Figure 6) we have that $r_{SM}+r_{EM} = 1\ AU = 1.5\times10^8$ km, and the above inequality becomes

$$r_{EM} < \frac{(m_E/m_S)^{1/2}}{1+(m_E/m_S)^{1/2}}\, AU \approx 2.5\times10^5\,\text{km},$$

since $m_S/m_E \approx 3\times10^5$. In this way, the Moon which is at a mean distance from the Earth of 3.85×10^5 km is clearly outside the sphere of gravitation of the Earth.

3.2 Spheres of influence

The concept of *sphere of influence* was introduced by Laplace in his work on the motion of a comet when it approaches Jupiter. It is useful to establish a criteria to choose the origin of coordinates along the different stages of the motion.

According with Laplace, in order to fix which body (Sun or Jupiter) has a dominant effect on the motion of a third body (comet), it is necessary to calculate the quotients of the disturbing force with respect to the Keplerian force (4) for both systems: Sun–comet–Jupiter and Jupiter–comet–Sun. The system with the smallest quotient will be the most suitable for describing the motion of the third body. Supposing r much less than ρ, the surface where both quotients are equal is almost spherical. For this reason, the limiting surface is called sphere of influence.

In order to settle the sphere of influence, we consider the motion of a body of mass m_3 (comet) under the influence of two bodies of masses m_1 (Sun) and m_2 (Jupiter). Next we are going to write the equations of the relative motion of m_3 with respect to m_1 and m_2 and to compare the magnitude of the disturbing forces. We write the equation (4) of the relative motion of m_3 with respect to

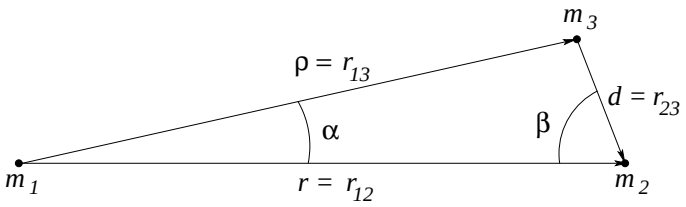

Figure 7: Sphere of influence.

m_1, taking into account the effect of m_2, as

$$\frac{d^2\boldsymbol{\rho}}{dt^2} = -G(m_1+m_3)\frac{\boldsymbol{\rho}}{\rho^3} - Gm_2\left(\frac{\mathbf{r}}{r^3}-\frac{\mathbf{d}}{d^3}\right) = \mathbf{F}_1^k + \mathbf{F}_1^p,$$

Similarly, the equation of motion of m_3 with respect to m_2, taking into account m_1, can be written as

$$\frac{d^2\mathbf{d}}{dt^2} = -G(m_2+m_3)\frac{\mathbf{d}}{d^3} - Gm_1\left(\frac{\mathbf{r}}{r^3}-\frac{\boldsymbol{\rho}}{\rho^3}\right) = \mathbf{F}_2^k + \mathbf{F}_2^p.$$

In both equations, the superscript k denotes the Keplerian term and p the disturbing one. The quotients between the modulus of the Keplerian and the

disturbing components of the acceleration are

$$\begin{aligned}\frac{F_1^p}{F_1^k} &= \frac{m_2\left[\left(\frac{\mathbf{r}}{r^3}-\frac{\mathbf{d}}{d^3}\right)\cdot\left(\frac{\mathbf{r}}{r^3}-\frac{\mathbf{d}}{d^3}\right)\right]^{1/2}}{\frac{m_1+m_3}{\rho^2}},\\ \frac{F_2^p}{F_2^k} &= \frac{m_1\left[\left(\frac{\mathbf{r}}{r^3}-\frac{\boldsymbol{\rho}}{\rho^3}\right)\cdot\left(\frac{\mathbf{r}}{r^3}-\frac{\boldsymbol{\rho}}{\rho^3}\right)\right]^{1/2}}{\frac{m_2+m_3}{d^2}}.\end{aligned} \tag{23}$$

If α is the angle between $\mathbf{r}$ and $\boldsymbol{\rho}$ and β the angle between $\mathbf{r}$ and $\mathbf{d}$ (see Figure 4), r can be expressed as

$$r = \rho\cos\alpha + d\cos\beta,$$

and

$$\cos\alpha = \frac{r}{\rho} - \frac{d}{\rho}\cos\beta.$$

Using this equality in (23), we obtain

$$\begin{aligned}\frac{F_1^p}{F_1^k} &= \frac{m_2}{m_1+m_3}\frac{\rho^2}{d^2}\left[1-2\,\frac{d^2}{r^2}\cos\beta+\frac{d^4}{r^4}\right]^{1/2},\\ \frac{F_2^p}{F_2^k} &= \frac{m_1}{m_2+m_3}\frac{d^2}{\rho^2}\left[1-2\,\frac{\rho}{r}\left(1-\frac{d}{r}\cos\beta\right)+\frac{\rho^4}{r^4}\right]^{1/2}.\end{aligned} \tag{24}$$

In order to determine the sphere of influence, we equate both expressions, obtaining

$$\left(\frac{d}{\rho}\right)^4 = \frac{m_2(m_2+m_3)}{m_1(m_1+m_3)}\left[\frac{1-2\,(d/r)^2\cos\beta+(d/r)^4}{1-2\,(\rho/r)\,(1-(d/r)\cos\beta)+(\rho/r)^4}\right]^{1/2} \tag{25}$$

Let us suppose that the mass of one primary is much greater than the other ($m_1 >> m_2$), and at the same time m_3 is much smaller than m_1 and m_2. In this situation, if the third body is on the sphere of influence of m_2, then $d >> r$. In fact, we would like to know of which order is the quotient d/r, so we will expand the right side of (25) in powers of d/r. First, we rewrite (25) as

$$\left(\frac{d}{r}\right)^4 = \frac{m_2(m_2+m_3)}{m_1(m_1+m_3)}\left(\frac{\rho}{r}\right)^4\left[\frac{1-2\,(d/r)^2\cos\beta+(d/r)^4}{1-2\,(\rho/r)\,(1-(d/r)\cos\beta)+(\rho/r)^4}\right]^{1/2} \tag{26}$$

Then, using the relation

$$\frac{\rho^2}{r^2} = 1+\frac{d^2}{r^2}-2\frac{d}{r}\cos\beta \tag{27}$$

(see Figure 4), we can expand the denominator of (26) in powers of (d/r), obtaining

$$\left[1-2\,\frac{\rho}{r}\left(1-d\frac{d}{r}\cos\beta\right)+\left(\frac{\rho}{r}\right)^4\right]^{1/2} = \left(\frac{d}{r}\right)\left(1+3\cos^2\beta-4\cos\beta\,\frac{d}{r}+O\left((d/r)^2\right)\right).$$

Substituting this expression and expanding the numerator in (26) and using (27), we get

$$\left(\frac{d}{r}\right)^5 = \frac{m_2(m_2+m_3)}{m_1(m_1+m_3)}\left[\frac{1}{\sqrt{1+3\cos^2\beta}} - 2\frac{\cos\beta(1+6\cos^2\beta)}{(1+3\cos^2\beta)^{3/2}}\,\frac{d}{r} + O((d/r)^2)\right],$$

and, therefore,

$$\frac{d}{r} = \left(\frac{m_2(m_2+m_3)}{m_1(m_1+m_3)}\right)^{1/5}\left(\frac{1}{(1+3\cos^2\beta)^{1/10}} + O(d/r)\right). \tag{28}$$

Finally, if we neglect the terms of order d/r on the right side, m_3 in front of m_1 and m_2 and use the fact that

$$1 < (1+3\nu^2)^{-1/10} < 1.15,$$

we get, approximately,

$$\frac{d}{r} \approx \left(\frac{m_2}{m_1}\right)^{2/5}.$$

The last expression defines a sphere around m_2 such that on its surface the quotient between the disturbing acceleration and the acceleration due to the primary are equal for both descriptions of the motion. Inside this sphere, called sphere of influence of m_2 with respect to m_3, we will consider the motion of m_3 taking m_2 as a origin of coordinates, while in the exterior of the sphere will be better to take m_1 as the origin.

Planet	R_{sph} (AU)	m_2/m_1	d (km)
Mercury	0.387099	0.000000164	112,000
Venus	0.723322	0.00000245	616,000
Earth	1.000000	0.00000304	929,000
Mars	1.523691	0.000000324	578,000
Jupiter	5.202803	0.000954786	48,200,000
Saturn	9.538843	0.000285584	54,500,000
Uranus	19.181951	0.000043727	51,900,000
Neptune	30.057779	0.000051776	86,800,000
Pluto	39.481687	0.0000000074	3,300,000

Table 2: Radius of the spheres of influence of planets

Next we will see a different approach to obtain the same equalities. As we have already seen, the terms $\mathbf{F}_1^k$ and $\mathbf{F}_1^p$ of the motion of m_3 under the influence of m_1 and considering m_2 as a perturbation can be written as

$$\mathbf{F}_1^k = -\frac{G(m_1+m_3)}{\rho^2}\,\mathbf{i}_{\boldsymbol{\rho}}, \quad \mathbf{F}_1^p = -\frac{Gm_2}{d^2}\left(\frac{d^2}{r^2}\,\mathbf{i}_{\mathbf{r}} - \mathbf{i}_{\mathbf{d}}\right),$$

where $\mathbf{i}_{\mathbf{r}}$, $\mathbf{i}_{\boldsymbol{\rho}}$, $\mathbf{i}_{\mathbf{d}}$ are unitary vectors in the directions of $\mathbf{r}$, $\boldsymbol{\rho}$ and $\mathbf{d}$, respectively. For the motion of m_3 considering m_2 as the principal body and m_1 the perturbing one, we use (13) to obtain

$$\mathbf{F}_2^k = -\frac{G(m_2+m_3)}{d^2}\,\mathbf{i}_{\mathbf{d}},\ \mathbf{F}_2^p = -\frac{Gm_1}{r^2}\sum_{k=1}^{\infty}\left(\frac{d}{r}\right)^k\left(P'_{k+1}(\cos\beta)\mathbf{i}_{\mathbf{r}} - P'_k(\cos\beta)\mathbf{i}_{\mathbf{d}}\right),$$

where $P_n(z)$ are the Legendre's polynomials. If we compute the quotients of the components of the accelerations

$$\frac{F_1^p}{F_1^k} = \frac{m_2}{m_1+m_3}\left(\frac{r}{d}\right)^2\left(\frac{\rho^2}{r^2}\right)\left[1-2\frac{d^2}{r^2}\cos\beta+\frac{d^4}{r^4}\right]^{1/2}$$

$$\frac{F_2^p}{F_2^k} = \frac{m_1}{m_2+m_3}\left(\frac{d}{r}\right)^3\sqrt{1+3\cos^2\beta}\left[1+\frac{6\cos^3\beta}{1+3\cos^2\beta}\left(\frac{d}{r}\right)+O\left(\frac{d}{r}\right)^2\right].$$

Equating these quantities, using (27) and that d/r is small, we get again the equation (28).

3.3 Hill's spheres

Together with the above two mentioned types of spheres, another type, namely, the Hill sphere, can also be distinguished. This concept appeared in connection with the restricted three body problem. It was shown by Hill that, at given values of the ratios of the masses of the two primaries m_1/m_2 and there is a definite zone (sphere) with radius R_H around m_2 (or m_1) within which the third body of small mass can stay for an infinitely time, initially with a closed orbit around the given body m_2 (or m_1). The radius of Hill's sphere R_H cannot be represented by a simple formula depending on the configuration of the masses. However, the computations lead to an important conclusion: the radius of Hill's sphere exceeds the radii of both spheres for any values of m_1 and m_2. Thus, e.g. in the case of the Moon Hill's sphere lies at $R_H = 700\ 000\ km$ from the Earth, whereas the distance between the Moon and the Earth varies between the limits 364 000 km and 402 000 km, being 384 000 km on average. Hence, the Moon lies deeply within Hill's sphere surrounding the Earth, and cannot leave this sphere.

The Jacobian integral of the RTBP, equation (18), can be used to obtain the velocity $V = \dot{x}^2+\dot{y}^2+\dot{z}^2$ of the third body at an arbitrary position. Therefore, for various values of C_J one can have different values of V at the same position of the small particle. As a matter of fact, equation (18) is nothing other than the equation of a surface on which the small body has a fixed velocity. In the case when $V = 0$ this equation becomes

$$x^2+y^2+\frac{2(1-\mu)}{(x-\mu)^2+y^2+z^2)^{1/2}}+\frac{2\mu}{(x-\mu+1)^2+y^2+z^2)^{1/2}} = C_J, \quad (29)$$

and gives the geometrical location of points at which the velocity of the infinitesimal body is zero. Obviously, on one side of this surface the velocity will be real and on the other complex. Though, when the velocity is real, we can say nothing about the orbit, at least we can be sure that, in that region, motions are possible.

The form of the family of zero velocity surfaces defined by equation (29) and corresponding to different values of C_J and μ should be rather complicated. To reveal the geometry of these surfaces, we can study their intersections with the coordinate planes. The forms of these intersections should reveal the structure of the surfaces.

If we set $z = 0$ in (29) we obtain

$$(x^2 + y^2) + \frac{2(1-\mu)}{(x-\mu)^2 + y^2)^{1/2}} + \frac{2\mu}{(x-\mu+1)^2 + y^2)^{1/2}} = C_J. \qquad (30)$$

We consider two limit cases:

1. *The motion takes place far from the primaries.*

   In this case x and y will be large and the second and third terms in (30) small, so the equation can be written in the form

   $$x^2 + y^2 = C_J - \epsilon(x, y), \qquad (31)$$

   where $\epsilon(x, y)$ is a small quantity. This equation defines a curve rather close to the circle of radius $(C_J - \epsilon(x, y))^{1/2}$. At large values of the Jacobi constant C_J, the curves tend to the circle of radius $\sqrt{C_J}$. With the decrease of C_J, the curves will be ovals within the mentioned circles and on decreasing the Jacobi constant the ovals contract.

2. *The motion takes place close to the primaries.*

   In this case x and y will be small and the first term of (30) is small compared with the second and third terms, so that we have

   $$\frac{2(1-\mu)}{(x-\mu)^2 + y^2)^{1/2}} + \frac{2\mu}{(x-\mu+1)^2 + y^2)^{1/2}} = C_J - \epsilon(x, y), \qquad (32)$$

   which is the equation of the equipotential curves for two gravitating centres. For large values of C_J the zero velocity curves are the two relatively lesser circles, which are slightly deformed. On increasing C_J the small ovals increase simultaneously deforming more and more.

In Fig. 8, the shape of the zero velocity curves for different values of the Jacobi constant are displayed. For large values of the Jacobi Constant the regions where the motion is possible are not connected, while for $C_\mathrm{J} < 3$ the surfaces do not intersect the plane $z = 0$ and planar motion is possible everywhere.

The equilibrium points of the RTBP play an important role in the shape of the zero velocity surfaces. The equilibrium points (also called Lagrangian points) are the solutions of the equations

$$\frac{\partial \Omega}{\partial x} = 0, \qquad \frac{\partial \Omega}{\partial y} = 0, \qquad \frac{\partial \Omega}{\partial z} = 0,$$

where $\Omega(x, y, z)$ is the function involved in the equations of motion (17). If the third particle is place in an equilibrium point with zero velocity, its acceleration will be zero as well, so it will stay there. There are five equilibrium points, all of them in the $z = 0$ plane, usually labelled L_1, L_2, L_3, L_4 and L_5. The first three points, also called collinear points, are on the horizontal synodical axis, while the last two, called triangular points, form equilateral triangles with the primaries. The collinear equilibrium points are situated at $(x_i, 0, 0)$, for $i = 1, 2, 3$, and it can be shown that

$$\begin{aligned} x_1 &= -1 - \left(\frac{\mu}{3}\right)^{1/3} - \frac{1}{3}\left(\frac{\mu}{3}\right)^{2/3} + \frac{28}{9}\left(\frac{\mu}{3}\right) + O(\mu^{4/3}), \\ x_2 &= -1 + \left(\frac{\mu}{3}\right)^{1/3} - \frac{1}{3}\left(\frac{\mu}{3}\right)^{2/3} + \frac{26}{9}\left(\frac{\mu}{3}\right) + O(\mu^{4/3}), \\ x_3 &= 1 + \frac{5}{12}\,\mu + O(\mu^3) \end{aligned} \qquad (33)$$

(see, for instance, [11]).

The shape of the zero velocity surfaces depends on the value of the Jacobi constant. There exists three critical values of the Jacobi constant for which the shape of the zero velocity surfaces change, which are the values of C_J at the collinear equilibrium points L_i, $i = 1, 2, 3$. Using the expressions (33) and (18), the values of the Jacobi constant at the equilibrium points are

$$\begin{aligned} C_{\mathrm{J}_1} &= 3 + 9\left(\frac{\mu}{3}\right)^{2/3} - 11\left(\frac{\mu}{3}\right) + O(\mu^{4/3}), \\ C_{\mathrm{J}_2} &= 3 + 9\left(\frac{\mu}{3}\right)^{2/3} - 7\left(\frac{\mu}{3}\right) + O(\mu^{4/3}), \\ C_{\mathrm{J}_3} &= 3 + 2\mu - \frac{49}{48}\,\mu^2 + O(\mu^3). \end{aligned}$$

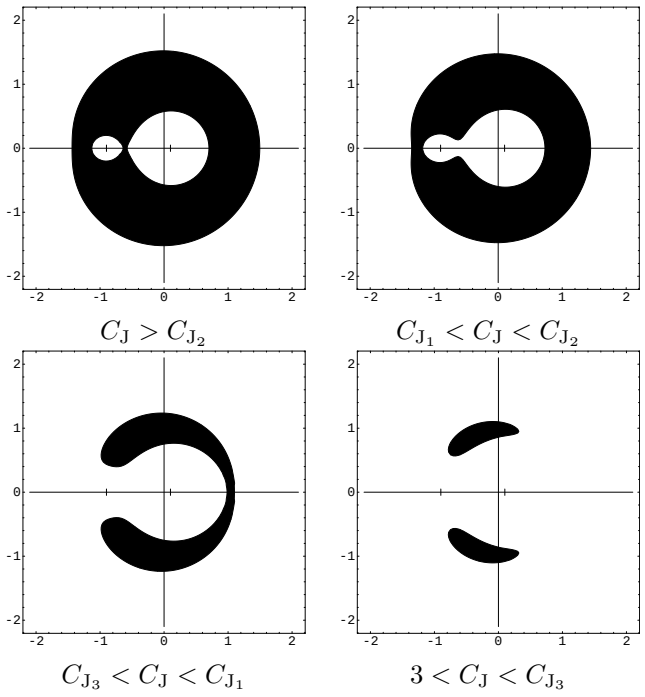

Figure 8: Zero velocity curves (the intersection of the zero velocity surfaces with the $z = 0$ plane) for $\mu > 0$. The motion is forbidden in the filled areas. The tick marks on the horizontal axis show the position of the primaries.

In Fig. 9, the shape of the zero velocity surfaces for the same range of values of the Jacobi constant are shown. As it can be seen, for $C_J < 3$, they do not intersect the plane $z = 0$.

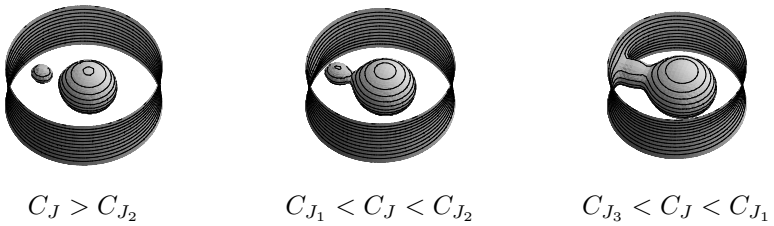

$C_J > C_{J_2}$ $C_{J_1} < C_J < C_{J_2}$ $C_{J_3} < C_J < C_{J_1}$

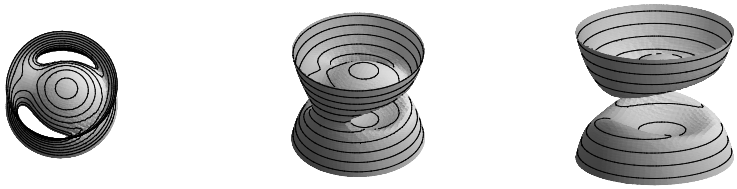

$C_{\mathrm{J}_3} < C_{\mathrm{J}} < C_{\mathrm{J}_1}$ $3 < C_{\mathrm{J}} < C_{\mathrm{J}_3}$

Figure 9: Zero velocity surfaces for $\mu > 0$.

4 Patched conics

The patched conics method allows the design of missions in which a spacecraft visits several bodies, such as planets or natural satellites, in the solar system. In a first approximation the mission analysis is done considering the trajectory of the spacecraft as a sequence of Keplerian orbits.

When approaching a mission by a sequence of two body problems, we can use conics for the different phases. For instance, for a Earth-Mars mission, the spacecraft starts its motion inside the gravisphere of the Earth and leaves this sphere following an hyperbolic trajectory with respect to the Earth. Once is out the sphere of influence of the Earth, the spacecraft follows an elliptic orbit with respect to the Sun until its close enough to Mars so us to be inside its sphere of influence. Once inside this sphere, its orbit with respect to Mars is hyperbolic.

When in the vicinity of a planet, a vehicle in a solar orbit experiences velocity perturbations. The velocity changes depend on the relative velocity between the vehicle and the planet and the distance separating the two at the point of closest approach. If only the gravitational field of the planet affected the motion of the spacecraft, the vehicle would make its approach along a hyperbolic path. Actually, the period time for which the planet's gravitation is significant is small when compared with the total time of the mission. Furthermore, during this time, the distance between the planet and the spacecraft is small when compared with its distance from the Sun. As a consequence, for the brief period of contact, solar gravity effects both the planet and the vehicle in essentially the same way. Therefore, in the discussion of planetary approach, solar gravity may be ignored with the assurance that its effects would not alter the results significantly.

4.1 Passage near a planet

We can view the effect of a planetary contact as an impulsive change in the velocity. At a sufficiently great distance, the motion of the space vehicle with respect to a target planet is essentially along the asymptotes of the approach/departure hyperbola and the velocity change corresponds to a rotation of its velocity vector with respect to the planet.

Let $\mathbf{R}(t)$, $\mathbf{V}(t)$ be the heliocentric position and velocity of the spacecraft at the epoch t, and $\mathbf{r}(t)$, $\mathbf{v}(t)$ the corresponding values with respect to a certain planet. This is, if $\mathbf{R}^{pl}(t)$ and $\mathbf{V}^{pl}(t)$ are the heliocentric position and velocity of the planet at the epoch t, then

$$\begin{array}{rcl} \mathbf{r}(t) & = & \mathbf{R}(t) - \mathbf{R}^{pl}(t), \\ \mathbf{v}(t) & = & \mathbf{V}(t) - \mathbf{V}^{pl}(t). \end{array} \tag{34}$$

After the hyperbolic fly-by of the planet, the gravity assist manoeuvre results in a rotation of the spacecraft velocity vector $\mathbf{v}$ around the angular momentum axis $\mathbf{c} = (c_1, c_2, c_3)^T = \mathbf{r}(t) \wedge \mathbf{v}(t)$. The rotation matrix of angle α around $\mathbf{c}$ is given by

$$R(\alpha) = \begin{pmatrix} \cos\alpha & \frac{c_3}{c}\sin\alpha & -\frac{c_2}{c}\sin\alpha \\ -\frac{c_3}{c}\sin\alpha & \cos\alpha & \frac{c_1}{c}\sin\alpha \\ \frac{c_2}{c}\sin\alpha & -\frac{c_1}{c}\sin\alpha & \cos\alpha \end{pmatrix}. \tag{35}$$

We define ν, as is shown in Figure 10, as the angle between the asymptote and the conjugate axis of the hyperbolic path of approach. In this way, if $\mathbf{r}(t_1)$, $\mathbf{v}(t_1)$, $\mathbf{r}(t_2)$ and $\mathbf{v}(t_2)$ are the input and output positions and velocities of the spacecraft at the sphere of influence of a certain planet ($|\mathbf{r}(t_1)| = |\mathbf{r}(t_2)| = R_{sph}$), we have that in the planetocentric reference system

$$\mathbf{r}(t_2) = R(\pi - 2\nu + 2\gamma)\mathbf{r}(t_1), \qquad \mathbf{v}(t_2) = R(2\nu)\mathbf{v}(t_1),$$

where, according to Figure 10,

$$\sin\gamma \;=\; \frac{d_\infty}{R_{sph}}, \qquad d_\infty \;=\; \frac{\mathbf{r}(t_1) \wedge \mathbf{v}(t_1)}{v(t_1)}. \tag{36}$$

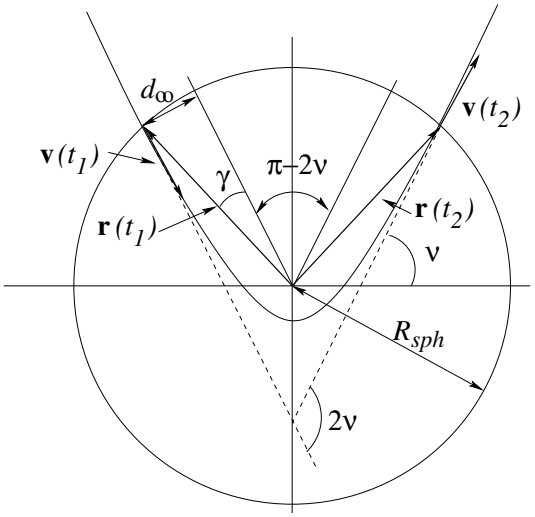

Figure 10: Gravity assist rotation of the spacecraft velocity in the sphere of influence of a planet ($|\mathbf{r}(t_1)| = |\mathbf{r}(t_2)| = R_{sph}$).

In order to compute the angle ν, recall that the modulus of the velocity for the hyperbolic motion is given by

$$v^2 = \mu\left(\frac{2}{r} + \frac{1}{a}\right),$$

where a is the eccentricity and semi-major axis of the hyperbolic orbit. So, since R_{sph} is large

$$v_\infty^2 = \frac{\mu}{a}, \tag{37}$$

from which we can compute a if the values of the gravitational constant of the planet $\mu = Gm_{pl}$ and $v_\infty = v(t_1)$ are known.

If e is the eccentricity of the hyperbola and r_p the distance from the vertex (point of closest approach of the spacecraft to the planet) to the focus, we have that

$$r_p = a(e-1) = \frac{\mu}{v_\infty^2}(e-1).$$

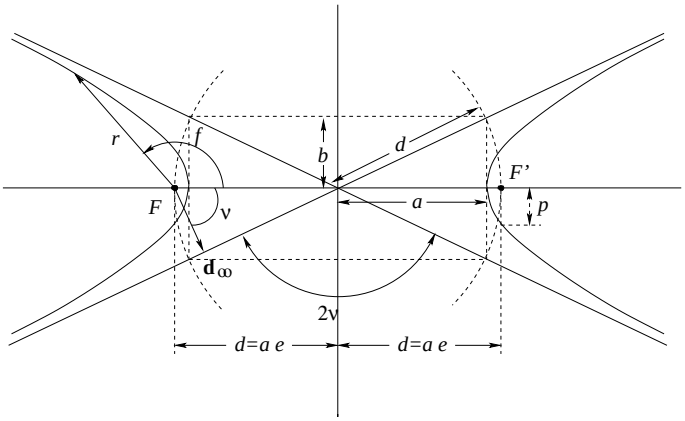

Figure 11: Hyperbolic motion.

Taking into account that (see Fig. 11)

$$e = \frac{d}{a} = \frac{1}{\sin \nu}, \tag{38}$$

we can compute ν as

$$\sin \nu = \frac{1}{1 + r_p v_\infty^2 / \mu}, \tag{39}$$

from which we get that the eccentricity of the hyperbolic orbit is

$$e = 1 + r_p \frac{v_\infty^2}{\mu}. \tag{40}$$

For some applications, it can be useful to compute ν as a function of the distance d_∞, where $\mathbf{d}_\infty$ is a vector from the focus of the hyperbola and perpendicular to one asymptote of the hyperbola. Since, according to Figure 11 and equation (38)

$$d_\infty = a\, e\, \cos \nu = \frac{a}{\tan \nu}, \tag{41}$$

we get, using (37), that

$$\tan \nu = \frac{\mu}{d_\infty v_\infty^2}. \tag{42}$$

Also, by eliminating ν between (39), (41) and (42) we get the value of the distance d_∞ as a function of r_p

$$d_\infty = r_p \sqrt{1 + \frac{2\mu}{r_p v_\infty^2}}. \tag{43}$$

The duration of the spacecraft motion inside the sphere of influence of the planet, Δt, will be computed in the next section.

Summarising: If t_1 and $t_2 = t_1 + \Delta t$ are, respectively, the epochs at which the spacecraft enters and exists the sphere of influence; $\mathbf{R}(t)$, $\mathbf{V}(t)$ denote the

heliocentric position and velocity of the spacecraft at the epoch t, and $\mathbf{R}^{pl}(t)$ and $\mathbf{V}^{pl}(t)$ are the heliocentric position and velocity of the planet, then

$$\begin{array}{rcl} \mathbf{R}(t_2) & = & \mathbf{R}^{pl}(t_2) + R(\pi - 2\nu + 2\gamma)\mathbf{r}(t_1), \\ \mathbf{V}(t_2) & = & \mathbf{V}^{pl}(t_2) + R(\pi - 2\nu)\mathbf{v}(t_1). \end{array} \tag{44}$$

where

$$\mathbf{r}(t_1) \; = \; \mathbf{R}(t_1) - \mathbf{R}^{pl}(t_1), \qquad \mathbf{v}(t_1) \; = \; \mathbf{V}(t_1) - \mathbf{V}^{pl}(t_1),$$

and the rotation matrix R as well as the angles ν and γ are given by (35), (39) and (36), respectively.

4.2 Hyperbolic motion inside the sphere of influence

In general it can be assumed that the time spent in the passage close the planet, Δt, is small when compared with the total time of the mission, so it can be considered that the spacecraft performs an instantaneous change of the in-bound velocity to the out-bound velocity. Nevertheless, this assumption cannot be always done. For example, in circumlunar trajectories the time spent within the sphere of influence is significant when compared with the total time.

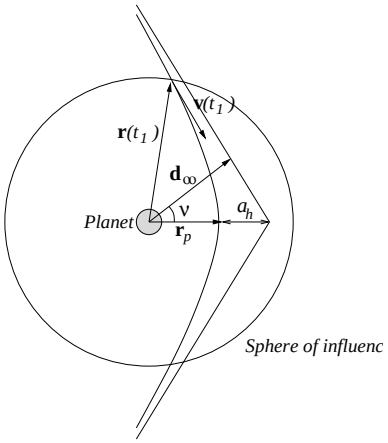

Figure 12: Hyperbolic motion inside the sphere of influence of a planet.

Let us suppose that the spacecraft follows an elliptic trajectory until it reaches the sphere of influence of a planet. Let $\mathbf{r}(t_1)$ and $\mathbf{v}(t_1)$ be the incoming position and velocity (at the sphere of influence) with respect to the planet (see Fig. 12). These vectors determine the hyperbolic trajectory with the planet at the focus. We want to calculate the elements of the hyperbolic orbit, a_h and e_h, as well as the minimum distance to the planet r_p and the time of flight from the incoming to the outgoing point.

First, using the energy of the orbit, the semi-major axis a_h of the hyperbola is

$$a_h = \left(\frac{v(t_1)^2}{\mu_p} - \frac{2}{r(t_1)} \right)^{-1}, \tag{45}$$

where μ_p is the gravitational constant of the planet.

Using that the radius vector magnitude for a hyperbolic orbit can be expressed in terms of the hyperbolic eccentric anomaly F as

$$r = a_h(e_h \cosh F - 1),$$

the minimum distance to the planet is $r_p = a_h(e_h - 1)$ or, using (38)

$$r_p = a_h(\csc \nu - 1). \tag{46}$$

Finally, to calculate the time spent inside the sphere of influence, Δt, we use the Kepler's equation

$$n(t - T_p) = e_h \sinh F - F, \tag{47}$$

where $n^2 a_h^3 = \mu_p$ and T_p is the epoch at pericenter. Using the symmetry of the orbit, $t = T_p - \Delta t/2$ at the incoming point, so

$$\Delta t = -2\sqrt{\frac{a_h^3}{\mu_p}}\,(e_h \sinh F - F), \tag{48}$$

where F is obtained from $r(t_1) = a_h(e_h \cosh F - 1)$, so

$$\cosh F = \left(\frac{r(t_1)}{a_h} - 1\right)\frac{1}{e_h}.$$

4.3 A simplified model for the gravity assist

Relations (44) represent the dynamic model of the spacecraft perturbation manoeuvre taking into account the size of the gravisphere of the planet as well as its motion during the perturbation manoeuvre.

The comparison of the size of the attracting planet with the radius of its orbit allows the following significant assumption: *the sphere of influence of the attracting body can be considered infinitesimal as compared to the radius of its orbit and infinitely large relative to the size of the attracting body itself.*

In accordance with the above assumption, the gravity assist manoeuvre can be approximated by an instantaneous rotation of the arrival velocity vector (at infinity) $\mathbf{v}_\infty$ with respect to the centre of the fly-by body and can be represented in accordance with the vector diagram of the velocities of the spacecraft and the attracting body (see Figure 13). In this case, the duration of the gravity assist manoeuvre is $\Delta t = t_2 - t_1 = 0$.

In the Figure 13, $\mathbf{V}(t_1)$ is the incoming inertial velocity of the spacecraft towards the fly-by body; $\mathbf{V}(t_2)$ is its outgoing velocity after the gravity assist manoeuvre; $\mathbf{v}_{\infty 1}$, $\mathbf{v}_{\infty 2}$ are respectively the initial and final hyperbolic velocities excesses of the spacecraft (directed along the incoming and outgoing asymptotes of the fly-by hyperbola) and

$$\|\mathbf{v}_{\infty 1}\| = \|\mathbf{v}_{\infty 2}\| = v_\infty.$$

The efficiency of the gravity assist manoeuvre depends on the rotation of the velocity vector $\mathbf{v}_{\infty 1}$ by the angle 2ν that is determined by the gravitational constant of the fly-by body and the fly-by altitude relative to its surface. According to (39), for a fixed value of v_∞, the angle ν increases as the distance r_{min} decreases, so we can write that the maximum value of ν is

$$\nu_{max} = \arcsin\left(\frac{\mu}{\mu + r_{min} v_\infty^2}\right), \tag{49}$$

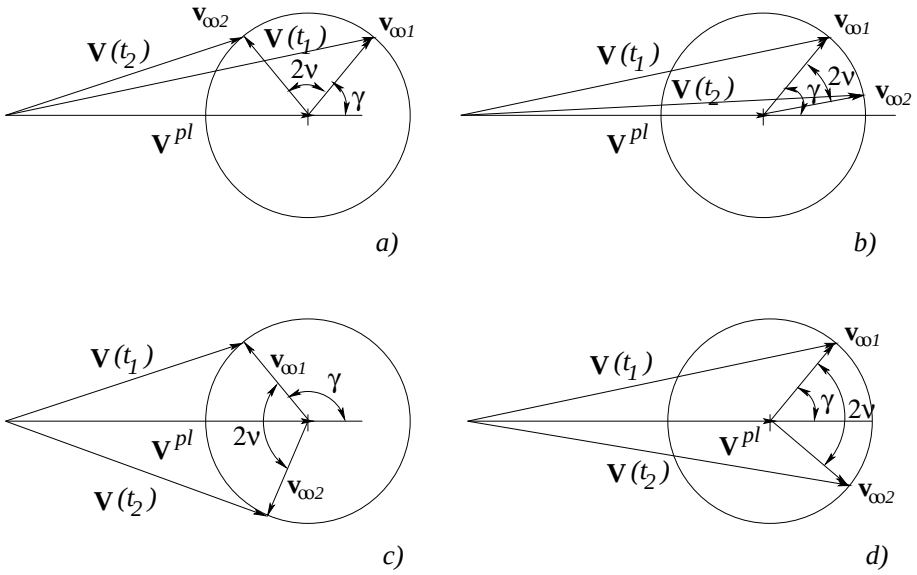

Figure 13: Vector diagram of the gravity assist manoeuvre.

where r_{min} is the minimum admissible distance to the centre of the planet at the pericenter of the fly-by hyperbola (which must be equal or greater than the radius of the planet plus the height of its atmosphere).

As can be seen from the diagrams in Figure 13, the rotation of $\mathbf{v}_{\infty 1}$ may produce either an increase $\|\mathbf{V}(t_2)\| > \|\mathbf{V}(t_1)\|$ (acceleration perturbation manoeuvre) or a decrease $\|\mathbf{V}(t_2)\| < \|\mathbf{V}(t_1)\|$ (deceleration perturbation manoeuvre) in the spacecraft outgoing velocity. In the case where the spacecraft passes through the point of intersection of the orbits before the fly-by body, angles ν and γ add up ($\mathbf{v}_{\infty 1}$ rotates counter-clockwise) and the spacecraft velocity decreases (case a). If the spacecraft flies behind the fly-by body, the angles ν and γ are subtracted ($\mathbf{v}_{\infty 1}$ rotates clockwise) and the spacecraft velocity increases (case b).

¿From Figure 13 it can be seen that the minimum value of the outgoing velocity $\mathbf{V}(t_2)$ can be attained when $2\nu + \gamma = \pi$ and the maximum value can be reached when the angles are subtracted $\gamma - 2\nu = 0$. In both cases, the spacecraft post-perturbation velocity will be collinear to the planet's velocity vector

$$\mathbf{V}_{min}(t_2) = \mathbf{V}^{pl}(t_2) - \mathbf{v}_{\infty 1}, \qquad \mathbf{V}_{max}(t_2) = \mathbf{V}^{pl}(t_2) + \mathbf{v}_{\infty 1}.$$

It should be noted that there are cases for which the change in the spacecraft velocity (increase or decrease) is the same whatever the direction of rotation of $\mathbf{v}_{\infty 1}$. This takes place when the spacecraft incoming velocity vector is collinear (or almost collinear) to the velocity vector of the fly-by body. If $V(t_1) < V^{pl}$, then only acceleration perturbation manoeuvres can occur. If $V(t_1) > V^{pl}$ a deceleration manoeuvre takes place. This is illustrated in Figure 13 (c and d respectively).

When analysing such cases, one should take into account that, depending on altitude of the spacecraft fly-by relative to the planetary surface, the angle

Mercury	3.01	Mars	3.55	Uranus	15.18
Venus	7.33	Jupiter	42.73	Neptune	16.75
Earth	7.91	Saturn	25.62	Pluto	1.10

Table 3: Maximum possible variations of the spacecraft velocity due to planetary fly-bys (in km/s).

of vector rotation $\mathbf{v}_{\infty 1}$ can vary from 0 to $2\nu_{max}$ (according to Eq. 49).

4.3.1 Maximum velocity variation

As it has been shown, a fly-by manoeuvre produces changes in both the modulus and direction of the spacecraft velocity. One of the criteria in assessing such manoeuvres is the value of the maximum change in velocity that can be obtained in a fly-by of a given body in the solar system.

The spacecraft velocity change is equal to

$$\Delta\mathbf{V} = \mathbf{V}(t_2) - \mathbf{V}(t_1).$$

In accordance with Figure 13 and using (39), we can write

$$\Delta V = \|\Delta\mathbf{V}\| = 2v_\infty \sin\nu = \frac{2v_\infty\mu}{\mu + r_p v_\infty^2},$$

where μ is the gravitational constant of the fly-by body and r_p is the pericentral distance of the fly-by hyperbola.

The maximum change in the modulus of the velocity ΔV, for a given value of v_∞ in the fly-by of a given body (e.g. a planet), is attained when r_p is equal to the minimum admissible distance to the centre of the planet (r_{min}). It is clear that one can not choose r_p equal to the radius of the planet r^{pl}, since this manoeuvre is impossible to implement, but it is of certain interest in assessing the potentialities of the fly-by body.

One can also study the values of hyperbolic velocity excess v_∞ that provide maximum possible change in the module of the spacecraft velocity vector for any fly-by body. From the condition

$$\left.\frac{\partial\Delta V}{\partial v_\infty}\right|_{r_p = r^{pl}} = 0,$$

it can be established that ΔV_{max} is attained when

$$v_\infty = \left(\frac{\mu}{r^{pl}}\right)^{1/2},$$

this is, the hyperbolic velocity excess should be equal to the velocity of the planet (assumed to be in circular motion). Table 3 gives the values of ΔV_{max} for all nine planets of the solar system to show the perturbation potentialities of the planets

4.4 Effect of perturbation manoeuvres on the spacecraft orbital characteristics

When analysing interplanetary missions with planetary fly-bys, it is of interest to estimate the effect of perturbation manoeuvres on the flight trajectory parameters (orbital constants or elements of the post-perturbation orbit) which determine the further motion of the spacecraft. With this knowledge, a gravity assist manoeuvre at an attracting body can be used to implement a controlled change of the spacecraft characteristics.

Generally speaking, the elements of post-fly-by spacecraft orbit can be estimated directly using the relations (44) which give $\mathbf{R}(t_2)$ and $\mathbf{V}(t_2)$. Obviously, such an estimate can be made only based on numerical calculations taking into account all the factors affecting the motion of both the spacecraft and the fly-by planet.

The simplified model of the preceding section, in which the gravisphere of the fly-by body is assumed to have zero radius, makes it easier to assess the perturbation effect of a planet on the characteristics of spacecraft post-fly-by orbit. In this case, the perturbation effect on the trajectory is a rotation of the spacecraft planetocentric velocity by an angle 2ν within the plane of the spacecraft fly-by hyperbola, which is uniquely determined by the incoming and outgoing spacecraft velocity vectors at the fly-by body. This makes it possible to conduct analysis on a vector diagram of velocities (see Figure 14).

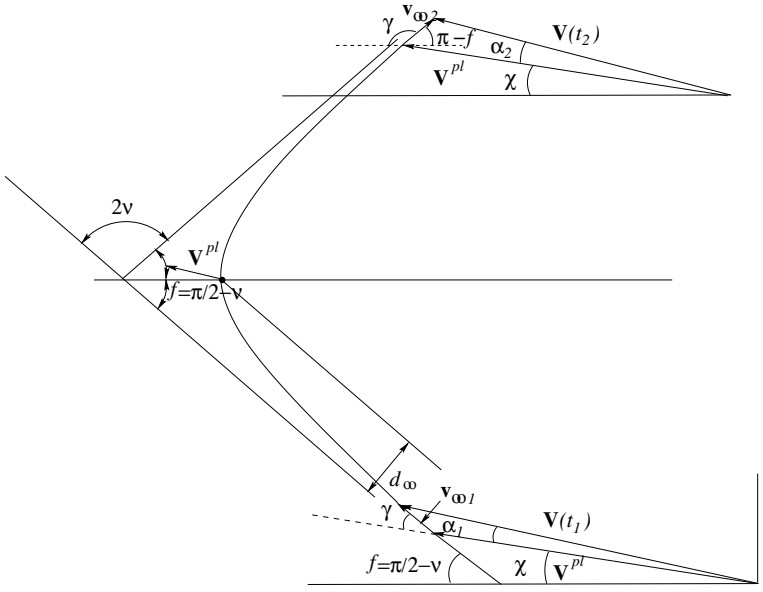

Figure 14: Schematic diagram of gravity assist manoeuvre.

Thus, the parameters of the post-fly-by orbit (both angular parameters and those determining the size and form of the spacecraft new orbit) will depend only on the parameters of the spacecraft hyperbolic velocity being formed in the gravitational field of the fly-by body. By varying the arrival angles and velocities, as well as the altitude at the fly-by body, the parameters of the post-

fly-by orbits can cover a relatively wide range.

4.4.1 Variations of the energy, angular momentum and line of apsides

The scheme of perturbation manoeuvre will be considered within the framework of the model described above. Suppose that a spacecraft and an attracting body with a gravitational constant μ_p move along coplanar orbits in the central gravitational field of a body (with a gravitational constant μ). Denote their locations and velocities at the moment of perturbation manoeuvre by $\mathbf{R}^{pl}$ and $\mathbf{V}^{pl}$ for the celestial body and by $\mathbf{R}(t_1)$ and $\mathbf{V}(t_1)$ for the spacecraft. After the gravity assist manoeuvre, $\mathbf{V}(t_1)$ transforms into $\mathbf{V}(t_2)$ (outgoing spacecraft velocity) as a result of an instantaneous rotation of the hyperbolic velocity excess $\mathbf{v}_{\infty 1}$ by an angle 2ν. In this case $\|\mathbf{v}_{\infty 1}\| = \|\mathbf{v}_{\infty 2}\| = v_\infty$. Projections of the spacecraft incoming and outgoing velocities onto the x and y axis (see Figure 14) can be written as

$$\begin{pmatrix} v_\infty \cos f + V^{pl} \cos\chi \\ v_\infty \sin f + V^{pl} \sin\chi \end{pmatrix}, \begin{pmatrix} v_\infty \cos(\pi - f) + V^{pl} \cos\chi \\ v_\infty \sin(\pi - f) + V^{pl} \sin\chi \end{pmatrix},$$

where $V^{pl} = \|\mathbf{V}^{pl}\|$, χ is the angle between the x axis (in the direction of the axis of the hyperbola) and $\mathbf{V}^{pl}$, f is the angle between the asymptote and the x-axis, which is related with ν by

$$f = \frac{\pi}{2} - \nu,$$

Since the rotation of the velocity vector in the fly-by point is assumed instantaneous, then $\mathbf{R}(t_1) = \mathbf{R}(t_2)$, and the change in the integral of the spacecraft energy resulting from the fly-by manoeuvre is determined only by the variation of the kinetic energy

$$\Delta h = V^2(t_2) - V^2(t_1) = -4 v_\infty V^{pl} \cos f \cos\chi.$$

Two cases can be considered:

1. A fly-by before the attracting body $\chi = f - \gamma$ (the perturbation manoeuvre reduces the spacecraft energy).
2. A fly-by behind the attracting body $\chi = f + \gamma$ (the perturbation manoeuvre increases the spacecraft energy).

We can write the change in the integral of the spacecraft orbital energy as

$$\Delta h = -4 v_\infty V^{pl} \cos f \cos(f \mp \gamma). \tag{50}$$

¿From the triangles of velocities we can determine the angle γ between the velocity vectors of the fly-by body $\mathbf{V}^{pl}$ and $\mathbf{v}_\infty$:

$$\sin\gamma = \frac{V(t_1)\sin\alpha_1}{v_\infty}, \qquad \cos\gamma = \frac{V(t_1)\cos\alpha_1 - V^{pl}}{v_\infty}.$$

Here α_1 is the angle between $\mathbf{V}^{pl}$ and $\mathbf{V}(t_1)$. Using equation (39) for the rotation angle 2ν, we write

$$\begin{aligned}
\cos f &= \sin\nu = \frac{1}{1+r_p v_\infty^2/\mu} = \frac{1}{1+mn^2},\\
\sin f &= \frac{n(m^2n^2+2m)^{1/2}}{1+mn^2},\\
v_\infty &= \left[V^2(t_1)+(V^{pl})^2-2V(t_1)V^{pl}\cos\alpha_1\right]^{1/2}.
\end{aligned}$$

Here, $m = r_p/r^{pl}$ is the relative pericentral distance of the hyperbola expressed in terms of radii of the fly-by body, $n = v_\infty/v_{cr}$ is the relative hyperbolic excess of the spacecraft velocity (in terms of local circular velocity at the surface of the fly-by body $v_{cr} = (\mu/r)^{1/2}$.

Returning to equation (50) and using the relationships obtained, we can write the expression for the spacecraft post-fly-by energy for any values of the initial energy h_1 and the spacecraft incoming angle α_1 as follows

$$h_2 = h_1 - 4V^{pl}(1+mn^2)^{-2}\left(V(t_1)\cos\alpha_1 - V^{pl} \pm V(t_1)\sin\alpha_1(2mn^2+m^2n^4)^{1/2}\right). \tag{51}$$

Here, the upper sign refers to the decrease and the lower sign to the increase of the spacecraft energy.

The change in the angular momentum of the orbit, as a result of the perturbation manoeuvre, in the coplanar model considered here is determined as

$$\Delta C = R\left[V(t_1)\cos\alpha_1 - V(t_2)\cos\alpha_2\right],$$

where $R = \|\mathbf{R}(t_1)\| = \|\mathbf{R}(t_1)\|$. Determining cosines of the spacecraft incoming and outgoing angles from velocity triangles

$$\cos\alpha_1 = \frac{V^2(t_1)+(V^{pl})^2-v_{\infty 1}^2}{2V(t_1)V^{pl}}, \qquad \cos\alpha_2 = \frac{V^2(t_2)+(V^{pl})^2-v_{\infty 2}^2}{2V(t_2)V^{pl}},$$

we get

$$\Delta C = R\frac{V^2(t_1)-V^2(t_2)}{2V^{pl}} = -R\frac{\Delta h}{2V^{pl}} = 2Rv_\infty\cos f\cos\chi. \tag{52}$$

The sum of the collinear vectors $\mathbf{C}(t_1)$ and $\Delta\mathbf{C}$ yields the post-fly angular momentum $\mathbf{C}(t_2)$.

Using equations (51) and (52) we write the final expression for the post-fly-by constant of areas of the spacecraft orbit for any values of the spacecraft initial velocity $\mathbf{V}(t_1)$ and in-going angle α_1 as follows

$$C(t_2) = C(t_1) + \frac{2R}{(1+mn^2)^2}\left(V(t_1)\cos\alpha_1 - V^{pl} \pm V(t_1)\sin\alpha_1(2mn^2+m^2n^4)^{1/2}\right). \tag{53}$$

Finally, we determine the perturbation change in the Laplace (eccentricity) vector controlling the location of the apsides of the spacecraft orbit in the plane of its orbital movement

$$\Delta\mathbf{e} = \mathbf{e}(t_2)-\mathbf{e}(t_1) = -\mathbf{C}(t_2)\wedge\mathbf{V}(t_2) - \frac{\mu\mathbf{R}(t_2)}{R(t_2)} + \mathbf{C}(t_1)\wedge\mathbf{V}(t_1) + \frac{\mu\mathbf{R}(t_1)}{R(t_1)}.$$

Since, as we have already said, $\mathbf{R}(t_1) = \mathbf{R}(t_2)$ we have that

$$\Delta\mathbf{e} = \mathbf{C}(t_1)\wedge\mathbf{V}(t_1) - \mathbf{C}(t_2)\wedge\mathbf{V}(t_2).$$

Therefore, the angle of rotation of apsides line δ of the orbit resulting from the perturbation manoeuvre is equal to the angle of rotation of the spacecraft velocity vector, and can be found as follows:

$$\cos\delta = \frac{V^2(t_1) + V^2(t_2) - \Delta V^2}{2V(t_1)V(t_2)}.$$

Using that

$$\Delta V = 2v_\infty \cos f = \frac{2v_\infty}{1 + mn^2},$$

we get

$$\cos\delta = \frac{(V^2(t_1) + V^2(t_2))(1 + mn^2) - 2v_\infty}{2V(t_1)V(t_2)}.$$

It is evident from (51) and (53) that with the use of the well known relationship we can obtain the value of the post-fly-by Laplace integral for any values of the spacecraft initial energy and incoming angles

$$\lambda(t_2) = (\mu^2 + h(t_2)C^2(t_2))^{1/2}.$$

Using the obtained values of constants h, $\mathbf{C}$ and $\mathbf{e}$ at $t = t_2$, it is easy to obtain the Keplerian elements of the post-fly-by orbit for the well-known relationships of celestial mechanics.

As can be seen from relationships (50) and (52), the conditions of maximum change in the constants of integrals of energy and areas are satisfied at the same value $v_\infty = \sqrt{\mu/r_p m}$ and $f = 60^o$. In this case, the values of the angle χ are

1. $\chi = 0$ in the case of decrease in Δh and increase in ΔC,
2. $\chi = \pi$ in the case of increase in Δh and decrease in ΔC.

The optimal angles $\alpha_{opt}(t_1)$ for approaching the attracting mass at a given value of the spacecraft orbital energy $h(t_1)$ can be selected based on the condition of maximising the increment of the energy constant

$$\Delta h_{max} = \max_{\alpha(t_1)} \Delta h(\mu, r, R, V(t_1), \alpha(t_1), m), \tag{54}$$

with $V(t_1) = ctant$ and $m = ctant$.

The computation of the optimal angles for the spacecraft to approach the fly-by body and to determine the maximum spacecraft energy change for incoming orbits bust be done numerically. Figures 15 and 16 represent the curves $\Delta h_{max}(h(t_1))$ which characterise the maximum spacecraft energy increase attainable from perturbation manoeuvres at each of the solar system planets. The corresponding optimal changes $\alpha_{opt}(h(t_1))$ of the spacecraft approaching the planet are shown in Figures 17 and 18 for m=1.

The given results show that Jupiter has the highest potentialities of all the planets ($\Delta h_{max} \approx 1100\ km^2/s^2$). Venus, Saturn and Earth display lesser potentialities ($\Delta h_{max} \approx 400$ to $500\ km^2/s^2$), and even lower potentialities are typical of Mercury, Mars, Uranus and Neptune ($\Delta h_{max} \approx 150$ to $250\ km^2/s^2$). It is worth mentioning that for the planets of the Jovian group, the values of Δh_{max} lie in the zone of high-energy incoming orbits (hyperbolic or parabolic) and their

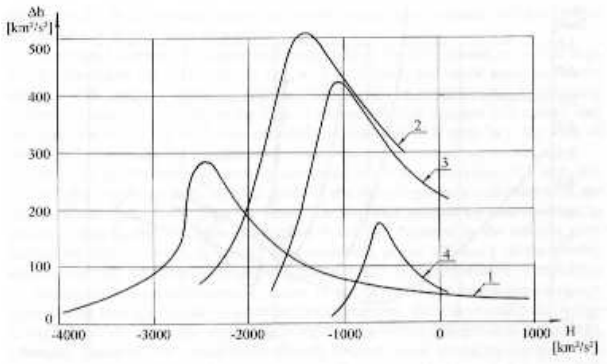

Figure 15: Maximum change in the spacecraft orbital energy constant at planets. 1 = Mercury, 2 = Venus, 3 = Earth, 4 = Mars.

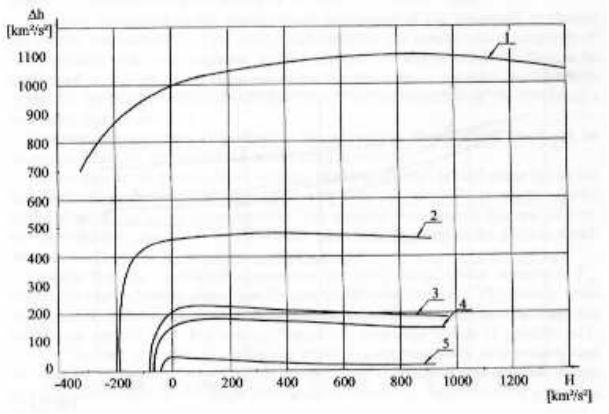

Figure 16: Maximum change in the spacecraft orbital energy constant at planets. 1 = Jupiter, 2 = Saturn, 3 = Uranus, 4 = Neptune, 5 = Pluto.

peaks are not distinct. For the planets of the Earth group, these maxima are more clearly defined, and are located in the zone of elliptic incoming orbits.

The optimal angles of the spacecraft approaching the fly-by planet are rather high for the planets of the Jovian group ($\alpha_{opt} \approx 1.5$ to 2.0 rad) and show small variations within a wide range of incoming energies. The planets of Earth's group have clearly defined minima (0.1–0.2 irad) in the zone of extreme change in spacecraft energy and increase drastically (up to 1 rad) especially in the case of a shift into the zone of orbits with low incoming energies.

The above results were obtained by numerical solution of equation (54) and refer to the fly-by where the pericentral altitude of the fly-by hyperbola coincides with the radius of the fly-by body. This obviously limiting case cannot be accomplished in practice (that is, the condition $m > 1$ must hold). An increase in the relative pericentral altitude m obviously results in a reduction in the efficiency of the gravity assist manoeuvre (in accordance with equation (51). An examination of the effect of changes in m on the maximum values of the

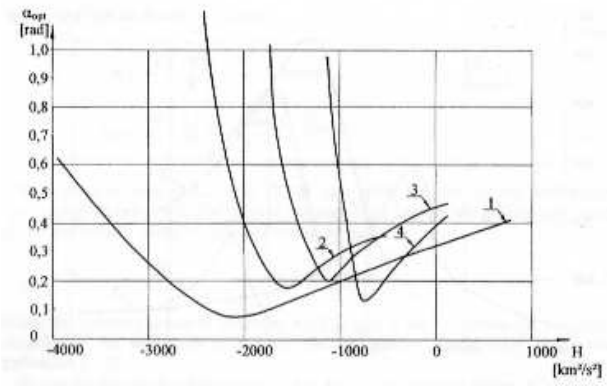

Figure 17: Optimal angle of approaching planets to perform a gravity assist manoeuvre. 1 = Mercury, 2 = Venus, 3 = Earth, 4 = Mars.

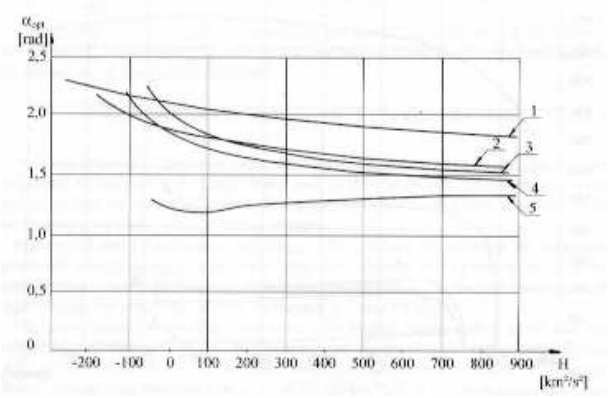

Figure 18: Optimal angle of approaching planets to perform a gravity assist manoeuvre. 1 = Jupiter, 2 = Saturn, 3 = Uranus, 4 = Neptune, 5 = Pluto.

perturbation increment in energy showed that throughout the range of incoming energies, there is virtually no change in the pattern curves (the growth in m results in a monotonic decrease in $\max \Delta h$, while the peaks of the curves move slightly toward lower incoming energies. The behaviour of the curves α_{opt} is similar. The optimal angles of the spacecraft approaching the fly-by body show insignificant variations (not more than $1^o - 2^o$) as the relative fly-by altitude m increases from 1 to 2. Thus, the values of α_{opt} show almost no dependence on deviations of m from its minimum value.

4.4.2 Variation of the semi-major axis

Assume that, before the close encounter, the spacecraft is moving in a Keplerian orbit of semi-major axis a_1, eccentricity e_1 and energy h_1, neglecting the influence of the planet. As always, we also assume that the planet fly-by performs an instantaneous change in velocity and it occurs at the periapsis (periapsis

vector $\mathbf{r}_p$ and phase angle η, see Fig. 19). After the fly-by, the spacecraft will be again on a Keplerian trajectory with respect to the Sun of semi-major axis a_2, eccentricity e_2 and energy h_2. We will also assume that the planet moves in a circular orbit, so that its orbital velocity $\mathbf{V}^{pl}$ is perpendicular to the Sun-planet radius $\mathbf{R}^{pl}$.

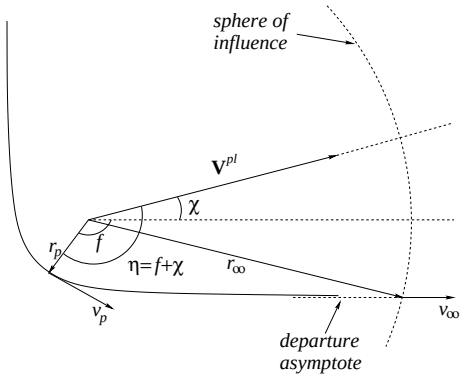

Figure 19: The phase angle η.

Using the expression of the energy, in terms of the semi-major axis of the spacecraft or in terms of its velocity and position with respect to the Sun, we can write

$$h_2 - h_1 = -\frac{\mu_S}{2}\left(\frac{1}{a_2} - \frac{1}{a_1}\right) = \frac{V^2(t_2) - V^2(t_1)}{2} - \mu_S \frac{R(t_1) - R(t_2)}{R(t_1)R(t_2)}, \qquad (55)$$

where $\mu_S = Gm_S$, being m_S the mass of the Sun. Assuming, as before, that $\mathbf{R}(t_1) = \mathbf{R}(t_2)$, we get

$$\frac{1}{a_2} - \frac{1}{a_1} = \frac{V_1^2 - V_2^2}{\mu_S}. \qquad (56)$$

Now, we want to express $V_1^2 - V_2^2$ in terms of $\mathbf{r}_p$ and the phase angle $\eta = f + \chi$. Obviously

$$V_2^2 - V_1^2 = (\mathbf{V}_2 + \mathbf{V}_1) \cdot (\mathbf{V}_2 - \mathbf{V}_1) = 2\mathbf{V}^{pl} \cdot (\mathbf{v}_2 - \mathbf{v}_1). \qquad (57)$$

Where we have used that $v_2^2 - v_1^2 = 0$, since the modulus of both the incoming and outgoing velocities is equal to v_∞. As the angle between $\mathbf{v}_1$ and $\mathbf{v}_2$ is 2ν (see Fig. 10), we have

$$\|\mathbf{v}_1 - \mathbf{v}_2\|^2 = v_1^2 + v_2^2 - 2v_1 v_2 \cos(2\nu) = 4v_\infty^2 \sin^2 \nu,$$

and using (39) and (40) we get that

$$\|\mathbf{v}_1 - \mathbf{v}_2\| = \frac{2v_\infty}{1 + r_p v_\infty^2/\mu_p} = \frac{2v_\infty}{e_p}, \qquad (58)$$

where $\mu_p = Gm_p$ and $e_p = 1 + r_p v_\infty^2/\mu_p$ is the eccentricity of the hyperbolic orbit. Due to the symmetry, the unity vector $\mathbf{i}_p$ in the periapsis direction can be written as

$$\mathbf{i}_p = \frac{\mathbf{v}_1 - \mathbf{v}_2}{\|\mathbf{v}_1 - \mathbf{v}_2\|}. \qquad (59)$$

Substituting (58) and (59) in (57) we obtain that

$$V_2^2 - V_1^2 = -2\|\mathbf{v}_1 - \mathbf{v}_2\|\,\mathbf{V}^{pl}\cdot\mathbf{i}_p = -\frac{4v_\infty V^{pl}\cos\eta}{e_p}. \tag{60}$$

Then, replacing the expression (60) in (56) and (55) we obtain an analytical expression for the semi-major axis a_2

$$\frac{1}{a_2} = \frac{1}{a_1} + \frac{4}{\mu_S}\,\frac{v_\infty V^{pl}\cos\eta}{e_p}. \tag{61}$$

¿From the expression obtained, we can observe how the semi-major axis changes depending on whether the planet is moving *away* or *towards* the spacecraft when it performs the fly-by. In the first case, $\pi/2 < \eta \leq \pi$ and $\cos\eta < 0$, so the semi-major will decrease (and the energy increase). In the second case, $0 \leq \eta < \pi/2$ and $\cos\eta > 0$, so the semi-major axis will increase (and the energy decrease). The maximum decrease and minimum increase will take place when $\eta = \pi$ and $\eta = 0$ respectively and r_p is minimum. For $\eta = \pi/2$ there will be not any change.

4.4.3 Variation of the eccentricity

Next, we will derive final eccentricity e_2 in terms of e_1, a_1, R^{pl}, r_p, η and v_∞. The initial and final eccentricity vectors are given by

$$\mathbf{e}_j = \left(\frac{V_j^2}{\mu_S} - \frac{1}{R_j}\right)\mathbf{R}_j - \frac{1}{\mu_S}(\mathbf{R}_j\cdot\mathbf{V}_j)\mathbf{V}_j,$$

for $j = 1, 2$. Using again that $\mathbf{R}_1 \approx \mathbf{R}^{pl}$ and $\mathbf{R}_2 \approx \mathbf{R}^{pl}$, as well as the relation

$$\frac{1}{a_j} = \frac{2}{R_j} - \frac{V_j^2}{\mu_S}$$

we can write

$$e_j^2 = \left(\frac{1}{R^{pl}} - \frac{1}{a_j}\right)^2 (R^{pl})^2 + \frac{1}{a_j\,\mu_S}(\mathbf{R}^{pl}\cdot\mathbf{V}_j)^2 \tag{62}$$

for $j = 1, 2$. We substitute (61) in (62) for $j = 2$ and we get that

$$e_2^2 = \left(\frac{1}{R^{pl}} - \frac{1}{a_1} - q\right)^2 (R^{pl})^2 + \left(\frac{1}{a_1} + q\right)\frac{(\mathbf{R}^{pl}\cdot\mathbf{V}_2)^2}{\mu_S}, \tag{63}$$

where $q = \dfrac{4v_\infty V^{pl}\cos\eta}{\mu_S e_p}$. The first term in (63) is already expressed in terms of the initial values. For the second term, we write $\mathbf{V}_2 - \mathbf{V}_1 = \mathbf{v}_2 - \mathbf{v}_1$ and using (57) and (59) we get that

$$\mathbf{V}_2 - \mathbf{V}_1 = -\frac{2v_\infty}{e_p}\,\mathbf{i}_p.$$

Therefore

$$\mathbf{R}^{pl}\cdot\mathbf{V}_2 = \mathbf{R}^{pl}\cdot\mathbf{V}_1 - \frac{2v_\infty R^{pl}}{e_p}\,\xi, \tag{64}$$

where ξ is the defined by $\mathbf{R}^{pl} \cdot \mathbf{i}_p = R^{pl}\xi$. From one hand,

$$\mathbf{R}^{pl} \cdot \mathbf{V}_1 = \mathbf{R}^{pl} \cdot (\mathbf{v}_1 + \mathbf{V}^{pl}) = \mathbf{R}^{pl} \cdot \mathbf{v}_1 = R^{pl} v_\infty \beta, \tag{65}$$

and from the other, the same product can be obtained from (62) for $j = 1$ as

$$(\mathbf{R}^{pl} \cdot \mathbf{V}_1)^2 = \mu_S(a_1 e_1^2 - a_1 + 2R^{pl} - (R^{pl})^2/a_1), \tag{66}$$

so that

$$\beta = \pm \frac{\sqrt{\mu_S(a_1 e_1^2 - a_1 + 2R^{pl} - (R^{pl})^2/a_1)}}{R^{pl} v_\infty}. \tag{67}$$

Finally, substituting (64), (65) and (66) in (63) we will get the final expression for e_2:

$$\begin{aligned} e_2^2 &= 1 - 2R^{pl}\left(\frac{1}{a_1} + q\right) + (R^{pl})^2\left(\frac{1}{a_1} + q\right)^2 + \\ &\quad + \left(\frac{1}{a_1} + q\right)\frac{1}{\mu_S}\left(\mathbf{R}^{pl} \cdot \mathbf{v}_1 - \frac{2v_\infty R^{pl}}{e_p}\,\xi\right)^2 \\ &= 1 + \left(\frac{1}{a_1} + q\right)\left(-2R^{pl} + \frac{(R^{pl})^2}{a_1} + q(R^{pl})^2 + a_1 e_1^2 - a_1 + 2R^{pl} - \frac{(R^{pl})^2}{a_1}\right) \\ &\quad + \frac{1}{\mu_S}\left(\frac{1}{a_1} + q\right)\left(-\frac{4v_\infty^2 (R^{pl})^2 \beta}{e_p}\,\xi + \frac{4v_\infty^2 (R^{pl})^2}{e_p^2}\,\xi^2\right) \\ &= e_1^2 + q\left((R^{pl})^2\left(\frac{1}{a_1} + q\right) + a_1(e_1^2 - 1)\right) \\ &\quad + \frac{4v_\infty^2 (R^{pl})^2}{e_p \mu_S}\left(\frac{1}{a_1} + q\right)\left(\frac{\xi}{e_p} - \beta\right)\xi. \end{aligned} \tag{68}$$

4.4.4 Variation of the inclination

Suppose that the spacecraft approaches the fly-by body, whose velocity is $\mathbf{V}^{pl}$ within the body's orbital plane. Let the spacecraft velocity by $\mathbf{V}(t_1)$. The gravity assist manoeuvre transforms the incoming spacecraft hyperbolic velocity excess $\mathbf{v}_{\infty 1}$ into the outgoing hyperbolic velocity $\mathbf{v}_{\infty 2}$. Figure 20 shows the sphere of possible locations of $\mathbf{v}_{\infty 2}$ after the manoeuvre. From the Figure it follows that the change in the angle of inclination, Δi, of the spacecraft orbital plane, after a single fly-by, can be written as

$$\sin \Delta i = \frac{v_\infty \sin 2\nu}{V^{pl}}.$$

Recall that the angle of rotation can be found from the formula

$$\sin \nu = \frac{1}{1 + r_p v_\infty^2/\mu},$$

and that for a fixed value of v_∞, ν is maximum when r_p is minimum, for instance if $r_p = r^{pl}$ where r^{pl} is the radius of the planet.

For a fixed value of v_∞, the maximum increment in the angle of inclination of the spacecraft orbital plane is given by

$$\sin \Delta i = \frac{v_\infty}{V^{pl}}. \tag{69}$$

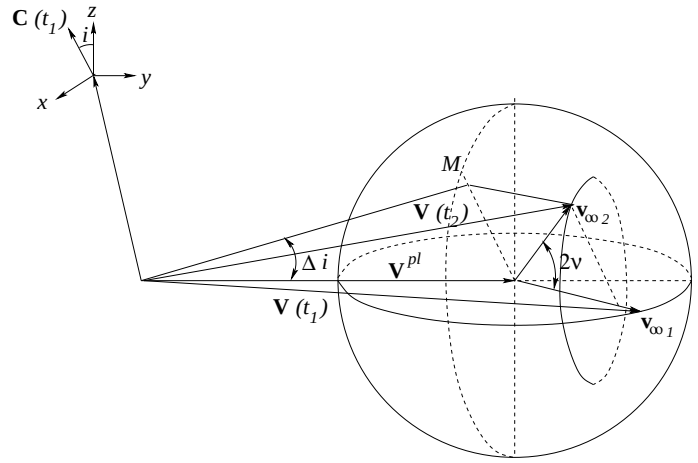

Figure 20: Changes in the inclination angle of the spacecraft orbit as a result of gravity assist manoeuvre.

Figure 21 gives the curves of maximum change in the spacecraft orbital plane inclination resulting from a single fly-by of different planets in the solar system. The data show that the highest potentialities for changing the spacecraft orbital plane in a single fly-by is typical of those large planets of the Jovian group – Jupiter, Saturn, Uranus, Neptune and Pluto. The potentialities of the Earth group planets –Earth, Venus, Mars and Mercury– are somewhat lower.

Multiple fly-bys of the attracting body allow a greater increase in the inclination angle of the spacecraft orbital plane by way of additional rotation of $\mathbf{v}_{\infty 2}$ during each fly-by.

It is evident that orbits with large inclination angles can be obtained. To do this, it is necessary to perform fly-bys with large $\mathbf{v}_\infty$, though the efficiency of the gravity assist manoeuvre in this case will decrease (in accordance with equation (49), growth in v_∞ results in a reduction in the rotation angle 2ν). This, in turn, will require the number N of fly-bys of the attracting body to be increased so as to attain the necessary Δi.

Gravity assist manoeuvres in space make it possible to significantly change the inclination of the spacecraft orbital plane. This can be particularly important in exploration beyond the ecliptic plane (e.g. in flights over the Sun) or in flights to celestial bodies whose orbits are notably inclined to the ecliptic plane.

4.5 Numerical estimations for close encounters

In a previous section, we have seen how the energy of the interplanetary trajectories with respect to the Sun changes after a close encounter with a planet. The effect caused by the encounter with the planet can be studied numerically using the Circular Restricted Three Body problem as a model. As the trajectory can be approximated by a hyperbola during the close approach, we can also restrict our attention to the planar case.

The aim is to classify a large variety of initial conditions of orbits with a close encounter with the small primary (the planet), according to the effects

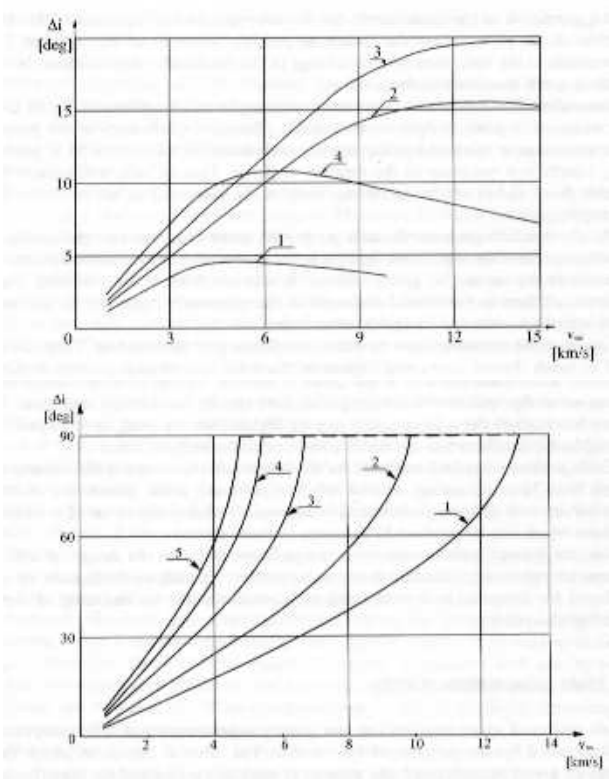

Figure 21: Maximum changes in the inclination angle of the spacecraft orbit as a result of gravity assist manoeuvre. In the top figure 1 = Mercury, 2 = Venus, 3 = Earth, 4 = Mars. In the bottom figure 1 = Jupiter, 2 = Saturn, 3 = Uranus, 4 = Neptune, 5 = Pluto.

due to the encounter with the planet. The classification are done evaluating the energy and the angular momentum of the third body before and after the passage near the planet. The orbits are identified by the Jacobi constant C_J of the third body, the angle ψ between the primaries line and the pericenter direction of the trajectory and the pericenter distance r_p (see Fig. 22).

Then, given arbitrary values for the Jacobi constant C_J, the minimum distance r_p and the angle ψ, the procedure has the following steps:

1. The position and the velocity at pericenter in the rotating synodical system (x, y) is given by

$$\mathbf{r}_p = (1 - \mu + r_p \cos\psi, r_p \sin\psi), \qquad \dot{\mathbf{r}}_p = (-v_p \sin\psi, v_p \cos\psi),$$

   where v_p, the modulus of the velocity, can be calculated from the Jacobi first integral.

2. Taking $\mathbf{r}_p$ as initial conditions, the equations of motion are integrated forward and backward until the distance between the third body and the planet is bigger than a certain fixed distance. For bigger distances, the

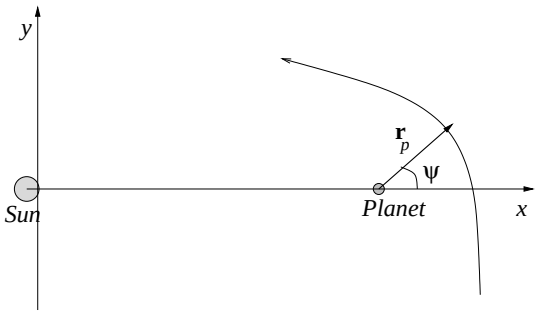

Figure 22: Close encounter in a rotating system. The passage near the planet has been magnified for greater clarity.

effect of the planet can be neglected and the energy and the angular momentum can be considered constants.

3. The energy and the angular momentum at final points of both integrations are computed.

The energy and the angular momentum (relative to the non-rotating sidereal system) can be expressed using the synodical coordinates $(x, y, \dot{x}, \dot{y})$ as

$$\begin{aligned} E &= \frac{1}{2}((x+\dot{y})^2 + (\dot{x}-y)^2) - \frac{1-\mu}{r_1} - \frac{\mu}{r_2}, \\ c &= x^2 + y^2 + x\dot{y} - y\dot{x}, \end{aligned} \tag{70}$$

and then, the Jacobi constant can be written as $C_J = E - wc$ (w the angular velocity of the system). Depending on the sign of both parameters E and c, the orbits are classified in:

- elliptic direct, when the energy is negative and the angular momentum is positive,
- elliptic retrograde, when both the energy and the angular momentum are negative,
- hyperbolic direct, when both the energy and the angular momentum are positive,
- hyperbolic retrograde, when the energy is positive and the angular momentum is negative,

Due to the change of the energy and the angular momentum after the close encounter, every orbit can be characterise by two of these categories. In Table 4, the labels A,B,...,O are assigned depending on the classification before and after the passage near the planet. There is a symmetry due to the fact that an orbit with angle ψ is different from an orbit with angle $\psi + \pi$ only by a time reversal. This means that there is a correspondence between the orbits of type B $\leftrightarrow$ E, C $\leftrightarrow$ I, D $\leftrightarrow$ M, G $\leftrightarrow$ J, H $\leftrightarrow$ N and L $\leftrightarrow$ O.

For a fixed value of the perigee distance, each point in the (ψ, C_J) plane represents an orbit that can be classified according the previous rules. This

After → / Before ↓	Direct Ellipse	Retrograde Ellipse	Direct Hyperbola	Retrograde Hyperbola
Direct Ellipse	A	E	I	M
Retrograde Ellipse	B	F	J	N
Direct Hyperbola	C	G	K	O
Retrograde Hyperbola	D	H	L	P

Table 4: Class of orbits depending on their classification before and after a close encounter with a planet.

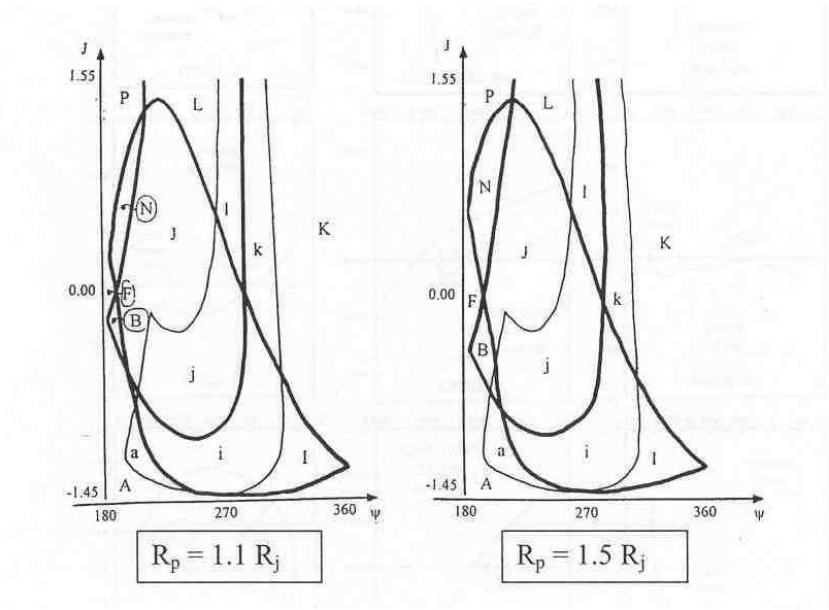

Figure 23:

gives a two-dimensional diagram where the regions corresponding to each type of orbit can be represented. In Fig. 23 these diagrams are shown for orbits with close encounters with Jupiter. The values of the perigee distance taken are 1.1 and 1.5 times the Jupiter's radius. In .... the orbits every orbit followed enough time to verify if the spacecraft has none, one or two possible encounter with the Earth. Orbits that do not cross the Earth's path around the Sun are labelled in capital letters, while lower letters represents orbits that cross the Earth's path around the Sun at least once.

4.6 Surface impact at a target planet

Consider the problem of pointing a vehicle in a direction to impact a planetary surface at a specific point. For simplicity, the following analysis assumes the point of impact to lie in the plane formed by the polar axis of the planet and the direction of the relative velocity vector (we are addressing the problem of impacting at a specified latitude). Generally, small adjustments in the orbit can alter the time of arrival to accommodate a desired longitude of impact. According to Figure 24, we see that the choice of latitude ϕ together with $\mathbf{v}_{\infty 1}$

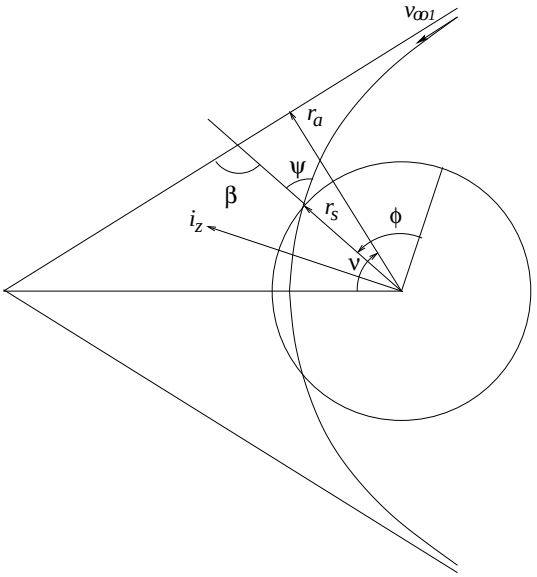

Figure 24: Impact at a target plane.

serves to determine the angle β and the point of impact $\mathbf{r}_s$. Writing $\mathbf{v}_{\infty 1}$ in a planetocentric equatorial system of coordinates, then

$$\sin(\beta - \phi) = \frac{\mathbf{i}_z \cdot \mathbf{v}_{\infty 1}}{v_\infty}.$$

Recall that the parameter of an hyperbolic orbit is given by

$$p = a(1 - e^2) = \frac{\mu}{v_\infty^2 \tan \nu}.$$

Thus we have

$$r_s = \frac{p}{1 + e\cos(\pi/2 - \beta + \nu)} = \frac{\dfrac{\mu}{v_\infty^2 \tan \nu}}{1 + \dfrac{\sin \beta}{\tan \nu} - \cos \beta}.$$

Using (42), we get the following quadratic equation for determining r_a in terms of β and v_∞.

$$r_a^2 - r_a r_s \sin \beta - \frac{\mu}{v_\infty} r_s (1 - \cos \beta) = 0.$$

The angle of incidence ψ, shown in Figure 24, is important for the atmospheric entry problem and may be determined from

$$\tan \psi = \frac{p}{r_s e \sin f},$$

where $f = \pi/2 - \beta + \nu$ is the true anomaly. Thus we have

$$\tan \psi = \frac{r_a^2}{r_s(r_a \cos \beta + \mu \sin \beta / v_\infty^2)}.$$

4.7 Tisserand's criterion

When a comet passes close to a planet, the elements of its orbit can be so drastically altered that the identity of the comet can be questionable. To solve this problem, Tisserand established a relationship among the comet elements which remains essentially unaltered by the perturbations. This same relationship can be used to analyse the effect of planetary contact on a spacecraft.

Tisserand's criterion is a particular interpretation of Jacobi's integral of the restricted three body problem. Thus, the first step is to rewrite that integral is an inertial (non-rotating) reference frame.

Recall that, in the synodic system, the Jacobi integral can be written as

$$\dot{x}^2 + \dot{y}^2 = w^2(x^2 + y^2) + \frac{2Gm_1}{r_1} + \frac{2Gm_2}{r_2} - C,$$

and using the identity

$$\mathbf{w} \wedge (\mathbf{w} \wedge \mathbf{r}) = -w^2(x\mathbf{i}_x + y\mathbf{i}_y),$$

we can write it as

$$v^2 = \dot{x}^2 + \dot{y}^2 = -\mathbf{r} \cdot \mathbf{w} \wedge (\mathbf{w} \wedge \mathbf{r}) + \frac{2Gm_1}{r_1} + \frac{2Gm_2}{r_2} - C. \tag{71}$$

In order to write it in the sidereal reference frame, recall that if R is a rotation matrix and we denote $\mathbf{r}^* = R\mathbf{r}$, then

$$\mathbf{v}^* = \frac{d\mathbf{r}^*}{dt} = \frac{dR}{dt}\mathbf{r} + R\frac{d\mathbf{r}}{dt} = R\left(R^T\frac{dR}{dt}\mathbf{r} + \frac{d\mathbf{r}}{dt}\right) = R\left(\Omega\mathbf{r} + \mathbf{v}\right), \tag{72}$$

where the matrix Ω is defined by

$$\Omega = R^T\frac{dR}{dt},$$

Derivating the identity $R^TR = I$, one gets that $\Omega^T = -\Omega$, so

$$\Omega = \begin{pmatrix} 0 & -w_z & w_y \\ w_z & 0 & -w_x \\ -w_y & w_x & 0 \end{pmatrix}.$$

Now, if we define $\mathbf{w}$ such that its components in the rotating reference system are (w_x, w_y, w_z), we can write

$$\mathbf{v}^* = R\left(\mathbf{w} \wedge \mathbf{r} + \frac{d\mathbf{r}}{dt}\right).$$

The vector $\mathbf{w}$ represents the angular velocity of the rotating frame with respect to the inertial one. From (72), we get

$$\mathbf{v}^* = R\left(\Omega\mathbf{r} + \mathbf{v}\right) = R\left(\Omega R^T\mathbf{r}^* + \mathbf{v}\right),$$

so

$$\mathbf{v} = R^T\left(\mathbf{v}^* - R\Omega R^T\mathbf{r}^*\right) = R^T\left(\mathbf{v}^* + \Omega^*\mathbf{r}^*\right),$$

where Ω^* is the matrix associated to $\mathbf{w}^* = -\mathbf{w}$ and verifies $\Omega^{*T} = R\,\Omega\,R^T$. From this identity we get

$$\begin{aligned}\mathbf{v}^T\mathbf{v} &= v^{*2} - \mathbf{r}^T\,\Omega\,\mathbf{v} + \mathbf{v}^T\Omega\,\mathbf{r} - \mathbf{r}^T\Omega\,\Omega\,\mathbf{r} \\ &= v^{*2} + 2\mathbf{w}\cdot\mathbf{r}\wedge\mathbf{v} - \mathbf{r}\cdot\mathbf{w}\wedge(\mathbf{w}\wedge\mathbf{r}) \\ &= v^{*2} + 2\mathbf{w}^*\cdot\mathbf{r}^*\wedge\mathbf{v}^* - r^{*2}w^{*2} - (\mathbf{w}^*\cdot\mathbf{r}^*)^2.\end{aligned}$$

Taking into account that

$$\mathbf{w}^* = -\mathbf{w}, \quad r^{*2} = r^2, \quad (\mathbf{w}^*\cdot\mathbf{r}^*)^2 = (\mathbf{w}\cdot\mathbf{r})^2$$

we obtain

$$v^2 = v^{*2} - 2\mathbf{w}\cdot\mathbf{r}^*\wedge\mathbf{v}^* - \mathbf{r}\cdot\mathbf{w}\wedge(\mathbf{w}\wedge\mathbf{r}),$$

Substituting this expression in (71)

$$v^{*2} = 2\mathbf{w}\cdot\mathbf{r}^*\wedge\mathbf{v}^* + \frac{2Gm_1}{r_1} + \frac{2Gm_2}{r_2} - C, \tag{73}$$

which is the Jacobi integral in sidereal coordinates.

If m_1 and m_2 are the masses of the Sun and a planet, respectively, then $m_2 << m_1$. Therefore, when a comet (or spacecraft) is not close to the planet, we may discard the term $2Gm_2/r_2$ in Jacobi integral. It is also verified that

$$w^2 = \frac{G(m_1+m_2)}{r_{12}^3} \approx \frac{Gm_1}{r_{12}^3} = \frac{\mu}{r_{12}^3},$$

where r_{12} is the distance from the Sun to the planet. Furthermore, $\mathbf{r}^*\wedge\mathbf{v}^*$ is just the angular momentum $\mathbf{c}$ of the small body with respect to the Sun, so that

$$\mathbf{w}\cdot\mathbf{r}^*\wedge\mathbf{v}^* = w\,c\,\cos i = w\sqrt{\mu\,a\,(1-e^2)}\cos i,$$

where i is the inclination angle of the body's orbital plane with respect to the ecliptic; a and e are, of course, the semi-major axis and eccentricity of the orbit of the small body. In addition, we can use the energy integral

$$v^{*2} = \mu\left(\frac{2}{r_1} - \frac{1}{a}\right).$$

When these are substituted in Jacobi integral, we obtain

$$\frac{1}{a} + 2\sqrt{\frac{a(1-e^2)}{r_{12}^3}}\cos i = \text{ctant},$$

which can also be written as

$$\frac{1}{a_1} + 2\sqrt{\frac{a_1(1-e_1^2)}{r_{12}^3}}\cos i_1 = \frac{1}{a_2} + 2\sqrt{\frac{a_2(1-e_2^2)}{r_{12}^3}}\cos i_2,$$

where a_1, e_1, i_1 are the semi-major axis, eccentricity and orbital inclination prior to the planetary contact and a_2, e_2, i_2 are the orbital elements after the contact. This last equation is generally referred as Tisserand's criterion for the identification of comets.

5 Optimal multi-purpose missions

5.1 Minimum energy flight paths

The most important requirement for a mission with one or several flybys is that it should **reduce the energy consumption** relative to an analogous direct flight. The criterion of minimum total energy can be based on different approximate models of the flight.

As has already been explained, the simplest model represents interplanetary trajectories as Keplerian arcs which begin and terminate on the orbits of the departure and destination planets (in circular and coplanar orbits). The energy expenditure for the interplanetary flight is estimated based on the total velocity needed for the spacecraft to fly from the orbit of departure to that of the destination planet. The gravity assist manoeuvre is approximated by an instantaneous rotation of the spacecraft velocity at the moment that the planet is passed.

For the simplest mission, and using the simplest model, the optimisation problem is reduced to searching for the minimum of the function

$$\min\left(\|\mathbf{V}_1 - \mathbf{V}^{pl1}\| + \|\mathbf{V}_2 - \mathbf{V}^{pl2}\|\right),$$

where μ is the gravitational constant of the arrival planet and

$$\begin{aligned}
\mathbf{V}^{pl1}, \mathbf{V}^{pl2} &= \text{velocities of the departure and destination planets,} \\
\mathbf{V}_1, \mathbf{V}_2 &= \text{spacecraft velocities at the departure and arrival points,} \\
&\quad (\mathbf{V}_i = \mathbf{V}(T_i, r_{pi}, R_i)), \\
T_i &= \text{period of the initial/final leg of the orbit,} \\
r_{pi} &= \text{pericentral distance of the initial/final leg of the orbit,} \\
R_i &= \text{orbital radii of the departure and destination planets.}
\end{aligned}$$

$V_\Sigma = \|\mathbf{V}_1 - \mathbf{V}^{pl1}\| + \|\mathbf{V}^{pl2} - \mathbf{V}_2\|$ is called the **total characteristic velocity** of the flight.

The orbital characteristics of the final (post-perturbation) leg of the flight (T_2, r_{p2}) are determined only by the altitude of the spacecraft flight $m_p = R_p/R^{pl2} > 1$ (in the pericenter of the flyby hyperbola) relative to the surface of the flyby planet and $V_\Sigma = V_\Sigma(T_1, r_{p1}, \mu)$.

It should be mentioned that the search for optimal solutions, even based on a model as simple as that, requires the use of the numerical methods and algorithms of nonlinear programming.

In a more accurate approach, the spacecraft trajectory is approximated by segments of unperturbed Keplerian movement, as in the previous model, but the planetary motion is represented more accurately, allowing elliptic and non-coplanar planetary orbits and taking into account the phasing of the planetary movement along the orbits. In this case the analysis is made for specific dates (or time intervals) of the interplanetary flight.

Now the approach works as follows: first, the segments of heliocentric motion from the Earth to the flyby planet and from the flyby planet to the destination planet are constructed. These segments of the interplanetary trajectory are matched, based on the asymptotic incoming and outgoing velocities relative to the flyby planet ($\mathbf{v}^-_{\infty\ i}$ and $\mathbf{v}^+_{\infty\ i}$), with possible application of a powered

manoeuvre. For multiple flybys trajectories, a similar construction is made for subsequent segments of the trajectory. The optimal trajectories are sought based on the criterion of minimum total characteristic velocity, which can be represented in the general form

$$\min V_\Sigma = \min \left(\|\mathbf{V}_0\| + \sum_{i=1}^{N} \|\mathbf{V}_i\| + \|\mathbf{V}_f\| \right),$$

where $\mathbf{V}_0$ is the starting impulse from the near-Earth orbit with radius R_0, $\mathbf{V}_i$ is the velocity impulse applied during the flyby of the i-th planet, $\mathbf{V}_f$ is the characteristic velocity of deceleration at the destination planet to enter a near-planetary orbit and N is the number of the flybys.

Here

$$\begin{aligned} \mathbf{V}_0 &= \mathbf{V}_0(T_1, T_0, \mathbf{R}_0), \\ \mathbf{V}_i &= \mathbf{V}_i(T_{i-1}, T_i, T_{i+1}, \boldsymbol{\rho}_i), \\ \mathbf{V}_f &= \mathbf{V}_f(T_N, T_f, \mathbf{R}_f), \end{aligned}$$

where T_0 is the date of the spacecraft launch, T_i are the dates of intermediate planetary flybys, T_f is the date of arrival at the destination planet ($T_f - T_0$ is the total flight time), $\mathbf{R}_0$ and $\mathbf{R}_f$ are the vector determining the departure and destination orbits and $\boldsymbol{\rho}_i$ is the radius vector of the point passing from the incoming to outgoing hyperbolas in the flyby of the i-th planet.

Thus, the problem of finding the optimal interplanetary trajectory with gravity assist manoeuvres is reduced to the minimisation of the mission characteristic velocity as a function of several variables

$$\min V_\Sigma(T_0, T_i, T_f, \mathbf{R}_0, \boldsymbol{\rho}_i, \mathbf{R}_f).$$

In the minimisation process, the problems of finding heliocentric and planetocentric legs of the flight path are considered separately within the framework of the different spheres of influence.

The problem of optimisation of a planetocentric flyby segment implies minimisation of energy expenditures for the inter-hyperbolic transfer, and is regarded as an internal problem with respect to the external heliocentric pre- and post-perturbation segments, which determine the values of hyperbolic velocity excess in the initial and end points of the flyby trajectory segment

$$\mathbf{v}^-_{\infty\ i} = \mathbf{v}(T_{i-1}, T_i), \qquad \mathbf{v}^+_{\infty\ i} = \mathbf{v}(T_i, T_{i+1}), \quad i = 1, ..., N-1.$$

The hyperbolic velocity excess uniquely determine the plane of the spacecraft planetocentric manoeuvre

$$[\mathbf{v}^-_{\infty\ i} \wedge \mathbf{v}^+_{\infty\ i}] \cdot \boldsymbol{\rho}_i = 0.$$

The calculation of the velocity impulse to be applied during flyby, $\min V_i$, in the case of a single-impulse manoeuvre reduces to find the impulse and the point of transfer $\boldsymbol{\rho}_i$ between the incoming and outgoing hyperbolas.

In terms of computations, the problem of search for the optimal multiple-fly-by interplanetary trajectory can be reduced to the successive minimisation of the function

$$\min V_\Sigma = \min_{T_1} \left(\min_{T_2} ... \left(\min_{T_{N-1}, T_f} V_\Sigma \right) \right),$$

with the optimisation of V_i at each stage. This problem can be solved by one of the nonlinear programming methods on the manifold of variables $T_1, ..., T_{N-1}, T_N$, $\boldsymbol{\rho}_i$, $\mathbf{R}_0, ..., \mathbf{R}_{N-1}, \mathbf{R}_f$.

5.2 Analysis of multi-purpose trajectories

Let M be the set of bounded coplanar orbits in a central gravitational field, comprising two subsets of circular and elliptic orbits

$$M = M_c \cup M_e.$$

Each element $N \in M$ can be mapped onto the space of orbital parameters. Several combinations of these parameters will be used, for instance the period of the orbit T and the pericentral distance r_p and we will write

$$N(T, r_p) \in M.$$

Given circular orbit with fixed radius R_k, $N(R_k)$, we select the set of elliptic orbits, M'_e, sharing at least one point with the given circular orbit

$$M'_e \subset M_e.$$

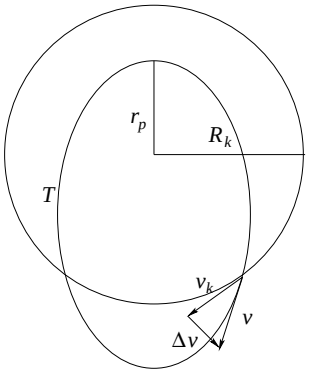

Figure 25: Single-impulse inter-orbital transfer.

Consider the problem of constructing the isoline field of relative velocities ($\Delta v = const$) in the intersection points of the circular orbit $N(R_k)$ with the orbits in the set M'_e. The velocity Δv (see Figure 25) is the relative velocity of transfer from a certain elliptic orbit to the given circular one (or vice versa) and can also be interpreted as the hyperbolic excess of the spacecraft velocity v_∞.

For the construction of the isoline field we first find the domain, in the (r_p, T) plane, into which the set M'_e is mapped, and then construct the field

$$\Delta v = \|\mathbf{v} - \mathbf{v}(R_k)\| = f(r_p, T) = const.$$

within this domain. Here, $\mathbf{v}$ and $\mathbf{v}(R_k)$ are the orbital velocities in the point of intersection of the elliptical and circular orbits.

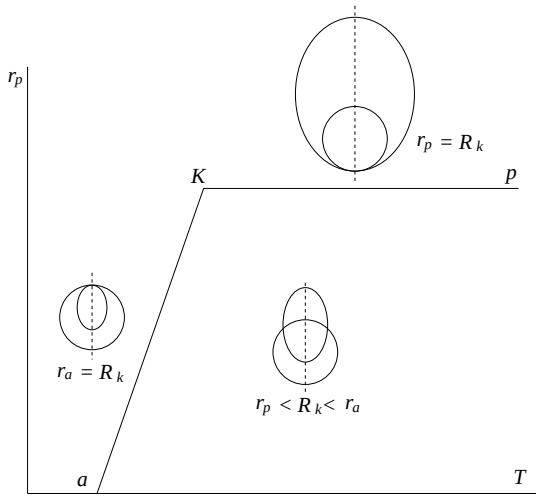

Figure 26: The domain of isolines $\Delta v = const$ of inter-orbital transfer.

The boundaries of the domain under consideration (see Fig. 26) are as follows: on the left is the line aK of the orbits tangent to the given circular orbit in their apocenters ($r_a = R_k$); the upper boundary is the line Kp of orbits tangent to the given circular orbit in the pericenter ($r_p = R_k$); from below, the domain is bounded by the $r_p = 0$ axis (rectilinear orbits); in the right boundary (at infinity) we find the parabolic orbits. The left and upper boundary lines have a common point, K, corresponding to a circular orbit that coincides with the given orbit (all points are shared and $\Delta v = 0$).

Let us consider in more detail the limiting lines and the position in them of the boundary points of the isolines $\Delta v = const$. The line aK can be determined analytically from the condition

$$T = 2\pi \left(\frac{a^3}{\mu}\right)^{1/2}, \qquad a = \frac{r_p + r_a}{2}.$$

Since $r_a = R_k = const.$ (from the tangency condition), we can write

$$T = \pi \sqrt{\frac{(r_p + R_k)^3}{2\mu}},$$

and solving for r_p we get

$$r_p = \left(\frac{T}{\pi}\right)^{2/3} (2\mu)^{1/3} - R_k.$$

This is, aK is a weakly convex segment limited by the points $r_p = 0$ and $r_p = R_k$. The values of Δv are determined from $\Delta v = v_p - v_a$, therefore, the position of the left ends of the isolines $\Delta v = const$ within the segment aK can be determined as

$$r_p = 2a - R_k = \frac{2\mu}{2V_k^2 - \Delta v^2} - r_k, \qquad \text{where} \qquad V_k = \sqrt{\frac{\mu}{R_k}}.$$

The boundary line Kp is parallel to the abscissa axis and is determined from the condition $r_p = R_k$; the location of the right ends of the isolines $\Delta v = const$ on it can be determined from the conditions

$$\Delta v = v_p - v_k, \qquad T = \frac{2\pi\mu}{(2V_k^2 - (\Delta v + v_k)^2)^{3/2}}.$$

It should be noted that each of the points lying within the domain aKp corresponds to an orbit $N(r_p, T)$ that has two shared points (intersections) with the circular orbit $N(R_k)$ under consideration. The isolines $\Delta v(r_p, T) = const$ can be constructed using the relationships of the triangle of velocities and the formulas describing undisturbed Keplerian motion of the spacecraft

$$\Delta v^2 - 2v_k \left(1 - v^2 + \frac{C^2}{R_K^2}\right) + v_k^2 - v^2 = 0,$$

where

$$\begin{aligned} v^2 &= \frac{2\mu}{R_k} - \left(\frac{2\pi\mu}{T}\right)^{2/3}, \\ C^2 &= 2r_p\mu - r_p^2 \left(\frac{2\pi\mu}{T}\right)^{2/3}. \end{aligned}$$

Figure 27 presents the isolines of relative velocities for central body with a gravity constant $\mu = 1$ and for a circular orbit with a radius $R_k = 1$. Each isoline represents a set of orbits for which the relative velocity of transfer to the orbit with unit radius $R_k = 1$ is constant. As can be seen from the Figure, the parameters of these orbits (r_p and T) change monotonically from the values corresponding to the orbits with apocentral tangency to the values of pericentral tangency with the orbit $R_k = 1$.

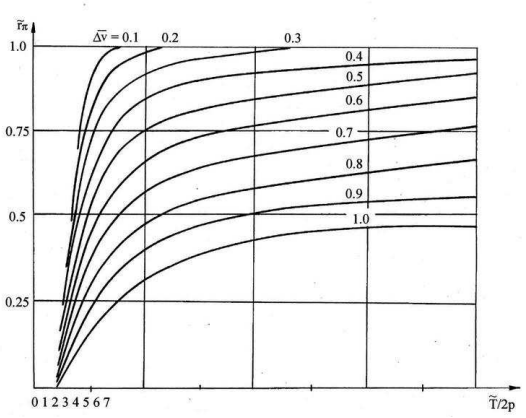

Figure 27: Isolines of relative velocities of single-impulse transfer to the circular orbit of radius 1.

Consider now several circular coplanar orbits with radii R_j, $j = 1, ..., n$ and let us see how to use the isoline field to analyse the conditions of inter-orbital

transfer. Each of these orbits will be represented by a point $N(R_j)$ on the plane of orbital parameters r_p and T.

To fix ideas, we will only consider four circular coplanar orbits $N(R_j)$, $j = 1, ..., 4$. For each of these orbits we can construct the appropriate subsets of intersecting orbits

$$M_j \subset M, \quad j = 1, ..., 4,$$

as well as the isolines of equal relative velocities. Figure 28 shows the location of the domains of isolines for the four orbits under consideration.

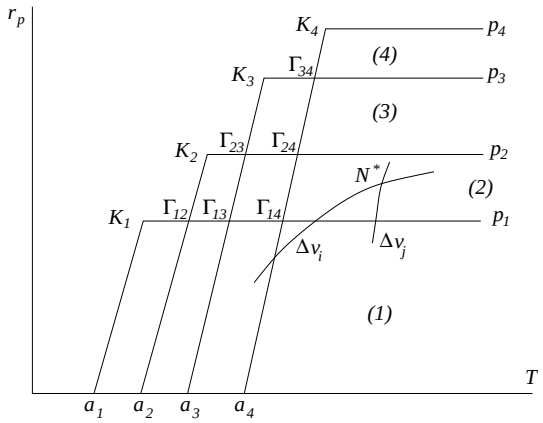

Figure 28: Domains of isolines $\Delta v = const$ for inter-orbital transfer between circular coplanar orbits.

The position of a point $N^*(r_p, T) \in M$ in this diagram allows, not only to judge the feasibility of certain inter-orbital transfers in the system of orbits under consideration, but also to make assessment in terms of energy. Isolines $\Delta v_j = const$ passing through N^* will determine the velocity required for this transfer, and the coordinates of the point $N^*(r_p, T)$ determine the transfer orbit.

Let us consider different possible positions of the image point $N^*(r_p, T)$ on the diagram:

1. $N^* \in \cap_{j=1}^{4} M_j$ implies that the selected orbit shares points with any given orbit. The inter-orbital transfer along the orbit N^* is possible in all cases.

2. $N^* \in M_i \cap M_j \cap M_k$, for all $i, j, k = 1, ..., 4$ and $i \neq j \neq k$ implies that the transfer along the orbit N^* is possible between the three given orbits.

3. $N^* \in M_i \cap M_j$ for all $i, j = 1, ..., 4$ with $i \neq j$ implies that the transfer along the orbit is possible between the two given orbits.

4. $N^* \in M_j$ or $N^* \notin M_j$, $j = 1, ..., 4$ implies that the inter-orbital transfer along the orbit N^* is impossible.

In addition, specific positions of the image point are possible:

1. $N^* \in a_j K_j$, implies that the orbit has an apocentral tangency with the j-th orbit.

2. $N^* \in K_j p_j$, implies that the orbit has an pericentral tangency with the j-th orbit.

3. $N^* = K_j$, implies that the orbit coincides with the j-th orbit.

4. $N^* = \Gamma_{ij} \in a_i K_i \cap K_j p_j$, with $i \neq j$, implies that the transfer orbit is tangent to the departure and arrival orbits.

The points Γ_{ij} on the diagram determine Hohmann transfer orbits between the circular orbits $N(R_j)$ considered.

This diagram can be used for a first approximate analysis, in terms of energy, for the transfers between the orbits under consideration and also to select optimal transfer options. Indeed, for any point $N^*(r_p^*, T^*)$ within the domains (see Fig. 28), one can find an isoline $\Delta v_j = const$, $j = 1, ..., 4$, that passes through this point and determines the velocity of a single impulse transfer between the selected orbit $N^*(r_p^*, T^*)$ and the j-th circular orbit (in the point of their intersection).

In the case where the point N^* is located in the zone of overlap between two domains, one can find two isolines such that $N^* \in \Delta v_i \cap \Delta v_j$, $i \neq j$. Then, the characteristic velocity of a two-impulse transfer between the two circular orbits can be determined as

$$\Delta v_1 = \Delta v_j, \quad \Delta v_2 = \Delta v_i, \quad \Delta v_\Sigma = \Delta v_1 + \Delta v_2.$$

In a similar way, more complicated trajectories in the system of orbits under consideration can be examined, and the optimal variant can be selected from them.

Incidentally, this kind of diagram clearly demonstrates that the Hohmann transfers provide minimum energy expenditure for the transfer from one orbit to another. The extreme left and top position of the points Γ_{ij} in the appropriate domains provides the minimum possible values both for Δv_1 and Δv_2 (and, hence, for the total characteristic transfer velocity Δv_Σ.

The above procedure can evidently be applied to the assessment of different space flights in terms of energy expenses (between the orbits of planets and their satellites, between orbits of planetary artificial satellites with different altitudes, interplanetary flights, etc.). To do this it is sufficient to construct combined isoline fields for relevant orbits.

5.3 Isolines for the analysis of the spacecraft orbit after the gravity assist manoeuvre

Gravity assist manoeuvres allow the change of the elements of the spacecraft orbit and, in particular, to increase or decrease the orbital period T and pericenter distance r_p.

Consider, for example, a natural satellite of a planet, with gravitation constant μ_s and radius r^s, moving along a circular orbit with a radius R in the central field of a planet with gravitational constant μ. We assume that the orbital planes of the natural satellite and a spacecraft are the same and that the spacecraft orbit is determined by its period T, pericentral distance r_p and pericentral longitude w_p.

The efficiency of a gravity assist manoeuvre is known to be determined by the conditions of the spacecraft approaching the celestial body: the spacecraft velocity $\mathbf{V}_1$ on approaching the natural satellite, the velocity of the satellite $\mathbf{V}^s$ and the minimum distance of the spacecraft from the satellite r_p. Figure 29 represents a vector diagram of this gravity assist manoeuvre, reflecting the formation of the spacecraft post-manoeuvre velocity $\mathbf{V}_2$ as a result of rotation of the asymptotic hyperbolic velocity $\mathbf{v}_\infty$ by the angle 2ν between the asymptote of the descending and ascending branches of the fly-by hyperbola.

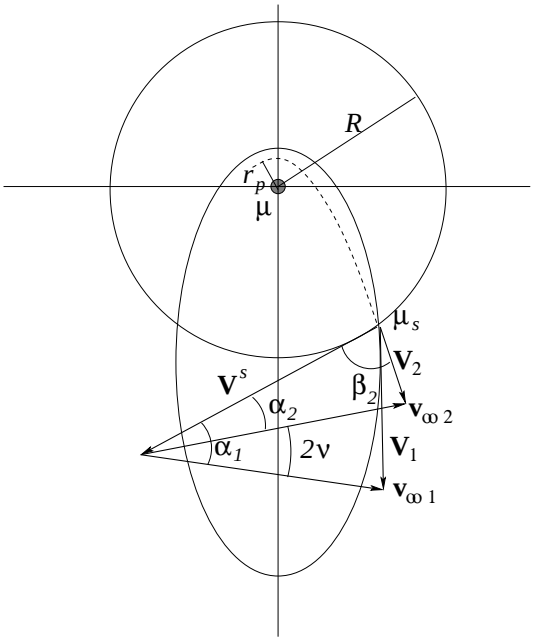

Figure 29: Diagram of velocities of the gravity assist manoeuvre.

Thus, the fly-by near an attracting body within the plane of its motion will cause a change in the parameters determining the size and shape of the spacecraft trajectory as well as the position of the orbit in the flight plane. That is, as the result of the perturbation manoeuvre with given r_p, the set of incoming trajectories $M_1(r_{p1}, T_1, w_1)$ is mapped into the set of post-perturbation orbits $M_2(r_{p_2}, T_2, w_2)$. This mapping associates each incoming orbit $O_1 \in M_1(r_{p1}, T_1, w_1)$ with a new (transformed) orbit $O_2 \in M_2(r_{p2}, T_2, w_2)$.

The determination of the subset of orbits $O_2^* \in M_2$ with a fixed value of T_2, allows the construction of an isoline $T_2 = const$ that can be determined in coordinates r_p and T. The isoline will represent the totality of all incoming spacecraft trajectories that will be transformed by the gravity assist manoeuvre near the satellite into iso-periodical orbits.

Let us consider an algorithm for the construction of the iso-periodic curves $T_2 = const$ in terms of the initial orbit parameters r_p and T.

The set of all the post-perturbation orbits with given T_2 is determined by

the value of outgoing velocity

$$V = \left(\left(\frac{2\pi\mu}{T_2} \right)^{2/3} - \frac{2\mu}{R} \right)^{1/2},$$

and the angle β_2 ($0 \leq \beta_2 \leq \pi$) between $\mathbf{V}^s$ and $\mathbf{V}_2$.

Given a values of β_2, we can determine the asymptotic incoming and outgoing velocities of the spacecraft from the natural satellite using

$$\begin{aligned} v_{\infty 2} &= ((V^s)^2 + V_2^2 - 2V^s V_2 \cos\beta_2)^{1/2}, \\ v_{\infty 1} &= v_{\infty 2}. \end{aligned}$$

The corresponding angles of the asymptotes with respect to $\mathbf{V}^s$ can be determined from the formulas

$$\begin{aligned} \alpha_2 &= \arccos\left(\frac{(V^s)^2 + + v_\infty^2 - V_2^*}{2^s v_\infty} \right), \\ \alpha_1 &= \alpha_2 \pm 2\nu, \end{aligned}$$

where

$$\nu = \arcsin \frac{\mu_s}{\mu_s + r_p v_\infty^2}.$$

Here, the plus sign corresponds to a decrease in the spacecraft energy (passing before the attracting body) and the minus sign to an increase in the spacecraft orbital energy (passing behind the attracting body).

Now let us compute the parameters of the incoming orbit of the spacecraft

1. The velocity of approach to the natural satellite is given by

$$V_1 = ((V^s)^2 + v_\infty^2 - 2V^s v_\infty \cos\alpha_1)^{1/2}.$$

2. Semi-major axis and eccentricity are

$$a = \left| -\frac{\mu}{h} \right|, \qquad e = \left(1 + \frac{hC^2}{\mu^2} \right)^{1/2},$$

where

$$h = V_1^2 - \frac{2\mu}{R}, \qquad C = V_1 R \cos\beta, \qquad \beta = \arcsin\left(\frac{v_\infty}{V_1} \sin\alpha_1 \right),$$

3. The pericentral distance r_p and period T of the incoming orbit of spacecraft are

$$r_p = a(1-e), \qquad T = 2\pi \left(\frac{a^3}{\mu} \right)^{1/2}.$$

In this way, the incoming orbit of the spacecraft for given values of T_2 and β_2 can been determined. Varying the values of β_2 within $[0, \pi]$, we can construct the isoline $r_p(T)$ for $T_2 = const$, and a field of isolines $T_2 = T_2(r_p, T)$ can be constructed for different values $T_{2j} = const$, $j = 1, ..., n$.

Figure 30 shows the isoline $T_2 = T_2(r_p, T) = 30$ days for the case of a spacecraft having a fly-by with Jupiter's natural satellite Ganymede. The two

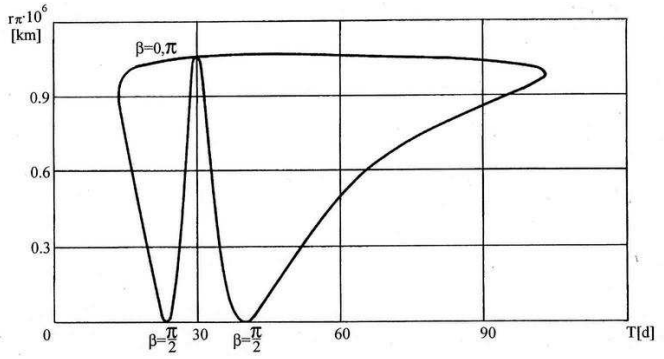

Figure 30: Isoline $T_2 = 30$ days for Ganymede (m=1).

parts of the isoline, left and right, correspond to the approaching spacecraft orbits requiring acceleration and deceleration manoeuvres respectively.

The isolines share a single point, $\beta_2 = 0$, that corresponds to the spacecraft orbit with a period $T = 30$ days and pericentral distance r_p equal to the radius of the bay-passed body's orbit. Both branches have points of tangency to the abscissa axis, which determine the degenerate rectilinear elliptic orbits of the spacecraft ($\beta = \pi/2$). As can be seen from the figure, the perturbation effect is strongly controlled by the selection of the incoming trajectory. Thus, the maximum perturbation effect (both decelerating and accelerating) is observed on the incoming orbits with $r_p \simeq 0.95R$. It should be mentioned that the isolines are constructed for $m = 1$ (where $m = r_p/r^s$), and in the above example, they reflect the maximum possible perturbation manoeuvre near the given celestial body. A decrease in the spacecraft fly-by altitude relative to the surface of the body will result in a reduction in the perturbation effect with the corresponding narrowing of the domain of possible incoming trajectories. Fig. 31 presents a family of isolines $T_2 = 30$ days, for a relative flyby distance varying within $1 \leq m \leq 2$.

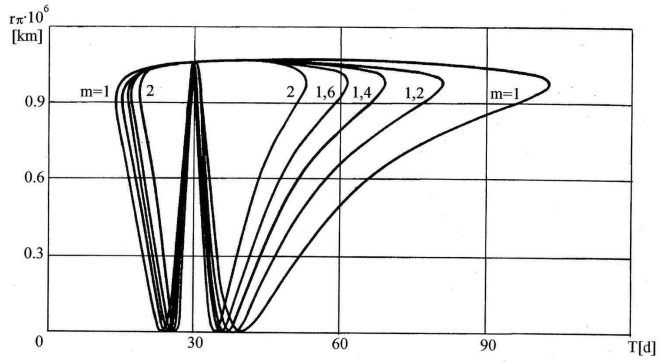

Figure 31: The family of isolines $T_2 = 30$ days for Ganymede ($1 \leq r_p/r^s \leq 2$).

Thus, the isoline constructed for $m = 1$ can be regarded as a boundary of

the domain of incoming orbits that can be transformed by the perturbation manoeuvre at the given body into iso-periodical orbits with a given period.

This circumstance holds for most planets and planetary satellites in the solar system. However, in the case of bypassing a planet with a strong gravitational field (the rotation angle can be $\nu \geq \pi/2$) the perturbation effect can be maximum for the values $m > 1$ determined from equation 51.

A comprehensive idea of the efficiency of perturbation manoeuvring can be derived from the isoline field for the parameter under study. By varying the values of $T_2 = const$ we can construct the field of isolines (isochrones) of the spacecraft post-perturbation trajectories for the fly-by of an attracting body. Fig. 32 shows a field of iso-periodical orbits constructed using the above algorithm and representing the perturbation effect due to Ganymede (for $m = 1$) on the spacecraft orbital periods.

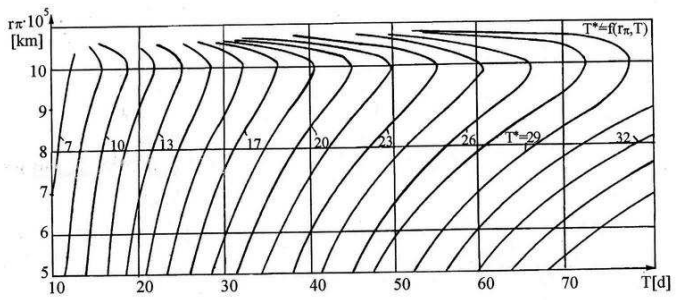

Figure 32: Field of iso-periodic curves for Ganymede (m=1).

In a similar way, we can construct isolines reflecting the post-perturbation orientation of the orbit Figs. 33 and 34 present isolines $\Delta w(r_p, T) = const$ and $\Delta i_{max}(v_\infty)$ for Ganymede. It is evident that the perturbation manoeuvre can result in considerable changes in the orientation of the orbit in its plane as well as in the orbital plane rotation.

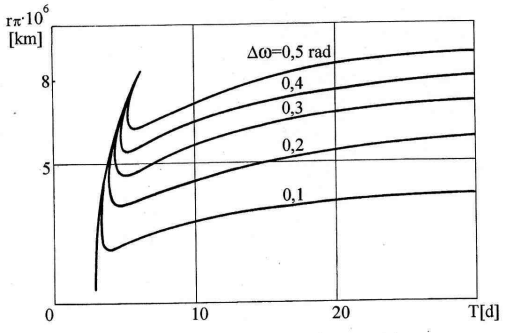

Figure 33: Isolines of angles of rotation of the orbital absides as a result of a gravity assist manoeuvre at Ganymede (m=1).

Constructing fields of isolines of orbital parameters for solar system plan-

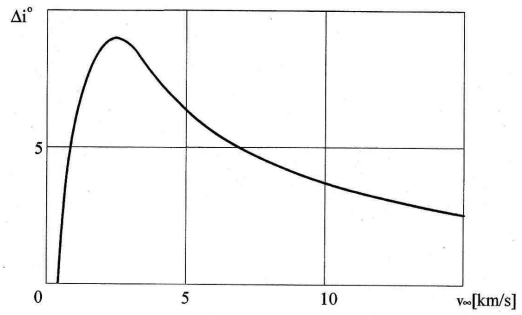

Figure 34: Maximum angles of rotation of the orbital plane as a result of gravity assist manoeuvre at Ganymede (m=1).

ets and their largest satellites will allow us to apply graphical analysis of the perturbation manoeuvring to the study of different paths of space flights.

6 The RTBP approximation

Let us consider a spacecraft moving in the solar system. The computation of fly-by interplanetary trajectories is greatly simplified when they are idealized as two (or more) heliocentric Keplerian orbits joined at one (or more) massless planet points, where the planetary attractions have been neglected. The departure from the departure planet, is patched to a launch hyperbola. Such a model, after a certain amount of trial and error on planetary passage dates, provides a first approximation to the launch velocity vectors for a family of fly-by trajectories covering a season of advantageous launch dates.

In a second step, the heliocentric ellipses have to be corrected for the influences of the other planets and matched in a neighbourhood of the arrival planet with local hyperbolas (see [5]). Furthermore, a local time-of-arrival bias that is strongly dependent on the distance of closest approach to the planet has to be taken into account. Firstly, the attraction of the departure planet can be ignored, although the attraction of the arrival planet and other planets is included. This analysis examines the correction to a nominal heliocentric ellipse from one massless planet to the next, which is due to the planetary perturbations as well as to variations on initial conditions. The expression for the corrected trajectory is called the 'outer expansion'.

In [5], the outer expansion relative to the arrival planet is examined at a distance (in AU) of order $\lambda^{1/2}$, where $\lambda = m_p/m_S$ is the mass ratio of the planet to the Sun, and it contains terms of powers of $\lambda^{1/2}$. This expansion has to be compared with an 'inner expansion', obtained by considering a planet-centered hyperbola plus the Sun's perturbation. Then the position at distance of order $\lambda^{1/2}$ can be examined. Adjusting the energy, angular momentum orientation and time of passage at pericenter of the hyperbola, the inner and outer expansions become identical up to order λ^2. This 'matching' procedure shows that the position and velocity of the incoming asymptote to the osculating hyperbola at closest approach as well as the velocity at infinity, differ from the corresponding quantities of the simple model by constant terms of order λ added to linear terms in the initial conditions variations and terms in other planet/Sun mass ratios. Nevertheless, the time of closest approach contains the nonlinear term $(Gm_p/v_\infty^3)\ln e$, where e is the eccentricity of the hyperbola and v_∞ the velocity at infinity. If the mass of the departure planet is also taken into account, the asymptote position and velocity corrections again contain biases and the time correction will contain the logarithm of the eccentricity of the planet-centered hyperbola.

An outline of the method would be the following one (for further details see [5]). The motion of a spacecraft in the gravitational field of the Sun (mass m_0) and n planets (masses m_i, $i = 1, .., n$), travelling from an arbitrary point in space to a small neighbourhood of the planet m_1, is described using perturbation techniques and the asymptotic matching. The equations of motion can be written as

$$\ddot{\mathbf{r}} = -\mu_0 \frac{\mathbf{r}}{r^3} + \mathbf{f}(\mathbf{r}, t),$$

where $\mathbf{r}$ is the position of the spacecraft relative to the Sun and

$$\mathbf{f}(\mathbf{r}, t) = -\sum_{i=1}^{n} \mu_i \left(\frac{\mathbf{r} - \mathbf{r}_i(t)}{|\mathbf{r} - \mathbf{r}_i(t)|^3} + \frac{\mathbf{r}_i(t)}{|\mathbf{r}_i(t)|^3} \right)$$

(see eq. (4)). Then, the perturbed solution describing the heliocentric trajectory can be developed as

$$\mathbf{r}(t) = \mathbf{r}^0(t) + \boldsymbol{\rho}^1(t) + \boldsymbol{\rho}^2(t) + \cdots ,$$

where $\mathbf{r}^0(t)$ represents the unperturbed conic, which is determined by the initial conditions at initial epoch t_0. The perturbation terms satisfy linear second-order non-homogeneous differential equations whose solution can be written in terms of the transition matrix

$$\frac{\partial(\mathbf{r}(t), \dot{\mathbf{r}}(t))}{\partial(\mathbf{r}(t_0), \dot{\mathbf{r}}(t_0))}.$$

In order to match the outer and inner approximations, the asymptotic behaviour of the perturbation solution as the spacecraft approaches the planet must be determined. For this purposed, it is supposed that at epoch t_1, the Sun centered trajectory arrives at the position of the massless planet m_1, this is, $\mathbf{r}^0(t_1) = \mathbf{r}_1(t_1)$. The only restriction imposed on the motion is that the relative velocity with which it approaches the planet $\mathbf{v}_1 = \dot{\mathbf{r}}^0(t_1) - \dot{\mathbf{r}}_1(t_1)$ is of $O(1)$. The process consists in knowing the behaviour of $\mathbf{r}^0(t)$, $\boldsymbol{\rho}^1(t)$ and $\boldsymbol{\rho}^2(t)$ as $t \to t_1$ and to obtain the corrected position relative to the planet at distances of order $O(\lambda^{1/2})$. This position can be expanded in ascending powers of $\lambda^{1/2}$.

Next, the inner trajectory (planet-centered motion) is described. The equations can be written as

$$\ddot{\boldsymbol{\rho}} = -\mu_1 \frac{\boldsymbol{\rho}}{\rho^3} + \mathbf{g}(\boldsymbol{\rho}, t),$$

where $\boldsymbol{\rho} = \mathbf{r} - \mathbf{r}_1$ and

$$\begin{aligned} \mathbf{g}(\boldsymbol{\rho}, t) \quad = \quad & -\mu_0 \left(\frac{\boldsymbol{\rho} - \mathbf{r}_1(t)}{|\boldsymbol{\rho} - \mathbf{r}_1(t)|^3} - \frac{\mathbf{r}_1(t)}{|\mathbf{r}_1(t)|^3} \right) \\ & - \sum_{i=2}^{n} \mu_i \left(\frac{\boldsymbol{\rho} + \mathbf{r}_1(t) - \mathbf{r}_i(t)}{|\boldsymbol{\rho} + \mathbf{r}_1(t) - \mathbf{r}_i(t)|^3} - \frac{\mathbf{r}_1(t) - \mathbf{r}_i(t)}{|\mathbf{r}_1(t) - \mathbf{r}_i(t)|^3} \right) . \end{aligned}$$

The unperturbed equations define an hyperbola $\boldsymbol{\rho}^0(t)$ with parameters (semimajor axis, eccentricity and time at pericenter) to be determined in the matching. Using the unperturbed hyperbola, the Sun and planetary perturbations near the planet m_1 can be bounded, such that again expansions series of the perturbed inner trajectory can be obtained.

The final step consists in matching the expressions obtained for the outer and inner expressions. Neglecting terms of order $O(\lambda^2)$, expressions for the velocity at infinity, the direction of the asymptote, the orientation of the plane of the hyperbola and the distance to the asymptote can be obtained. Thus, the planet-centered hyperbola is completely determined.

In the case where the trajectory of the spacecraft originates in a small neighbourhood of one planet and reaches a small neighbourhood of a different one, the asymptotic matching must be done at both ends of the Sun centered conic.

In the above method, all planets are considered, so it is necessary to deal with all the perturbation terms due to the planetary attractions. In order to describe the inner and outer solutions, a simpler model can be considered. We take as the underlying model the 3D circular Restricted Three Body Problem, in which the motion of a massless particle (the third body) under the gravitational attraction

of the Sun and a planet (the primaries) is described. If the third body has a close encounter with the planet, part of the motion takes place far from it and another part, inside a neighbourhood of it. We will take as a neighbourhood of the planet the sphere B of radius $\mu^{1/3}$ around it, where μ is the mass parameter of the RTBP. Then, the outer solution and the inner solution will correspond with the motion outside and inside B respectively. More concretely, we fix the initial epoch at the moment in which the third body leaves B, this is, the initial conditions in an rotating frame $(\boldsymbol{\rho}_i, \dot{\boldsymbol{\rho}}_i)$ are such that

$$\rho_{2i} = |\boldsymbol{\rho}_i - \boldsymbol{\rho}_{_P}| = \mu^{1/3} \quad \text{and} \quad \boldsymbol{\rho}_{2i} \cdot \dot{\boldsymbol{\rho}}_i \geq 0, \tag{74}$$

where $\boldsymbol{\rho}_{_P}$ is the position of the planet. The inner solution corresponds with the solution of the equations of the RTBP with these initial conditions and moving backwards in time. The outer solution has two parts: before entering the sphere and after leaving it. The later corresponds with the solution of the equations with the same initial conditions and moving forward in time. It will be enough to study and give an analytical approximation of this part of the outer solution because the same arguments allow to obtain the same result for the part of the outer solution before entering the sphere.

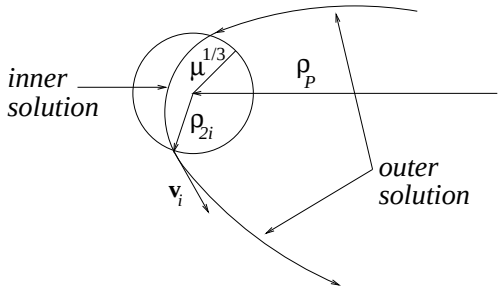

Figure 35: Outer and inner solutions.

6.1 The outer solution

The outer solution takes place far from the small primary, so the motion of the third body can be approximated by a keplerian orbit. We want to see how big is the error involved in this approximation.

Let us begin writing the equations of the RTBP as a first order system in a sidereal coordinate system as

$$\dot{\mathbf{q}} = \begin{pmatrix} \dot{\mathbf{r}} \\ -(1-\mu)\dfrac{\mathbf{r}-\mathbf{r}_{_S}}{r_1^3} \end{pmatrix} + \begin{pmatrix} 0 \\ -\mu\,\dfrac{\mathbf{r}-\mathbf{r}_{_P}}{r_2^3} \end{pmatrix} = G(\mathbf{q},\mu) + F(\mathbf{q},\mu), \tag{75}$$

where $\mathbf{q} = (\mathbf{r}, \dot{\mathbf{r}})$, $\mathbf{r}_{_S}$ and $\mathbf{r}_{_P}$ are the position vectors of the Sun and the planet and

$$\dot{\mathbf{q}} = G(\mathbf{q}, 0) \tag{76}$$

is the Kepler's equation. Let $\mathbf{q}(t)$ and $\mathbf{q}_0(t)$ be the solutions of (75) and (76) respectively, with the same initial condition $\mathbf{q}_i$. Since the equations (75) are

autonomous, we can consider that the initial condition occurs at $t = 0$. As $\mathbf{q}_i$ is on the sphere B and leaving it, we have that

$$r_2(0) = r_{2i} = |\mathbf{r}_i - \mathbf{r}_P| = \mu^{1/3} \text{ and } r_2(t) > \mu^{1/3} \tag{77}$$

for some $t > 0$. We will also suppose that the motion is bounded and takes place far from the Sun to avoid a collision with it.

In order to obtain an upper bound of $|\mathbf{q}(t) - \mathbf{q}_0(t)|$, we write the solutions of the equations (75) and (76) as

$$\begin{aligned} \mathbf{q}(t) &= \mathbf{q}_i + \int_0^t \Big(G(\mathbf{q}(\tau), \mu) + F(\mathbf{q}(\tau), \mu) \Big)\, d\tau\,, \\ \mathbf{q}_0(t) &= \mathbf{q}_i + \int_0^t G(\mathbf{q}_0(\tau), 0)\, d\tau. \end{aligned} \tag{78}$$

On one hand, the assumptions made on the motion of the massless particle implies that r is bounded and cannot be arbitrarily small, so we have that

$$G(\mathbf{q}(t), \mu) = G(\mathbf{q}(t), 0) + O(\mu),$$

and from the mean value theorem we obtain that

$$|G(\mathbf{q}(t), \mu) - G(\mathbf{q}_0(t), 0)| \leq K|\mathbf{q}(t) - \mathbf{q}_0(t)| + C\mu. \tag{79}$$

On the other hand, the function $F(\mathbf{q}, \mu)$ in (75) can be bounded using (77) as follows:

$$|F(\mathbf{q}(t), \mu)| = \frac{\mu}{r_2^2} \leq \frac{\mu}{\mu^{2/3}} = \mu^{1/3}. \tag{80}$$

Using (78), (79) and (80) we get that

$$\begin{aligned} |\mathbf{q}(t) - \mathbf{q}_0(t)| &\leq \mu^{1/3} t + Ct\mu + K \int_0^t |\mathbf{q}(\tau) - \mathbf{q}_0(\tau)|\, d\tau \\ &\leq \widetilde{C}\mu^{1/3} t + K \int_0^t |\mathbf{q}(\tau) - \mathbf{q}_0(\tau)|\, d\tau, \end{aligned} \tag{81}$$

for all the time such that (77) is verified.

At this point we use the following lemma[1]:

Lemma 1 *Let $g \in \mathcal{C}^1$ such that $g(t) \geq 0$.*

1. *If $g(t) \leq K_0 t + K_1 \displaystyle\int_0^t g(\tau)\, d\tau$ for $t \geq 0$, with $K_0, K_1 > 0$, then*

$$g(t) \leq K_0 t e^{K_1 t}$$

   for all $t \geq 0$.

2. *If $g(t) \leq K_0|t| + K_1 \displaystyle\int_t^0 g(\tau)\, d\tau$ for $t \leq 0$, with $K_0, K_1 > 0$, then*

$$g(t) \leq K_0 |t| e^{K_1 |t|},$$

   for all $t \leq 0$.

[1]The results are similar to Gronwall's Lemma.

Then, applying the first result of this Lemma to the inequality (81) we obtain that

$$|\mathbf{q}(t) - \mathbf{q}_0(t)| \leq \widetilde{C}\mu^{1/3} t e^{Kt}, \tag{82}$$

which means that if t is bounded, the error involved in the approximation of the outer solution by a keplerian orbit is, at least, of order $O(\mu^{1/3})$, this is

$$\mathbf{q}(t) = \mathbf{q}_0(t) + O(\mu^{1/3}), \tag{83}$$

for $t \in [0, M]$ and a fixed M.

This result depends strongly on (80). The bigger the distance to the small primary, the fewer the error. For instance, it is clear that for any time interval for which $r_2(t) \geq \mu^{1/6}$, then

$$|\mathbf{q}(t) - \mathbf{q}_0(t)| = O(\mu^{2/3}).$$

Initially, the orbit leaves B, $r_2(0) = \mu^{1/3} < \mu^{1/6}$, so the question is if the error done in (83) can be improved up to order $\mu^{2/3}$ for all time interval for which $\mu^{1/3} \leq r_2(t) \leq \mu^{1/6}$. The answer is affirmative if the initial velocity is not tangent to the sphere. In that case, for t close to the initial epoch, the third body is moving away from the planet and its distance grows. More accurate calculations prove that

$$r_2(t) \geq \mu^{1/3} + kt,$$

for a certain k not arbitrarily small and then

$$\int_0^t |F(\mathbf{q}(\tau), \mu)|\, d\tau = \int_0^t \frac{\mu}{r_2(\tau)^2}\, d\tau \leq \frac{\mu^{2/3}}{k}.$$

Using this result we obtain that

$$\mathbf{q}(t) = \mathbf{q}_0(t) + O(\mu^{2/3}), \tag{84}$$

for $t \in [0, M]$ and a fixed M.

6.2 Resonant orbits

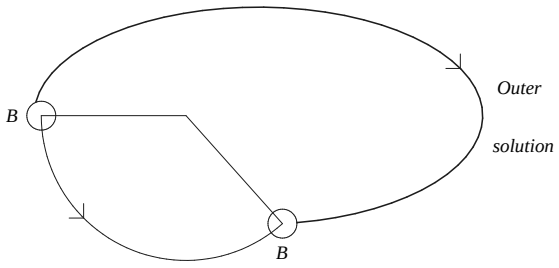

Figure 36: Qualitative representation of the outer solution of an orbit which leaves and goes back to the sphere B centered at the planet.

Missions with two or more flybys of one or more attracting bodies can be considered in order to reduce the energy requirements. A simpler way to achieve

this reduction in a interplanetary trajectory from one Earth to another plant is considering one gravity assist to a third planet. Nevertheless, the energy savings can be considered insufficient. One way to improve this performance is considering one or more gravity assists to the arrival planet. This kind of solutions have been considered by Yen in [12] in the framework of the analysis of a Mercury mission, where several resonant returns to Mercury are used in order to reduce the orbit capture Δv requirements. The Δv saving is made at the expense of flight time, because the spacecraft must return to the planet at about the same position in space to obtain a gravity assist. For example, performing two gravity assists to Mercury a substantial reduction of the v_∞ at Mercury, from 5.7 km/s to 4.7 km/s, can be achieved, although there is a penalty in the flight time of 270 days, which is three Mercury years.

Let us considerer a resonant orbit as a trajectory of the infinitesimal body with consecutive approaches to the small primary such that between two close encounters, both the massless particle and the planet perform an entire (not necessarily equal) number of revolutions around the Sun. In order to characterize the resonant orbits around a planet, we can use the analytical approximation of the outer solution given by (84).

The resonant orbits satisfy the restrictions made in the previous section: they leave a neighbourhood of a planet, which we will suppose is the sphere B, and go back to the same neighbourhood in a finite time. This implies that the outer solution of the resonant orbits can be approach by an elliptic orbit. More precisely, we say that an orbit is a p-q resonant orbit if the time spent in leaving the sphere B and returning for the first time to the same sphere is

$$T = 2\pi q + \varepsilon \mu^{1/3} + O(\mu^{2/3}) = 2\pi p \tau + \delta \mu^{1/3} + O(\mu^{2/3}), \tag{85}$$

where $p, q \in \mathbb{N}$ are relatively prime, ε and δ are suitable constants and $2\pi\tau$ is the period of the approximated ellipse $\mathbf{q}_0(t)$.

In order to characterize the resonant orbits, we will obtain a set of conditions on the initial position and velocity coming from two restrictions: the orbits leave the sphere B and return to it in time T. The process will be the following: we will compute the energy of the approximated ellipse, its angular momentum and the final position on the sphere B at the return time T and we will give developments for all of them in terms of powers of $\mu^{1/3}$. Equating terms of the same order (of the appropriate developments) we will obtain the set of conditions that define the resonant orbits.

Since the initial conditions are taken on the sphere B at $t = 0$, they can be expressed in spherical coordinates in the rotating frame as

$$\begin{aligned} \boldsymbol{\rho}_i &= \begin{pmatrix} x_i \\ y_i \\ z_i \end{pmatrix} = \begin{pmatrix} \mu - 1 + \mu^{1/3} \cos\varphi \, \cos\theta \\ \mu^{1/3} \cos\varphi \, \sin\theta \\ \mu^{1/3} \sin\varphi \end{pmatrix}, \\ \dot{\boldsymbol{\rho}}_i &= \begin{pmatrix} \dot{x}_i \\ \dot{y}_i \\ \dot{z}_i \end{pmatrix} = v_i \begin{pmatrix} \cos\overline{\phi} \, \cos\overline{\psi} \\ \cos\overline{\phi} \, \sin\overline{\psi} \\ \sin\overline{\phi} \end{pmatrix}. \end{aligned} \tag{86}$$

For a fixed position on B (this is, fixed φ and θ), there are different velocities for which the orbit comes back to the same sphere (see Fig. 37). For this reason

we write the spherical coordinates of the velocity, $\overline{\phi}$ and $\overline{\psi}$, as

$$\begin{array}{rcl} \overline{\phi} & = & \phi + \Delta\phi\, \mu^{1/3} + O(\mu^{2/3}), \\ \overline{\psi} & = & \psi + \Delta\psi\, \mu^{1/3} + O(\mu^{2/3}). \end{array} \tag{87}$$

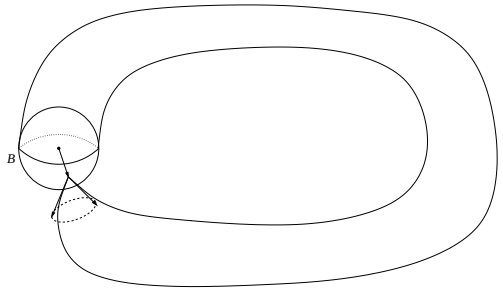

Figure 37: Fixed the initial position on the sphere B, there are different initial velocities such that the orbit comes back to B. The curves on the figure are the qualitative representation of two solutions of the RTBP that come back to B tangentially.

To guarantee that the orbit leaves B at the initial epoch, it is necessary to avoid the tangent direction, so the initial conditions must verify that

$$0 < \frac{\boldsymbol{\rho}_{2i} \cdot \dot{\boldsymbol{\rho}}_i}{\mu^{1/3} v_i} = \cos\overline{a}, \tag{88}$$

where $v_i = |\boldsymbol{\rho}|$ and a is the angle between $\boldsymbol{\rho}_{2i}$ and $\dot{\boldsymbol{\rho}}_i$. Using (86) and (87), we can write

$$\cos\overline{a} = \cos a + O(\mu^{1/3}) \tag{89}$$

where

$$\cos a = \cos\varphi\, \cos\phi\, \cos(\theta - \psi) + \sin\varphi\, \sin\phi,$$

and (88) can be expressed as $\varepsilon \leq \cos a$, for some ε.

Furthermore, using the Jacobi integral (18) and (86), the initial synodical velocity v_i can be written in terms of C_J and μ as

$$v_i^2 = 3 - C_J + (\cos^2\varphi\,(1 + 3\cos^2\theta) + 1)\mu^{2/3} + O(\mu). \tag{90}$$

This equation implies that $C_J < 3$. In the planar problem this means that there are no zero velocity curves, but in the spatial case still zero velocity surfaces (and so, forbidden regions for the motion) exist, although they do not intersect the $z = 0$ plane.

As we have said, the outer solution of a resonant orbit can be approximated by a keplerian orbit which must be an ellipse. Both, the outer solution and the ellipse, have the same initial conditions, so we can compute the energy h in terms of the spherical coordinates φ, θ, ϕ, ψ, the Jacobi constant and μ. We will use the relations (86), (87) and (90). The energy of the keplerian orbit is given by

$$h = \frac{|\dot{\mathbf{r}}_\mathbf{i}|^2}{2} - \frac{1}{|\mathbf{r}_i|}. \tag{91}$$

On one hand,

$$r_i^2 = 1 - 2\mu^{1/3}\cos\varphi\,\cos\theta + O(\mu^{2/3}). \tag{92}$$

On the other hand, we use the relation between the sidereal and synodical velocities

$$|\dot{\mathbf{r}}|^2 = |\dot{\boldsymbol{\rho}}|^2 + 2(x\dot{y} - \dot{x}y) + x^2 + y^2,$$

which at the initial condition gives

$$|\dot{\mathbf{r}}_\mathbf{i}|^2 = 4 - C_J - 2\sqrt{3 - C_J}\cos\phi\sin\psi + O(\mu^{1/3}). \tag{93}$$

Introducing (92) and (93) in (91) we can develop h in terms of $\mu^{1/3}$, obtaining the following expression for the energy

$$h = h_0 + O(\mu^{1/3}) = 1 - \frac{C_J}{2} - \sqrt{3 - C_J}\cos\phi\,\sin\psi + O(\mu^{1/3}). \tag{94}$$

Let us introduce the fact that the orbit is a resonant orbit. As we know, the energy h and the period τ (modulus 2π) of a keplerian orbit verify that

$$\tau^{2/3} = \frac{1}{2|h|}. \tag{95}$$

¿From (85) τ can be written as

$$\tau = \frac{q}{p} + \frac{\varepsilon - \delta}{2\pi p}\,\mu^{1/3} + O(\mu^{2/3}),$$

and, therefore,

$$\tau^{2/3} = \left(\frac{q}{p}\right)^{2/3} + \frac{1}{3}\left(\frac{p}{q}\right)^{1/3}\frac{\varepsilon - \delta}{\pi p}\mu^{1/3} + O(\mu^{2/3}). \tag{96}$$

Using (95) and equating the terms of order zero of (94) and (96), we get that

$$C_J - 2 + 2\sqrt{3 - C_J}\cos\phi\,\sin\psi = \left(\frac{p}{q}\right)^{2/3}. \tag{97}$$

¿From this expression we can get several information. First of all, we notice that (97) implies that the energy is negative, because $h_0 < 0$. Next, we observe that $(p/q)^{2/3} \leq C_J - 2 + 2\sqrt{3 - C_J} \leq 2$, so p and q must verify

$$\frac{p}{q} \leq 2\sqrt{2}. \tag{98}$$

Moreover, (97) implies that $\left|2 - C_J + \left(\frac{p}{q}\right)^{2/3}\right| \leq 2\sqrt{3 - C_J}$, from which we get that $C_J \in [C_{J_1}, C_{J_2}]$ where

$$C_{J_{1,2}} = \left(\frac{p}{q}\right)^{\frac{2}{3}} \mp 2\sqrt{2 - \left(\frac{p}{q}\right)^{\frac{2}{3}}}. \tag{99}$$

The next condition to be required is to avoid collision with the big primary, which implies that the angular momentum $\mathbf{c}$ cannot vanish. As before, we can

compute $\mathbf{c}$ of the keplerian orbit in terms of the initial conditions from the expression

$$\mathbf{c} = \mathbf{r}_i \wedge \dot{\mathbf{r}}_i = \boldsymbol{\rho}_i \wedge \dot{\boldsymbol{\rho}}_i + \mathbf{w}_i,$$

where $\mathbf{w}_i = (-x_i z_i, -y_i z_i, x_i^2 + y_i^2)$. Using again (86), (87) and (90) the modulus of $\mathbf{c}$ can be expressed as

$$c^2 = (3 - C_J)\sin^2\phi \, + \, (1 - \sqrt{3 - C_J}\cos\phi \, \sin\psi)^2 + O(\mu^{1/3}), \tag{100}$$

and the condition $\mathbf{c} \neq 0$ can be expressed as

$$(3 - C_J)\sin^2\phi \, + \, (1 - \sqrt{3 - C_J}\cos\phi \, \sin\psi)^2 \neq 0.$$

As this expression is the sum of two squares, it will be sufficient if one of them is different from zero. The first one do not vanish if $\phi \neq 0$. If $\phi = 0$, then it will be necessary that $\sin\phi \neq 1/\sqrt{3 - C_J}$, which using (97) is equivalent to $C_J \neq (p/q)^{2/3}$. Thus, the condition will be

$$\phi_0 \neq 0, \qquad \text{or} \qquad C_J \neq \left(\frac{p}{q}\right)^{2/3}. \tag{101}$$

Observe that, for planar orbits, using the same developments as above, the angular momentum can be written as

$$\mathbf{c} = \left(0, 0, \frac{1}{2}\left(C_J - \left(\frac{p}{q}\right)^{2/3}\right)\right) + O(\mu^{1/3}).$$

According to the classification given in a previous section depending on the sign of the energy and the angular momentum, the orbits with values of the Jacobi constant $C_J < (p/q)^{2/3}$ are elliptic retrograde, whereas the orbits are elliptic direct if $C_J > (p/q)^{2/3}$.

Summarizing, for a fixed values of p and q, the range of admissible values for C_J is $[C_{J_1}, C_{J_2}] \subset (-2\sqrt{2}, 3)$. Moreover, if the initial velocity is parallel to the $z = 0$ plane ($\phi = 0$), then $C_J \neq (p/q)^{2/3}$. In Fig. 38 the restrictions for the Jacobi constant are represented.

At this point, the spherical coordinates of the initial conditions and the Jacobi constant of orbits with period given by (85), initial negative energy and such that leave the sphere B avoiding the tangent direction, have been characterized. The restrictions are given by (88), (97) and (100). There is a final condition to be imposed on the orbits and comes from the fact that they must come back to B at time T. To deal with it, we will derive an explicit expression for the out map, which is associated to follow the flow forward in time and applies the initial conditions $\mathbf{q}_i$ to the position and velocity $\mathbf{q}_e = \mathbf{q}(T)$ at the return time T.

In order to obtain an expression for the final position and velocity, we use(85) and the approximation by the elliptic orbit given by (84):

$$\begin{aligned} \mathbf{r}(T) &= \mathbf{r}_0(T) + O(\mu^{2/3}) = \mathbf{r}_0(2\pi p\tau + \delta\mu^{1/3}) + O(\mu^{2/3}) \\ &= \mathbf{r}_0(2\pi p\tau) + \dot{\mathbf{r}}_0(2\pi p\tau)\delta\mu^{1/3} + O(\mu^{2/3}) \\ &= \mathbf{r}_i + \dot{\mathbf{r}}_i\delta\mu^{1/3} + O(\mu^{2/3}), \end{aligned} \tag{102}$$

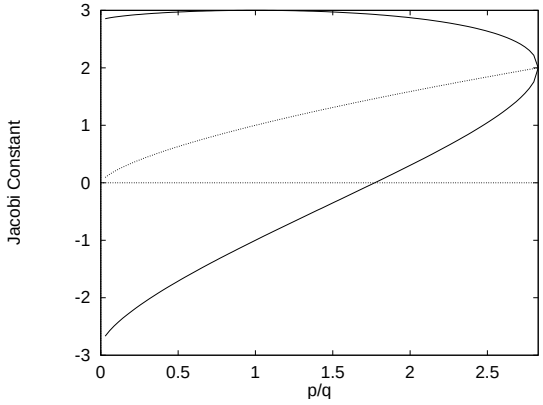

Figure 38: The area limited by the continuous curve defines the range of variation of the Jacobi constant of the resonant orbits as a function of p/q. The dotted curve represents the values $C_J = (p/q)^{2/3}$ which must be excluded if $\phi = 0$. The upper and lower regions correspond to direct and retrograde orbits respectively.

where we have used that $2\pi p\tau$ is the period of the elliptic orbit $\mathbf{q}_0$, and $\mathbf{r}_i$ and $\dot{\mathbf{r}}_i$ are its initial conditions. Analogously, the position of the planet at epoch T can be expressed as

$$\mathbf{r}_{_P}(T) = \mathbf{r}_{_P}(2\pi q + \varepsilon\mu^{1/3}) + O(\mu^{2/3}) = \mathbf{r}_{_P}(0) + \dot{\mathbf{r}}_{_P}(0)\varepsilon\mu^{1/3} + O(\mu^{2/3}) \quad (103)$$

The condition we need is $|\mathbf{r}(T) - \mathbf{r}_{_P}(T)| = \mu^{1/3}$. Using (102) and (103) we write

$$|\mathbf{r}(T) - \mathbf{r}_{_P}(T)| = |\mathbf{r}_i - \mathbf{r}_{_P}(0) + \mu^{1/3}(\dot{\mathbf{r}}_i\delta - \dot{\mathbf{r}}_{_P}(0)\varepsilon)| + O(\mu^{2/3}),$$

which can be expressed as $|\mathbf{r}(T) - \mathbf{r}_{_P}(T)| = \mu^{1/3}|\mathbf{w}| + O(\mu^{2/3})$ where

$$\begin{aligned} |\mathbf{w}|^2 \quad = \quad & 1 + (\varepsilon-\delta)^2 + (3-C_J)\delta^2 + 2(\varepsilon-\delta)\delta\sqrt{3-C_J}\,\cos\phi\,\sin\psi \\ & +2\delta\sqrt{3-C_J}\,(\cos\varphi\,\cos\phi\,\cos(\psi-\theta) + \sin\varphi\,\sin\psi) \\ & +2(\varepsilon-\delta)\cos\varphi\,\sin\theta. \end{aligned}$$

The condition we will ask is $\mathbf{w} = 1$, or equivalently

$$\begin{aligned} (\varepsilon-\delta)^2 + \delta^2(3-C_J) + \,2\,(\varepsilon-\delta)\cos\varphi\,\sin\theta \\ +\,2\delta\sqrt{3-C_J}\,\cos a + 2(\varepsilon-\delta)\delta\,\sqrt{3-C_J}\cos\phi\,\sin\psi \quad = \quad 0. \end{aligned} \quad (104)$$

Thus, ε and δ, the terms of order $\mu^{1/3}$ of the return time T, have to verify equation (104). This equation represents an ellipse in the $(\delta, \varepsilon-\delta)$ plane, except if $1 = \cos^2\phi\sin^2\psi$. In these cases, equation (104) represents two lines, so δ and $\varepsilon-\delta$ can take any real value and then T could be arbitrarily large. To avoid this, it is necessary to impose that $\cos^2\phi\sin^2\psi \neq 1$ which, using (97), is equivalent to $C_J \neq C_{J_{1,2}}$.

6.2.1 The out-map

The out map applies the initial position and velocity $(\mathbf{r}_i, \dot{\mathbf{r}}_i)$ to the final position and velocity on B at the return time T, $(\mathbf{r}_e, \dot{\mathbf{r}}_e)$. We have seen in (102) that

$$\mathbf{r}_e = \mathbf{r}_i + \dot{\mathbf{r}}_i\delta\mu^{1/3} + O(\mu^{2/3}).$$

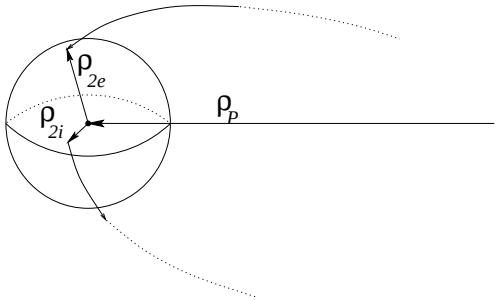

Figure 39: Qualitative representation of the out map in a synodical reference system.

Analogously it can be derived an expression for the velocity:

$$\begin{aligned}\dot{\mathbf{r}}(T) &= \dot{\mathbf{r}}_0(2\pi p\tau + \delta\mu^{1/3}) + O(\mu^{2/3}) \\ &= \dot{\mathbf{r}}_0(2\pi p\tau) + \ddot{\mathbf{r}}_0(2\pi p\tau)\delta\mu^{1/3} + O(\mu^{2/3}) \\ &= \dot{\mathbf{r}}_i - \frac{\dot{\mathbf{r}}_i}{r_i^3}\,\delta\mu^{1/3} + O(\mu^{2/3}).\end{aligned}$$

Using that $r_i = 1 + O(\mu^{1/3})$, we get that the out-map in the sidereal coordinates is given by the expressions

$$\begin{aligned}\mathbf{r}_e &= \mathbf{r}_i + \dot{\mathbf{r}}_i\delta\mu^{1/3} + O(\mu^{2/3}) \\ \dot{\mathbf{r}}_e &= \dot{\mathbf{r}}_i - \mathbf{r}_i\delta\mu^{1/3} + O(\mu^{2/3}).\end{aligned} \tag{105}$$

These expressions give us the position and velocity at the return time on the sphere B in terms of the initial conditions.

In [6], orbits which undergo consecutive close encounters with the small primary in the planar RTBP are considered. The numbers of revolutions of the small bodies around the larger one between consecutive encounters can be chosen to be two arbitrary sequences (p_n, q_n), with constraints depending on the Jacobi constant.

6.3 The inner solution

As the third body approaches the small primary, the influence of the big one can be considered as a perturbation. The inner solution takes place inside the sphere B, so the orbit will be, approximately, an hyperbolic orbit. As for the outer solution, we want to study the difference between the real solution and the approximated hyperbola, for which it will be convenient to remove the singularity of the system due to the small primary. To achieve this we begin regularizing the equations of motion.

Let $(\boldsymbol{\rho}, \dot{\boldsymbol{\rho}})$ be the solution of the equations of motion (17) in a synodic reference system with initial condition on the sphere B, this is, the solution of

$$\ddot{\boldsymbol{\rho}} + A_3\dot{\boldsymbol{\rho}} = \nabla\Omega(\boldsymbol{\rho}), \quad \boldsymbol{\rho}(0) = \boldsymbol{\rho}_i,\ \dot{\boldsymbol{\rho}}(0) = \dot{\boldsymbol{\rho}}_i, \tag{106}$$

where $\Omega(\boldsymbol{\rho}) = \dfrac{1}{2}(x^2+y^2) + \dfrac{1-\mu}{r_1} + \dfrac{\mu}{r_2}$ and $A_3 = \begin{pmatrix} 0 & -2 & 0 \\ 2 & 0 & 0 \\ 0 & 0 & 0 \end{pmatrix}$.

Simultaneously to the regularization we will perform a change of scale in order to transform the sphere B into a sphere of radius 1, so we will introduce the parameter $\mu^{1/3}$ into the equations. This will allows us to develop the equations of motion in powers of $\mu^{1/3}$ and, truncating at first order, we will obtain an approximated solution of the real orbit.

To regularize, we use Kustaanheimo-Stiefel (KS) transformation, which is defined by

$$\boldsymbol{\rho} = \boldsymbol{\rho}_{_P} + \mu^{1/3} L(\mathbf{u})\mathbf{u}, \quad \frac{dt}{ds} = r_2, \tag{107}$$

where $\mathbf{u} = (u_1, u_2, u_3, u_4)$, a zero fourth component to the vector $\boldsymbol{\rho}$ and $\boldsymbol{\rho}_{_P}$ has been added and

$$L(\mathbf{u}) = \begin{pmatrix} u_1 & -u_2 & -u_3 & u_4 \\ u_2 & u_1 & -u_4 & -u_3 \\ u_3 & u_4 & u_1 & u_2 \\ u_4 & -u_3 & u_2 & -u_1 \end{pmatrix}.$$

We observe that $L(\mathbf{u})^T L(\mathbf{u}) = |\mathbf{u}|^2 I_4$ (I_4 identity matrix 4×4), so $r_2 = \mu^{1/3}|\mathbf{u}|^2$. Therefore, the sphere B transforms into the sphere $B^* = \{\mathbf{u} \in \mathbb{R}^4;\ |\mathbf{u}| \leq 1\}$.

The change of coordinates (107) introduces a change in time, as well. As the inner solution is the solution of the equation (106) when the third body moves backwards in time, we can write the relation between t and s (time in KS coordinates) as

$$t = -\mu^{\alpha} \int_s^0 |\mathbf{u}(\tau)|^2 d\tau. \tag{108}$$

We denote $' = d/ds$. To write the new equations of motion, we will make use of the following Lemma ([10]):

Lemma 2 *Let $\mathbf{u}, \mathbf{w} \in \mathbb{R}^4$ satisfying the bilinear relation*

$$l(\mathbf{u}, \mathbf{w}) = u_1 w_4 - u_2 w_3 + u_3 w_2 - u_4 w_1 = 0.$$

Then

1. $L(\mathbf{u})\mathbf{w} = L(\mathbf{w})\mathbf{u}$
2. $\langle \mathbf{u}, \mathbf{u} \rangle L(\mathbf{w})\mathbf{w} - 2\langle \mathbf{u}, \mathbf{w} \rangle L(\mathbf{u})\mathbf{w} + \langle \mathbf{w}, \mathbf{w} \rangle L(\mathbf{u})\mathbf{u} = 0$

Once we get the equations of motion, it can be proved that $l(\mathbf{u}, \mathbf{u}')$ is a first integral. This means that

$$l(\mathbf{u}(s), \mathbf{u}'(s)) = u_4' u_1 - u_3' u_2 + u_3 u_2' - u_4 u_1' = 0, \tag{109}$$

has to be fulfilled at just one point, for instance at the initial condition ($s = 0$). We will take this into account when we choose the initial conditions.

We want to write the left side of (106) in terms of the new variables. Let us suppose that (109) is satisfied $\forall\, s$. Then using the first property of the Lemma we get that

$$\dot{\boldsymbol{\rho}} = \frac{2}{|\mathbf{u}|^2} L(\mathbf{u})\mathbf{u}', \tag{110}$$

and deriving this expression and using the second property of the Lemma we get that

$$\ddot{\mathbf{r}}^s = \frac{2\mu^{-1/3}}{|\mathbf{u}|^4} \left(L(\mathbf{u})\mathbf{u}'' - \frac{|\mathbf{u}'|^2}{|\mathbf{u}|^2} L(\mathbf{u})\mathbf{u} \right). \tag{111}$$

We also need to express $\nabla\Omega(\boldsymbol{\rho})$ in terms of the new coordinates. First we write

$$\begin{aligned}\nabla\Omega(\boldsymbol{\rho}) &= \begin{pmatrix} x \\ y \\ 0 \end{pmatrix} - \frac{1-\mu}{r_1^3}\begin{pmatrix} x-\mu \\ y \\ z \end{pmatrix} - \frac{\mu}{r_2^3}\begin{pmatrix} x-\mu+1 \\ y \\ z \end{pmatrix} \\ &= \mathbf{p} - \left(\frac{1-\mu}{r_1^3} + \frac{\mu}{r_2^3}\right)\boldsymbol{\rho}_2 + (1-\mu)\left(\frac{1}{r_1^3} - 1\right)\mathbf{e}_1,\end{aligned} \tag{112}$$

where $\mathbf{p} = (x-\mu+1, y, 0)$ and $\mathbf{e}_1 = (1,0,0)$. Next, we are going to expand the expression (112) in terms of powers of $\mu^{1/3}$. Using (107) we have that

$$\begin{aligned} r_2 &= \mu^{1/3}|\mathbf{u}|^2, \\ r_1^2 &= 1 - 2u_x\mu^{1/3} + \mu^{2/3}|\mathbf{u}|^4, \\ \frac{1}{r_1^3} &= 1 + 3\mu^{1/3}u_x + O(\mu^{2/3}), \end{aligned}$$

where u_x and u_y are given by $x - \mu + 1 = \mu^{1/3}u_x$ and $y = \mu^{1/3}u_y$. Introducing these relations in (112) we get that

$$\nabla\Omega(\boldsymbol{\rho}) = \mu^{1/3}\left[\mathbf{p} + \left(1 + \frac{1}{|\mathbf{u}|^6}\right)L(\mathbf{u})\mathbf{u} + 3u_x\mathbf{e}_1\right] + O(\mu^{2/3}), \tag{113}$$

where we have used that $|\mathbf{u}|$ is bounded because we are interested in the motion inside B^*.

Now, substituting (110), (111) and (113) into (106) we get that

$$\begin{aligned} L(\mathbf{u})\mathbf{u}'' - \frac{|\mathbf{u}'|^2}{|\mathbf{u}|^2}L(\mathbf{u})\mathbf{u} &= \frac{\mu^{1/3}}{2}|\mathbf{u}|^4\left(-\frac{2}{|\mathbf{u}|^2}A_3L(\mathbf{u})\mathbf{u}' + \nabla\Omega(\boldsymbol{\rho})\right) \\ &= -\mu^{1/3}|\mathbf{u}|^2A_3L(\mathbf{u})\mathbf{u}' + \frac{\mu^{2/3}}{2|\mathbf{u}|^2}L(\mathbf{u})\mathbf{u} + O(\mu^{2/3}). \end{aligned} \tag{114}$$

In order to get the final equations of motion (where the singularity do not appear) it will be necessary to introduce the Jacobi integral $|\dot{\boldsymbol{\rho}}|^2 = 2\Omega(\mathbf{r}) - C_J$. On one hand, from (110) we get that

$$|\dot{\boldsymbol{\rho}}|^2 = \frac{4}{|\mathbf{u}|^4}L(\mathbf{u})\mathbf{u}' \cdot L(\mathbf{u})\mathbf{u}' = 4\frac{|\mathbf{u}'|^2}{|\mathbf{u}|^2}\,.$$

¿From another hand,

$$\begin{aligned} 2\Omega(\boldsymbol{\rho}) &= x^2 + y^2 + 2\frac{1-\mu}{\sqrt{(x-\mu)^2+y^2+z^2}} + 2\frac{\mu}{\sqrt{(x-\mu+1)^2+y^2+z^2}} \\ &= (\mu - 1 + \mu^{1/3}u_x)^2 + \mu^{2/3}u_y^2 + \frac{2(1-\mu)}{\sqrt{1-2\mu^{1/3}u_x + O(\mu^{2/3})}} + \frac{2\mu^{2/3}}{|\mathbf{u}|^2} \\ &= 1 - 2\mu^{1/3}u_x + 2(1+\mu^{1/3}u_x) + 2\frac{\mu^{2/3}}{|\mathbf{u}|^2} + O(\mu^{2/3}) \\ &= 3 + 2\frac{\mu^{2/3}}{|\mathbf{u}|^2} + O(\mu^{2/3}). \end{aligned}$$

Then, the expression of the Jacobi constant in terms of powers of $\mu^{1/3}$ is

$$\frac{|\mathbf{u}'|^2}{|\mathbf{u}|^2} = \frac{3 - C_J}{4} + \frac{\mu^{2/3}}{2|\mathbf{u}|^2} + O(\mu^{2/3}). \tag{115}$$

Substituting (115) in (114) we finally obtain the equations of motion in KS coordinates expressed in powers of $\mu^{1/3}$:

$$\mathbf{u}'' = \frac{3 - C_J}{4}\,\mathbf{u} - \mu^{1/3}|\mathbf{u}|^2 L(\mathbf{u})^t A_3 L(\mathbf{u})\mathbf{u}' + O(\mu^{2/3}). \tag{116}$$

The initial conditions $(\mathbf{u}_i, \mathbf{u}_i')$ are chosen such that $\mathbf{u}_i$ is any solution of the equation $\boldsymbol{\rho}_i = \mu^{1/3} L(\mathbf{u}_i)\mathbf{u}_i$ (observe that there is one degree of freedom) and $\mathbf{u}_i'$ is such that verifies $\mathbf{u}_i' = \frac{1}{2} L(\mathbf{u}_i)^t \dot{\mathbf{r}}_i^s$. This choice ensures that $l(\mathbf{u}_i, \mathbf{u}_i') = 0$.

The equation (116) can be written as a first order system as

$$\begin{array}{c} \mathbf{U}'' = C\mathbf{U} + O(\mu^{1/3}) \\ \mathbf{U}(0) = \mathbf{U}_i \end{array} \tag{117}$$

where $\mathbf{U} = (\mathbf{u}, \mathbf{u}')$,

$$C = \begin{pmatrix} 0 & I_4 \\ c\, I_4 & 0 \end{pmatrix},$$

and $c = (3 - C_J)/4$. Let $\mathbf{U}(s)$ be the solution of (117) (this is, the inner solution) and $\mathbf{U}_0(s)$ be the solution of the truncated equation $\mathbf{U}'' = C\mathbf{U}$ with the same initial conditions (the hyperbolic orbit). Then, applying the same Lema as in the approximation of the outer solution we get that

$$|\mathbf{U}(s) - \mathbf{U}_0(s)| \leq |s| K \mu^{1/3} e^{\bar{c}|s|}, \tag{118}$$

for all time s for which the orbit is inside the sphere B^* and where $\bar{c} = \max(1, (3 - C_J)/4)$. This result states that if the orbit remains inside B^* for a bounded time the error done in the approximation is of order $\mu^{1/3}$. In order to know the magnitude of the error in synodic coordinates, it is necessary to undo the change of variables. It is immediately from (107) that the error will be of order $\mu^{2/3}$ for the synodical positions. Nevertheless, for the synodical velocities we have to use (110).In this case, if $|\mathbf{u}(s)|$ cannot be arbitrarily small, the error will be of order $\mu^{1/3}$.

As for the outer solution, (118) can be improved. It will be necessary to keep more terms in the equations (116). The problem is that the term of order $\mu^{1/3}$, is not linear. In order to solve this difficulty, it is necessary to introduce a change of coordinates previous to the K-S coordinates, which allows us to write the equations as

$$\mathbf{u}'' = \frac{3 - C_J}{4}\mathbf{u} + \mu^{1/3} f(\mathbf{u}, \mathbf{u}')\mathbf{u} + O(\mu^{2/3}),$$

where $f(\mathbf{u}, \mathbf{u}') = -u_2 u_1' + u_1 u_2' - u_4 u_3' + u_3 u_4'$. Then, using (118) and explicit expressions for $\mathbf{U}_0$ it can be easily seen that

$$f(\mathbf{U}) = f(\mathbf{U}_0) + O(\mu^{1/3}) = k + O(\mu^{1/3})$$

for some constant k. This implies that the equations can be written as

$$\mathbf{u}'' = c\mathbf{u} + O(\mu^{2/3}), \tag{119}$$

where now $c = (3 - C_J)/4 + k\mu^{1/3}$. Then, if we consider the solution of the linear part of the equations (119) as an approximation of the solution of the

whole equations, we get that the error will be of order $\mu^{2/3}$ in K-S coordinates, and of order μ and $\mu^{2/3}$ for the synodical positions and velocities respectively.

For the moment, it will be sufficient to consider the approximation given by (118). As we have said, it is necessary to ensure that the time spent inside the sphere is finite and that the minimum distance to the planet is not too small. For this, we will compute the time spent for the hyperbolic orbit inside B^* and its distance to the origin at the pericenter as well.

The solution $\mathbf{u}_0$ can be written explicitly in terms of the initial conditions as

$$\mathbf{u}_0(s) = \cosh(\sqrt{c}s)\mathbf{u}_i + \frac{\sinh(\sqrt{c}s)}{\sqrt{c}}\mathbf{u}_i'. \tag{120}$$

Let us denote $V_i = |\mathbf{u}_i'|$ and η_i such that $\mathbf{u}_i \cdot \mathbf{u}_i' = V_i \cos\eta_i$. The modulus $|\mathbf{u}(s)|$ can be written as

$$|\mathbf{u}(s)|^2 = \frac{1}{2}\left(1 + \frac{V_i^2}{c}\right)\cosh(2\sqrt{c}s) + \frac{V_i\cos\eta_i}{\sqrt{c}}\sinh(2\sqrt{c}s) + \frac{1}{2}\left(1 - \frac{V_i^2}{c}\right), \tag{121}$$

where we have use that $|\mathbf{u}_i| = 1$. Deriving this expression and equating to zero, we will obtain the time of passage at pericenter, which is

$$s_p = \frac{1}{4\sqrt{c}}\ln\left(\frac{m_i - n_i}{m_i + n_i}\right), \tag{122}$$

where

$$m_i = 1 + \frac{V_i^2}{c} \quad \text{and} \quad n_i = 2\frac{V_i\cos\eta_i}{\sqrt{c}}.$$

V_i and η_i can be expressed in terms of the synodical initial conditions. From the expression of the Jacobi constant (115), we get that

$$V_i^2 = c + O(\mu^{2/3}), \tag{123}$$

and from (107) and (110)

$$\boldsymbol{\rho}_{2i} \cdot \dot{\boldsymbol{\rho}}_i = 2\mu^{1/3}\mathbf{u}_i \cdot \mathbf{u}_i', \tag{124}$$

which implies that $v_i \cos\overline{a} = 2V_i\cos\eta$. We use again the spherical coordinates for the synodical initial conditions introduced in (86). Then, using $v_i = 2\sqrt{c} + O(\mu^{2/3})$ (obtained from (90)), (123), (88) and (89), the expression (124) gets that

$$\cos\eta_i = \cos\overline{a}\,(1 + O(\mu^{1/3})). \tag{125}$$

Observe that $m_i \geq n_i$ and $n_i > 0$, so $s_m < 0$. We can also write m_i and n_i in terms of the initial conditions. From (123), $m_i = 2 + O(\mu^{2/3})$ and $n_i = 2\cos\eta_i + O(\mu^{2/3})$. Then

$$\begin{array}{rcl} m_i^2 - n_i^2 & = & 4(1 - \cos^2\eta_i) + O(\mu^{2/3}) = 4\sin^2\eta_i + O(\mu^{2/3}), \\ m_i - n_i & = & 2(1 - \cos\eta_i) + O(\mu^{2/3}) = 2(1 - \cos a) + O(\mu^{1/3}), \\ m_i + n_i & = & 2(1 + \cos\eta_i) + O(\mu^{2/3}) = 2(1 + \cos a) + O(\mu^{1/3}). \end{array} \tag{126}$$

Introducing the two last equations in (122) we get that the time of passage at pericenter can be written as

$$s_p = \frac{1}{3 - C_J}\ln\left(\frac{1 - \cos a}{1 + \cos a}\right) + O(\mu^{1/3}), \tag{127}$$

provided that $1-\cos a$ is not too small. This implies that we have to avoid the case in which the third body leaves the sphere in the direction of the radius vector. When the third body moves backwards in time, this is the direction to the center of the sphere, this is, the direction to collision with the small primary.

Furthermore, the time s_f spent in B^* by the third body is twice the time of passage at pericenter, so s_f will be bounded whenever

$$1-\cos a \geq \epsilon > 0,$$

for some ϵ. Assuming this, from (108) we can obtain an approximate expression for the synodical time spent in B. Using the approximation given by $\mathbf{u}_0$ and (121) and after some calculations, we can write

$$t_f = -\mu^{1/3}\int_{s_f}^{0} |\mathbf{u}_0|\, ds + O(\mu^{2/3}) = -\mu^{1/3}\frac{\cos a}{\sqrt{c}} + O(\mu^{2/3}).$$

So, the time spent within B is of order $\mu^{1/3}$. In previous sections, we have supposed that close encounters to a planet performs an impulsive change in the velocity. This can be done if the time t_f can be neglected, this is, for small values of the mass parameter μ.

Finally, we can also get the minimum distance to the origin. Substituting s_p into the expression (121) it can be obtained that

$$|\mathbf{u}(s)|^2 = 1-\frac{1}{2}(m_i-\sqrt{m_i^2-n_i^2}) = \sin a + O(\mu^{1/3}).$$

Again, assuming that the angle a cannot be small, the minimum distance to the small primary is bounded.

6.3.1 The in-map

Analogously to the out-map, the in-map applies the initial position and velocity $(\mathbf{r}_i, \dot{\mathbf{r}}_i)$ to the final position and velocity on B at the return time T, $(\mathbf{r}_f, \dot{\mathbf{r}}_f)$, when the third body moves backwards inside the sphere B. To derive expressions for $(\mathbf{r}_f, \dot{\mathbf{r}}_f)$, we can use the approximation given by (118). First, an explicit expression for the in-map of the hyperbolic approximation $\mathbf{U}_0$ can be obtain from (120), using that

$$s_f = \frac{1}{2\sqrt{c}}\ln\left(\frac{m_i-n_i}{m_i+n_i}\right),$$

and

$$\begin{aligned}
\cosh(\sqrt{c}\, s_f) &= \frac{1}{2}\sqrt{\frac{m_i-n_i}{m_i+n_i}}) + \frac{1}{2}\sqrt{\frac{m_i+n_i}{m_i-n_i}}) = \frac{m_i}{\sqrt{m_i^2-n_i^2}},\\
\sinh(\sqrt{c}\, s_f) &= \frac{1}{2}\sqrt{\frac{m_i-n_i}{m_i+n_i}}) - \frac{1}{2}\sqrt{\frac{m_i+n_i}{m_i-n_i}}) = \frac{-n_i}{\sqrt{m_i^2-n_i^2}}.
\end{aligned}$$

Then, the in-map in K-S coordinates writes as

$$\begin{aligned}
\mathbf{u}_f &= \frac{1}{\sqrt{m_i^2-n_i^2}}\left(m_i\mathbf{u}_i - \frac{n_i}{\sqrt{c}}\mathbf{u}_i'\right) + O(\mu^{1/3}),\\
\mathbf{u}_f' &= \frac{1}{\sqrt{m_i^2-n_i^2}}\left(-\sqrt{c}\, n_i\mathbf{u}_i + m_i\mathbf{u}_i'\right) + O(\mu^{1/3}).
\end{aligned}$$

In order to obtain the in-map in synodical coordinates, it is necessary to undo the change of variables given be (107) and (110) and the properties of Lemma 2 . After some calculations, it can be obtained that

$$\begin{aligned} \boldsymbol{\rho}_f &= \boldsymbol{\rho}_i - \frac{\cos a}{\sqrt{c}}\,\mu^{1/3}\dot{\boldsymbol{\rho}}_i + O(\mu^{2/3}) \\ \dot{\boldsymbol{\rho}}_f &= \dot{\boldsymbol{\rho}}_i + O(\mu^{1/3}), \end{aligned} \tag{128}$$

which express the final position and velocity in terms of the initial conditions.

The second equation in (128), which do not gives the explicit terms of order $\mu^{1/3}$, can be improved. This can be done using the appropriate changes of variables which improve the approximation given by (118) up to order $\mu^{2/3}$. In that case, it can be shown that

$$\dot{\boldsymbol{\rho}}_f = \dot{\boldsymbol{\rho}}_i + \frac{\cos a}{\sqrt{c}}\,\mu^{1/3} A_3 \dot{\boldsymbol{\rho}}_i + O(\mu^{2/3}). \tag{129}$$

The in-map allows us to obtain a development in powers of $\mu^{1/3}$ for the change of the (keplerian) energy (with respect to the big primary) after a passage near the small primary. The result obtained is similar to (61), in the sense that it can be explained the increase or decrease of the energy in terms of the initial velocity.

6.4 Resonant orbits and periodic solutions

The interest in resonant orbits comes from their application to the design of spacecraft missions and because of their role as natural motions of comets, as well. In the case of spacecraft missions, multiple flybys to one planet can be done, such that the approach energy is reduced each time the spacecraft makes a near resonant return to the planet for a gravity assist, reducing the orbit capture ΔV requirements.

Let us suppose that a massless particle is moving in a resonant orbit after a flyby to a planet. So after some time, it will return to the same neighbourhood of the same planet. Considering the motion in the framework of the Restricted Three Body Problem, the passage near the small primary corresponds to the inner solution, and the resonant orbit to the outer solution. Both solutions match at the junction point where the third body leaves the neighbourhood (the initial condition for both inner and outer solution), but not at the return point in which the third body enters the neighbourhood of the small primary. The in-map and the out-map allow us to measure the distance between these two positions. From (105) and (128), we have that

$$\boldsymbol{\rho}_e - \boldsymbol{\rho}_f = \left(\delta + \frac{\cos a}{\sqrt{c}}\right)\,\mu^{1/3}\dot{\boldsymbol{\rho}}_i + O(\mu^{2/3}). \tag{130}$$

A reduction of this distance can be done matching the corresponding expressions up to order $\mu^{2/3}$, so that

$$\delta = -\frac{\cos a}{\sqrt{c}}. \tag{131}$$

Nevertheless, we have to take into account that resonant orbits have to verify the restrictions (97), (101) and (104). Given a value for p and q, it will be

enough to choose a value for the Jacobi constant and the spherical coordinates of the initial conditions (at the epoch where the orbit leaves the neighbourhood of the small primary) verifying (97), (101) and ε such that $\varepsilon - \delta = 0$ to ensure (104).

In particular, in the planar case ($\phi = \varphi = 0$) the resonant families can be described as follows. For each $p, q \in \mathbb{N}$ relatively prime with $p/q \leq 2\sqrt{2}$, there is a family of p–q resonant orbits with the Jacobi constant, $C_J \in (C_{J_1}, C_{J_2}) \setminus \{(p/q)^{2/3}\}$ (see (99)) and the polar angle of the velocity ψ given (from (97)) by the relation

$$\sin\psi = \frac{2 - C_J + (p/q)^{2/3}}{2\sqrt{3 - C_J}}. \tag{132}$$

Only a very reduced subset of these orbits will be periodic. If we just ask for periodicity in configuration space, the difference Δv between the velocities $\dot{\boldsymbol{\rho}}_e$ and $\dot{\boldsymbol{\rho}}_f^s$ for this orbits can be computed numerically. In Figure 40 the behaviour of Δv as a function of C_J for different p–q families are shown. As we can see, there are ranges of values of the Jacobi constant for which the Δv keeps bounded, while for values near its minimum C_{J_1} and maximum C_{J_2} value, Δv increases.

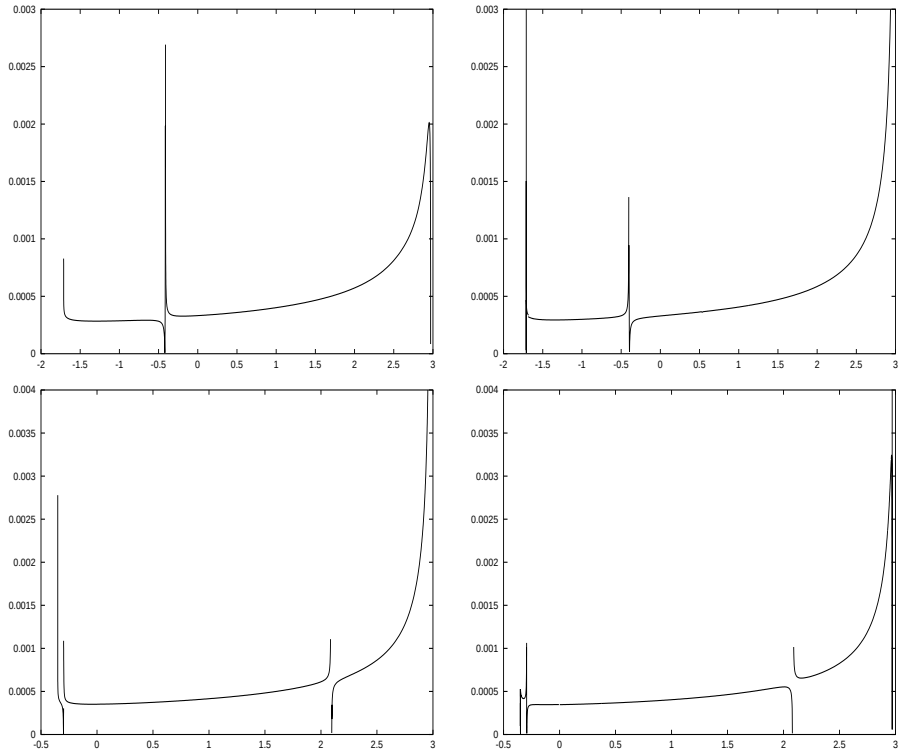

Figure 40: C_J (x axis) vs Δv (y axis) for the orbits of two p–q resonant families. The left hand side curves correspond to values of $\psi \in (-\pi/2, \pi/2)$ and the right hand side to $\psi \in (\pi/2, 3\pi/2)$. From top to bottom, the values of p–q are 1–2 and 3–2 respectively.

References

[1] Barrabés, E. and G. Gómez: 'Spatial p-q resonant orbits of the RTBP'. *Celestial Mechanics and Dynamical Astronomy* **84**(4), 387–407, 2002.

[2] Barrabés, E. and G. Gómez: 'Three dimensional p-q resonant orbits close to second species solutions'. *Celestial Mechanics and Dynamical Astronomy* **85**(2), 145–174, 2003.

[3] Barrabés, E. and G. Gómez: 'A note on Second Species Solutions generated from p-q resonant orbits'. *Celestial Mechanics and Dynamical Astronomy* **88**(3), 229–244, 2004.

[4] Battin, R.H.: *An Introduction to the Mathematics and Methods of Astrodynamics.* AIAA Education Series, AIAA, 1987.

[5] Breakwell, J. and L. Perko: 'Matched asymptotic expansions, patched conics, and the computation of interplanetary trajectories'. *Prog. Astronaut. Aeronaut.* **17**, 159–182, 1996.

[6] Font, J., A. Nunes, and C. Simó: 2002, 'Consecutive quasi-collisions in the planar circular RTBP'. *Nonlinearity* **15**(1), 115–142.

[7] Gómez, G. and J. Masdemont and J.M. Mondelo: 'Solar System Models with a Selected Set of Frequencies'. *Astronomy & Astrophysics* **390**(2), 733–749, 2002.

[8] Labunsky, A.V., O.V. Papkov, and K.G. Sukhanov. *Multiple Gravity Assist Interplanetary Trajectories*. Gordon and Breach Science Publishers, 1998.

[9] Prado, A.F.B.A. and R.A. Broucke. 'Transfer Orbits in Restricted Problem'. *Journal of Guidance, Control and Dynamics* **18** (3) 593–599, 1995.

[10] Stiefel, E. and G. Scheifele: *Linear and regular celestial mechanics.* Die Grundlehren der mathematischen Wissenschaften. Band 174. Berlin-Heidelberg-New York: Springer-Verlag. 1971.

[11] Szebehely, V.: *Theory of Orbits. The Restricted Problem of Three Bodies.* Academic Press, Inc. 1967.

[12] Yen, C.: 'Ballistic Mercury Orbiter Mission via Venus and Mercury Gravity Assists'. *AAS/AIAA Astrodynamics Specialist Conference, Paper AAS 85–346, 1985.*